Freie Universität Berlin

Inaugural-Dissertation

towards the academic degree

Doctor rerum naturalium (Dr. rer. nat.)

Synthesis, structure and reactivity of well defined Stannoxanes, Indoxanes and Thalloxanes

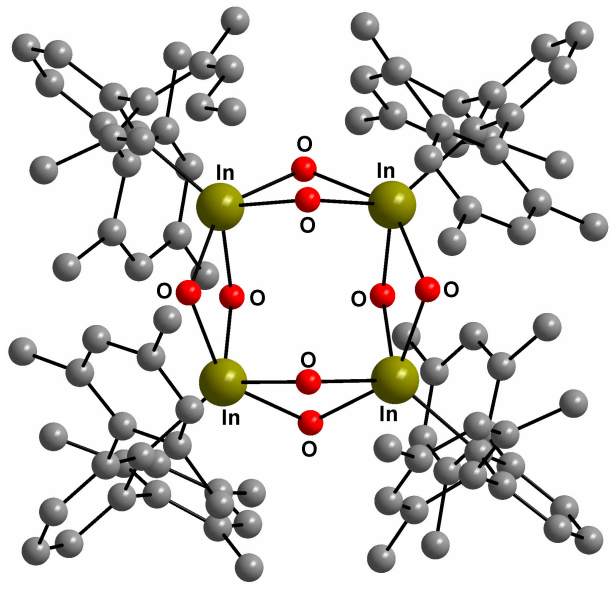

Submitted to the Department of Biology, Chemistry and Pharmacy,

Freie Universtät Berlin

S. Usman Ahmad, Pakistan

January 2011

The present work was carried out under the supervision of Prof. Dr. Jens Beckmann from April 2007 to December 2010 at the Institute of Chemistry and Biochemistry, at the Freie Universität Berlin.

1st Referee: Prof. Dr. Jens Beckmann

2nd Referee: Prof. Dr. Ulrich Abram

Date of Defense: 18. 02. 2011

Acknowledgements

I wish to express my deepest and sincere gratitude to Prof. Dr. Jens Beckmann for providing me the opportunity to carry out the research work under his supervision. His admirable supervision and encouragement were crucial towards the successful completion of the work.

I am deeply grateful to Prof. Dr. Ulrich Abram for reviewing this thesis and the annual reports for the scholarship extension.

I thank the employees of the facilities and service departments of the FU Berlin for the administrative tasks, the recording of spectra, elemental analysis, glassware and technical support.

I thank Dr. Andrew Duthie of the School of Life and Environmental Sciences, Deakin University, Australia, for the measurement of ESI MS and MAS NMR spectra.

Dr. Vadapalli Chandrasekhar of the Indian Institute of Technology Kanpur, is to be thanked for a gift of pentamethylphosphetanic acid.

I wish to thank all the former and present group members of the research group especially Marian Grassmann, Jens Bolsinger, Alexandra Schütrumpf, Pamela Finke, Maxie Hesse, Ole Mallow and Nelly Rivas for an exceptionally supportive, pleasant and enjoyable working atmosphere. Here, I consider this especially important to acknowledge and thank Dr. Malte Hesse, who not only measured a number of crystal structures for me but also always had very useful and handy tips throughout the research work.

I am grateful to the Higher Education Commission (HEC), Pakistan in collaboration with the Deutscher Akademischer Austausch Dienst (DAAD), Germany for the financial support.

My special gratitude is due for my parents, my brothers and sisters and their families for their love and support.

Last, but never the least, I am grateful to all my friends especially Sylwia, Adnan, Husnain, Ahsan, Farooq, Asma and Sajjad for being my surrogate family during the many years I have stayed in Germany.

Contents

1. Introduction

The first step towards a theory of chemical reactions was taken by Georg Ernst Stahl in 1697 when he proposed the *phlogiston* theory. He concluded that phlogiston (from the Greek *phlogistos*, "to burn") is consumed whenever something burns. The phlogiston theory was the basis for research in chemistry for most of the 18th century.

Although the credit for the discovery of oxygen goes to Carl Wilhelm Scheele and Joseph Priestly, Antoine Lavoisier in 1775, was the first to recognize it as an element and proposed the name *oxygene* (literally, "acid-former") for the substance absorbed from air when a compound burns. He chose this name because the products of the combustion of nonmetals such as phosphorus are acids when they dissolve in water. Such reactions embarked the era of intensive research in the field of main group element oxides and hydroxides and it was a matter of time that the oxygen chemistry of the light main group elements was established.

Group 14 element oxo acids

Carboxylic acids RC(O)OH represent a large family of organic compounds that find widespread applications in organic synthesis. The oxides of carbon differ from the other members of group 14 in that carbon has the tendency to form double bonds with the oxygen atoms as observed in the carbonyl group of carboxylic acids.

Organosiloxane chemistry has evolved rapidly combining the functional characteristics of the siloxane backbone with the functionality of organics. The widespread applications range from daily use plastic materials to heterogeneous catalysis,[1] supramolecular chemistry,[2] nanotechnology[3] and advanced materials.[4]

Although a variety of routes are used for the synthesis of siloxanes, the reaction of silicon halides with alcohols to give the corresponding silylethers is the most common Si-O bond formation reaction.[5]

Among various classes of siloxanes, the silsesquioxanes are a unique class that has attracted a great deal of interest from polymer industry. The term silsesquioxane refers to all structures with the empirical formula $(RSiO_{1.5})_n$ and the related hydrates, where R can be hydrogen, methyl, phenyl, or a higher molecular weight organic group.

Silanetriols $RSi(OH)_3$[6] are valuable precursors for silsesquioxanes[7] and metallasiloxanes.[8] A general pathway for the preparation of silanetriols and related compounds is the controlled hydrolysis of appropriated precursors, e.g. organotrichlorosilanes $RSiCl_3$. An example of alkyl silantriols is *t*BuSi$(OH)_3$ obtained by the hydrolysis of *t*BuSiCl_3 (Figure 1). In the solid-state *t*BuSi$(OH)_3$ is involved in extensive hydrogen bonding.[9]

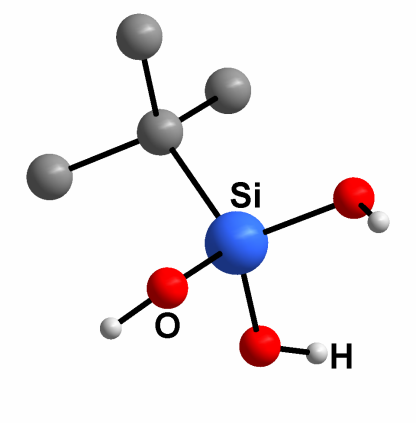

Figure 1: Molecular structure of *t*butyl silanetriol *t*BuSi$(OH)_3$.

An example of an aryl silanetriol is 2,6-$Mes_2C_6H_3Si(OH)_3$ which is also involved in hydrogen bonding showing different polymorphs and pseudopolymorphs (Figure 2).[10]

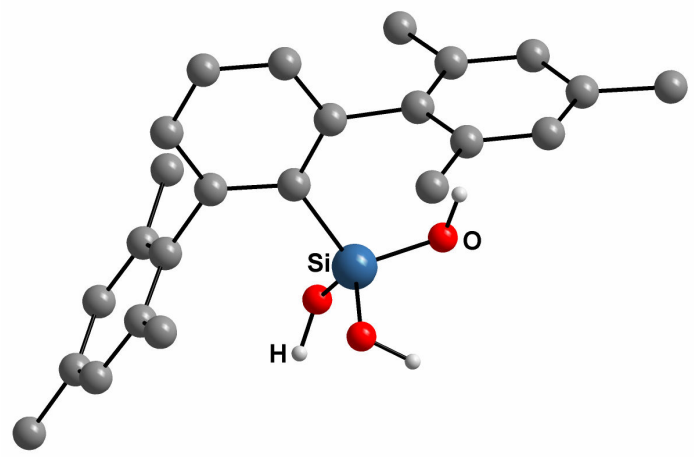

Figure 2: Molecular structure of *m*-terphenyl silanetriol 2,6-$Mes_2C_6H_3Si(OH)_3$.

The condensation products of silanetriols are oligo- or polysiloxanes.[11] The primary condensation product of *t*BuSi$(OH)_3$ is $(t\text{BuSi})_2O(OH)_4$ (Figure 3).[12]

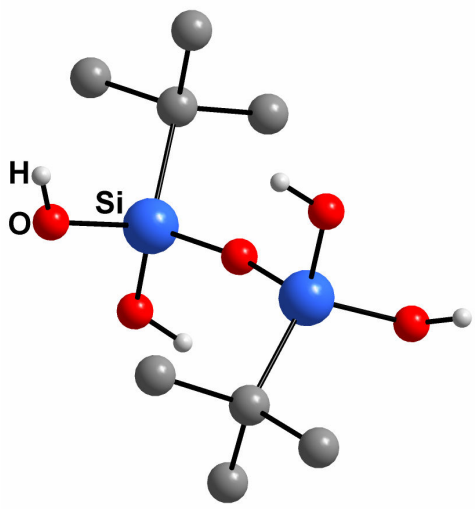

Figure 3: Molecular structure of (tBuSi)$_2$O(OH)$_4$.

The primary condensation product of two *m*-terphenyl silanetriol molecules is (*m*-TerSi)$_2$O(OH)$_4$.[13] However the crystal structure for the dimeric compound K$_2$(*m*-TerSi$_2$O)$_2$(OH)$_3$(O)$_2$ is reported through synthesis of the compound by applying excess of KOH to triflorosilane 2,6-Mes$_2$C$_6$H$_3$SiF$_3$.[13] This compound is not comparable to the (tBuSi)$_2$O(OH)$_4$ because it is a K-silanolate. In the solid state two disiloxane units are bridged by K^+ cations (Figure 4). The interaction of the potassium cation with the aromatic π-systems of the *m*-terphenyl substituent seems to significantly stabilize aggregation.[14]

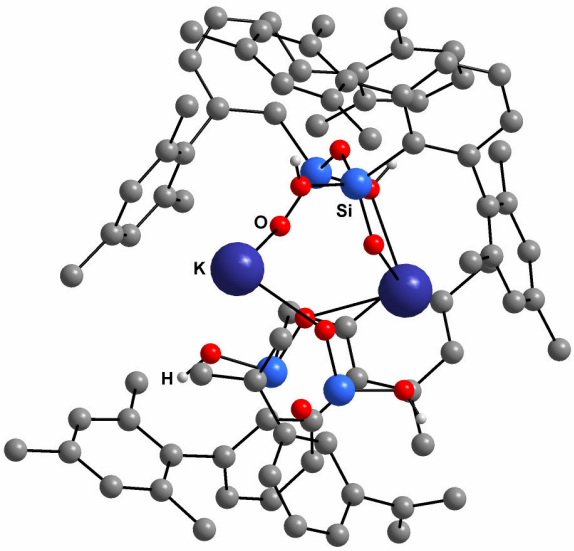

Figure 4: Molecular structure of [K$_2$(*m*-TerSi$_2$O)$_2$(OH)$_3$(O)$_2$].

The condensation product of an alkylsilanetriol namely *i*PrSi(OH)$_3$ is a trimeric cyclotrisiloxanetriol [*i*PrSiO(OH)]$_3$ with a virtually planar Si-O ring that was obtained by the dearylchlorination using HCl/AlCl$_3$ and subsequent hydrolysis of the cyclotrisiloxanes [Ar(*i*Pr)SiO]$_3$ (Ar = Ph, *o*-MeC$_6$H$_4$) (Figure 5).[15]

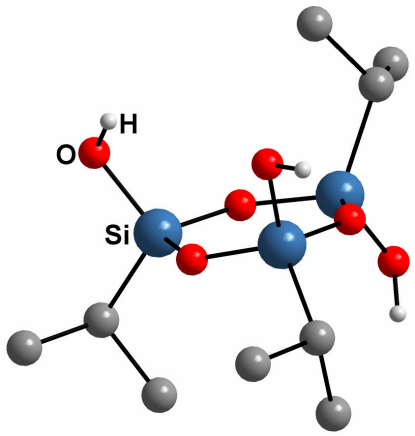

Figure 5: Molecular structures of *trans*-[*i*PrSiO(OH)]$_3$.

Another silanetriol namely *cis*-[(Me$_3$Si)$_2$CSiO(OH)]$_3$ has all hydroxy groups oriented in the same direction with respect to the Si$_3$O$_3$ ring plane (Figure 6).[16]

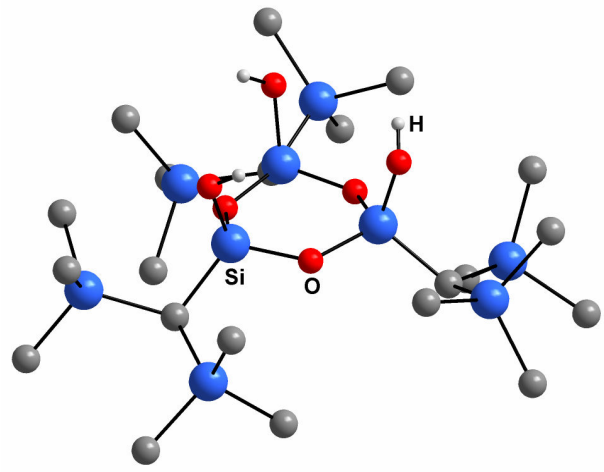

Figure 6: Molecular structure of *cis*-[(Me$_3$Si)$_2$CSiO(OH)]$_3$.

Further condensation of such oligomeric silsesquioxanes may result in a variety of polyhedral oligomeric silsesquioxanes designated by the abbreviation POSS. These may have random structures, ladder structures, cage structures and partial cage structures. The cage structures (RSiO$_{1.5}$)$_n$ can adopt different geometries for example adamantane (n = 4), prism (n = 6), cube (n = 8) etc (Scheme 1).

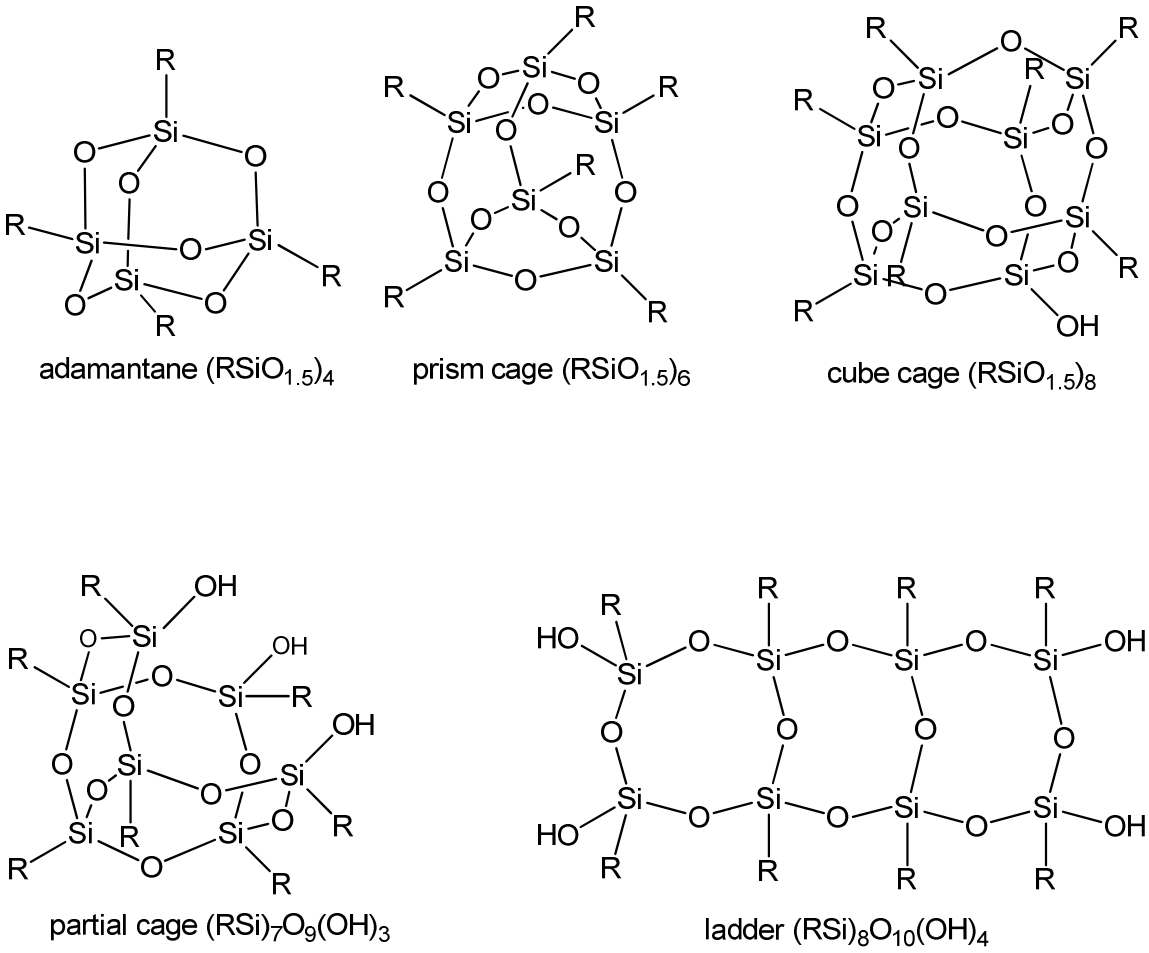

Scheme 1: Structures of silsesquioxanes.

Among such oligomeric silsesquioxanes (POSS) is included the cage silsesquioxane $(t\text{BuSiO}_{1.5})_6$ which is the condensation product of $t\text{BuSi(OH)}_3$ (Figure 7).[12]

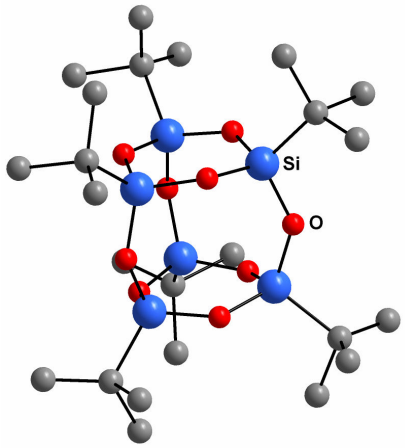

Figure 7: Molecular structure of $(t\text{BuSiO}_{1.5})_6$.

An incompletely condensed silsesquioxane (tBuSi)$_7$O$_9$(OH)$_3$ is extracted from a mixture of several condensation products when tBuSi(OH)$_3$ is treated with NaH (Figure 8).[12]

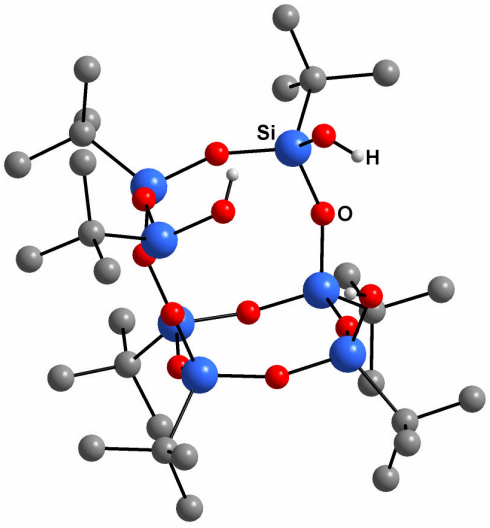

Figure 8: Molecular structure of (tBuSi)$_7$O$_9$(OH)$_3$.

The heavier analogues of silsesquioxanes are called germasesquioxanes represented by the general formula (RGeO$_{1.5}$)$_n$. The Ge-O-Ge linkage is labile compared with the siloxane bond in silsesquioxanes. This opens up the possibility of further chemical modification of the polymeric architecture.[17] Generally for galloxanes (RGeO$_{1.5}$)$_n$, the numeral n is smaller as for siloxanes (RSiO$_{1.5}$)$_n$.

Hydrolysis of alkylgermanium trichloride gives cage hexakis alkylgermasesquioxane, (RGeO$_{1.5}$)$_6$ (R = iPr, tBu, $cyclo$-C$_6$H$_{11}$).[18] The structure of ($cyclo$-C$_6$H$_{11}$Ge)$_6$O$_9$ displays two six-membered Ge$_3$O$_3$ rings that are joined co-facially by Ge-O bridges (Figure 9).[18]

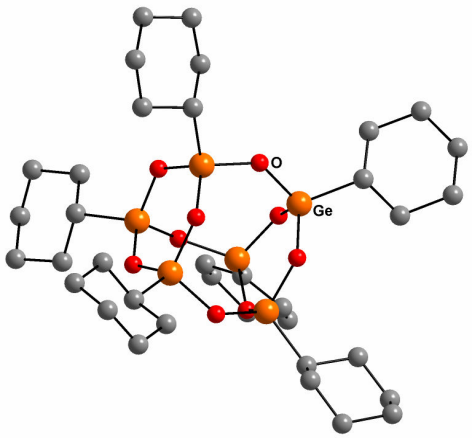

Figure 9: Molecular structure of ($cyclo$-C$_6$H$_{11}$Ge)$_6$O$_9$.

Both silsesquioxanes and germasesquioxanes display a coordination number of four for silicon and germanium.

Previous work on organotin oxo clusters has revealed an extensive structural diversity, which depends on the method of preparation, the degree of hydrolysis and most importantly, the bulk of the organic substituent which provide the kinetic stabilization.[19] Tin displays hypercoordination in many of its oxygen cluster compounds. Hydrolysis of organotin halides has shown to proceed in a stepwise fashion, with the nature of the products increasing in complexity with increasing halide content of the precursor.

The final hydrolysis product of a monoorganotintrihalide is a stannonic acid $[RSn(O)OH]_n$ or the corresponding anhydride $(RSnO_{1.5})_n$ (R = alkyl, aryl). The first organostannonic acid $[MeSn(O)OH]_n$ was obtained more than 120 years ago by the reaction of $SnCl_2$ with methyl iodide in the presence of aqueous KOH.[20] A more general hydrolysis scheme with possible hydrolysis products of the monoorganotin(IV) trichloride is shown in Scheme 2.

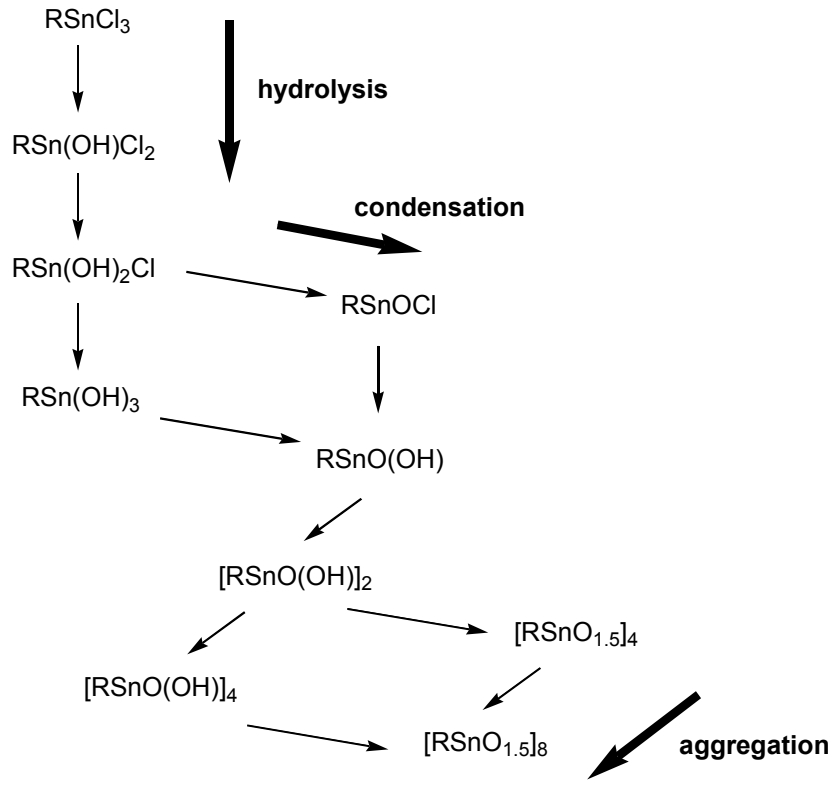

Scheme 2: General hydrolysis scheme for monoorganotin(IV) trichloride.

Subsequent work showed that organostannonic acids and related compounds are more generally prepared by the base hydrolysis of organotin trichlorides and related compounds (Scheme 2).[21] Most previously known organostannonic acids are amorphous, high melting polymers with cross-linked random structures.[22] The aggregation and hypercoordination of the tin atoms was unambiguously proven by the seminal work of Puff and Reuter who carefully studied the base hydrolysis of *i*PrSnCl$_3$ and reported a series of well-defined molecular organostannoxy chlorides, such as [*i*PrSn(OH)Cl$_2$·H$_2$O]$_2$,[23] (*i*PrSn)$_9$O$_8$(OH)$_6$Cl$_5$,[24] and [(*i*PrSn)$_{12}$O$_{14}$(OH)$_6$]Cl$_2$,[25] which can be regarded as intermediates on the way to polymeric organostannonic acids [RSn(O)OH]$_n$ and related compounds (Figure 10).

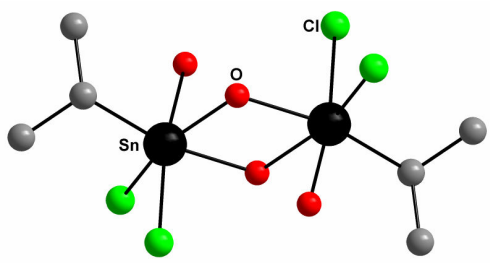

[*i*PrSn(OH)Cl$_2$·H$_2$O]$_2$

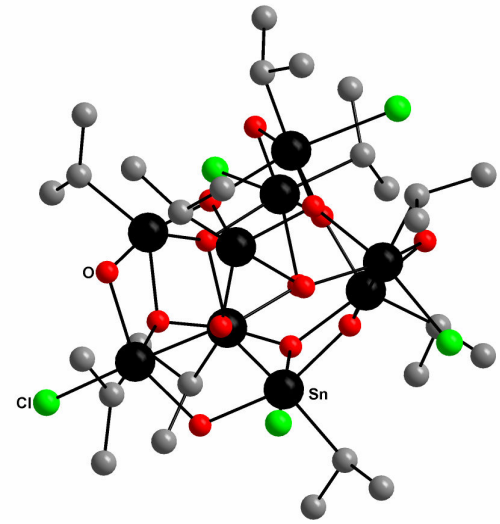

(*i*PrSn)$_9$O$_8$(OH)$_6$Cl$_5$

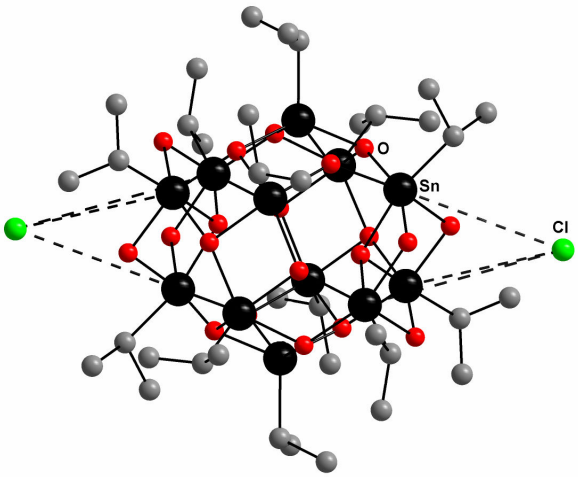

[(*i*PrSn)$_{12}$O$_{14}$(OH)$_6$]Cl$_2$

Figure 10: Molecular structures of the hydrolysis products of *i*PrSnCl$_3$.

Within this series, the degree of aggregation increases with the number of oxygen atoms replacing the chlorine atoms.

The first molecular organostannonic acids were obtained only recently by using the kinetic stabilization of bulky organic substituents. These include the *cis*-$[(Me_3Si)_3CSn(O)OH]_3$[26] comprising an aggregated six-membered ring type structure with all the three hydroxy groups *cis* to each other (Figure 11).

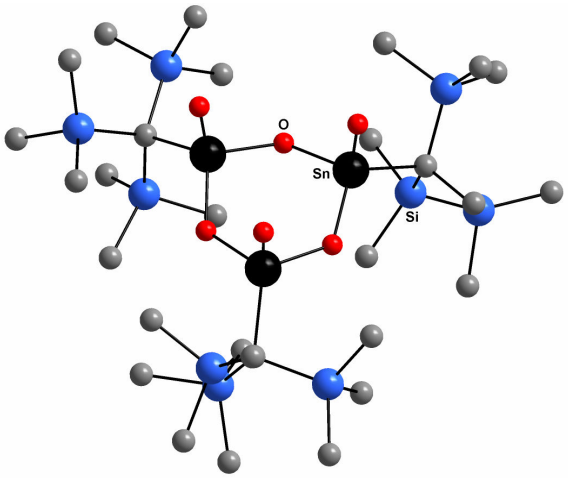

Figure 11: Molecular structure of monoorganostannonic acid *cis*-$[(Me_3Si)_3CSn(O)OH]_3$.

Another recently reported stannonic acid is $[2,4,6\text{-}i Pr_3C_6H_2Sn(O)OH]_{6,}$[27] comprising a hexanuclear cluster type structure (Figure 12).

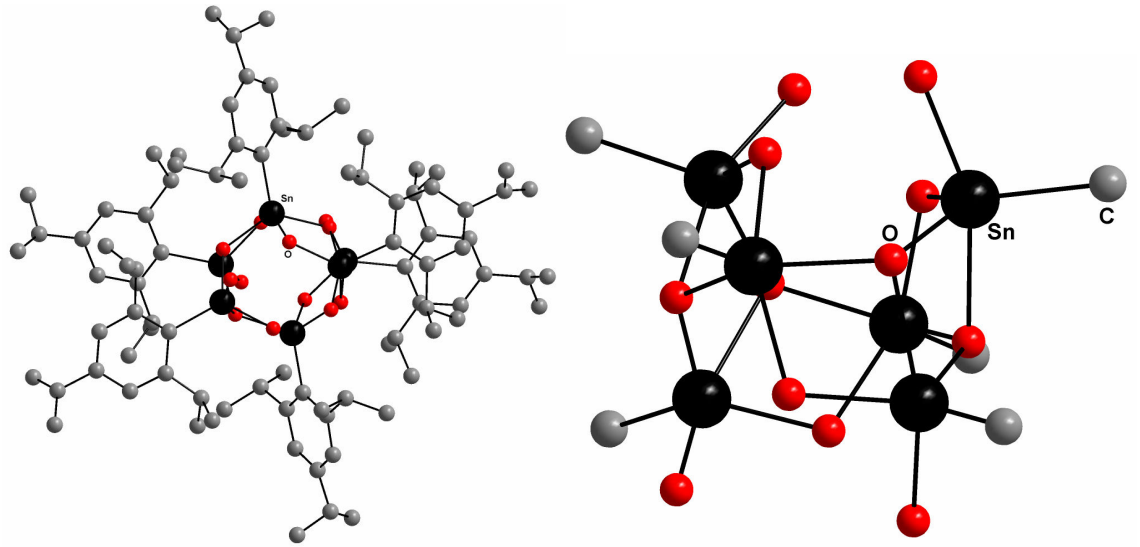

Figure 12: Molecular structure and the inorganic core of organostannonic acid $[(2,4,6\text{-}i Pr_3C_6H_2Sn(O)OH]_6$.

Also noteworthy is the related organotin oxide $[(Me_3Si)_3CSn]_4O_6$ comprising an adamantane type structure,[28] which can be regarded as an stannonic acid anhydride, a condensation product of an organostannonic acid. During the course of this study, another molecular organostannonic acid $[2,6\text{-}(Me_2NCH_2)_2C_6H_3Sn(O)OH]_6$ containing a cluster type structure with a Sn_6O_{12} core structure was obtained by the electronic stabilization of an intramolecularly coordinating *N*-donor substituent (Figure 13).[29]

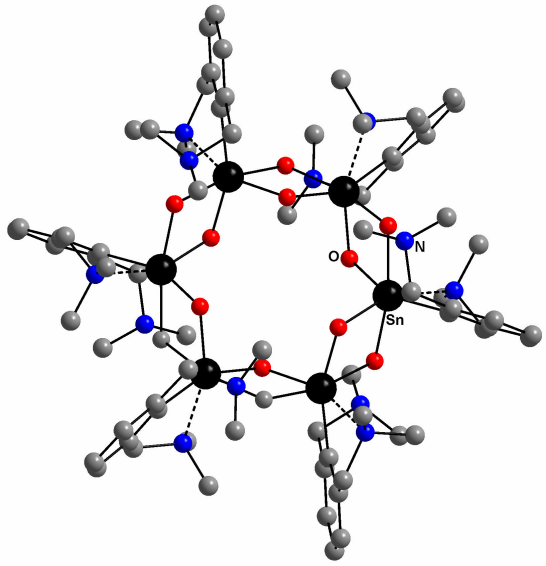

Figure 13: Molecular representation of $[2,6\text{-}(Me_2NCH_2)_2C_6H_3Sn(O)OH]_6$.

Group 13 element oxo acids

The boronic acids, $RB(OH)_2$, and the related boroxine rings, $(RBO)_3$, are crucial for many branches of chemistry. The most prominent application involves the use as reagents for transition metal catalyzed cross-coupling reactions[30] and as intermediates predominantly in the Suzuki coupling. The noble prize for chemistry 2010 is shared by three scientists including Akira Suzuki which is the manifestation of the importance of these coupling reactions. Boronic acids are also of current interest as building blocks in supramolecular chemistry[31] and for applications in carbohydrate sensing.[32]

The industrial use of polymeric methylalumoxane $(MeAlO)_n$ as co-catalyst for the polymerization of ethylene (Ziegler-Natta reaction) has stimulated active research on alumoxanes. While the exact structure of $(MeAlO)_n$ is unknown, considerable work has been done on the structural determination of alumoxanes (RAlO) containing bulkier organic substituents to elucidate their role in polymerization. RAlO is the formal condensation product of elusive $RAl(OH)_2$ (R = alkyl, aryl). Aluminium has the

tendency to extend the coordination number generally to four. Examples include [*t*BuAl(μ_3-O)]$_6$[33] and [(Me$_3$Si)$_3$CAl]$_4$(μ-O)$_2$(μ-OH)$_4$ (Figure 14).[34]

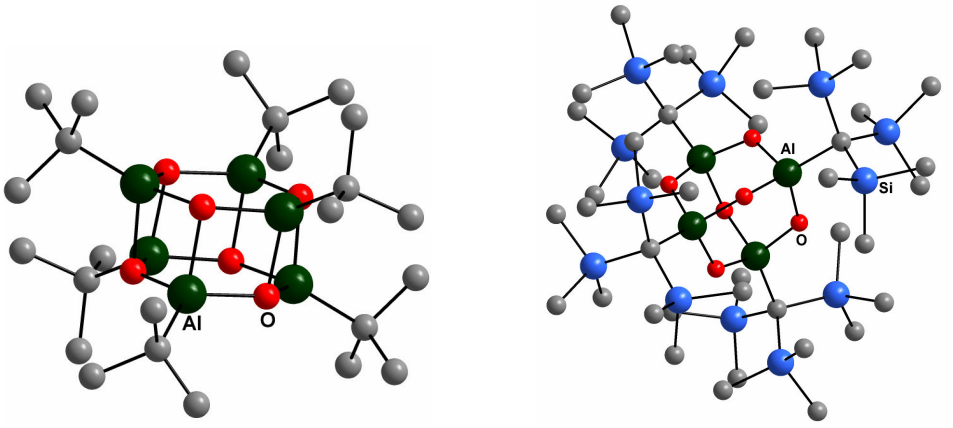

[*t*BuAl(μ_3-O)]$_6$ [(Me$_3$Si)$_3$CAl]$_4$(μ-O)$_2$(μ-OH)$_4$

Figure 14: Molecular structures of two tetracoordinate alumoxanes.

Several workers have postulated the existence of five-coordinate aluminium in alumoxanes.[35] Indeed the hydrolysis of [*t*BuAl(μ_3-O)]$_6$ resulted in (*t*BuAl)$_6$(μ_3-O)$_4$ (μ-OH)$_4$ with pentacoordinated aluminum centers (Figure 15).[36]

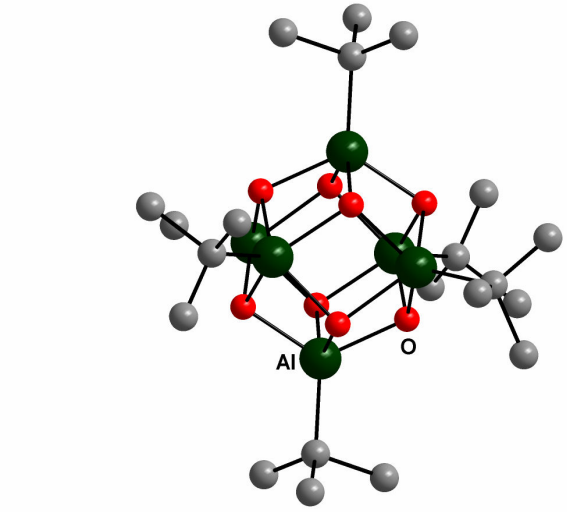

Figure 15: Molecular structure of pentacoordinate alumoxane (*t*BuAl)$_6$(μ_3-O)$_4$(μ-OH)$_4$.

Alumoxanes with a coordination number of three at the aluminum centre can be represented by a tetrameric organoaluminum oxide [(2,4,6-*t*Bu$_3$C$_6$H$_2$Al)$_4$(μ-O)]$_4$ cluster in which further increase in coordination number is hindered by a bulky substituent (Figure 16).[37]

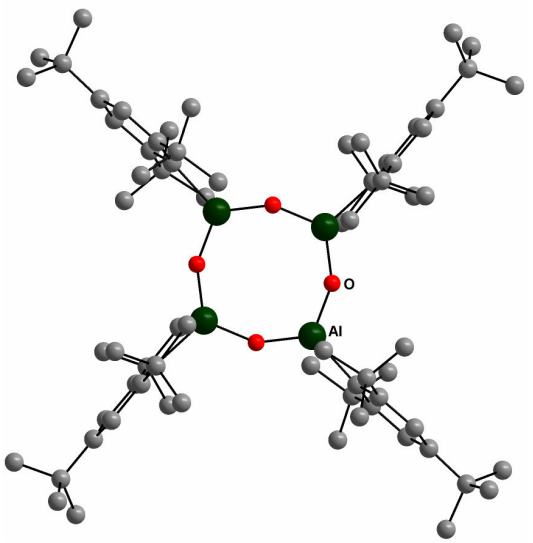

Figure 16: Molecular structure of tricoordinate alumoxane $[(2,4,6\text{-}t\text{Bu}_3\text{C}_6\text{H}_2\text{Al})_4(\mu\text{-O})]_4$.

Just like the alumoxanes, the chemistry of galloxanes $(\text{RGaO})_n$ has also progressed at a rapid pace as highlighted by a recent review.[38] The structure of $(\text{MesGaO})_9$ (Figure 17) was found to be analogous to $(t\text{BuAlO})_9$.[39] The cage structure of both clusters consists of two M_3O_3 (M = Al, Ga) rings connected by three M-(μ_3-O) units.

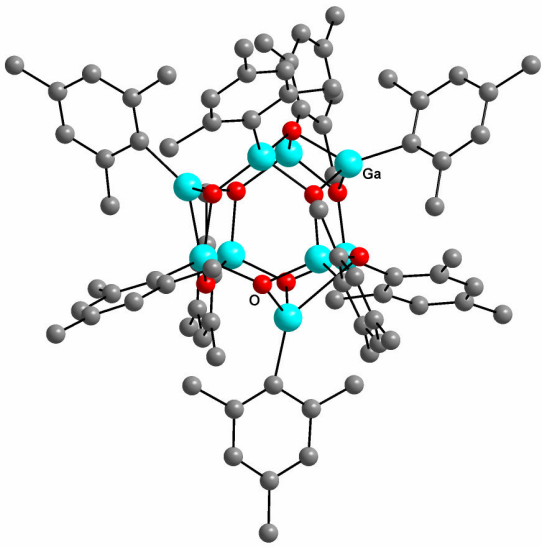

Figure 17: Molecular structure of galloxane $(\text{MesGaO})_9$.

Another example of a galloxane cluster is $(t\text{BuGa})_{12}(\mu_3\text{-O})_8(\mu\text{-O})_2(\mu\text{-OH})_4$ with twelve vertex-sharing tetrahedra (Figure 18).[36]

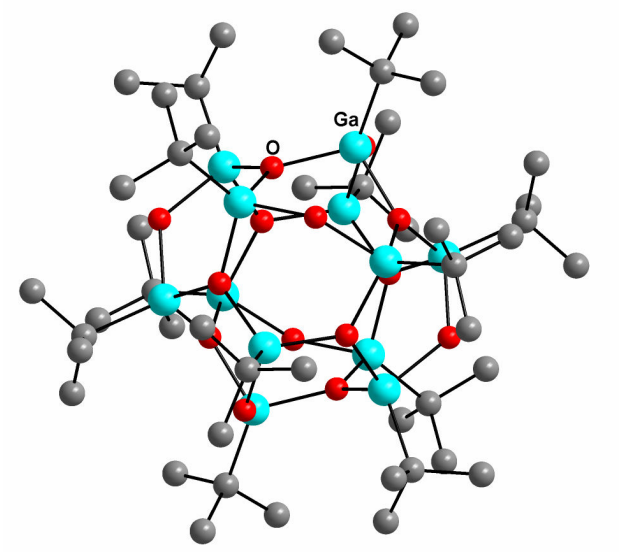

Figure 18: Molecular structure of galloxane $(t\text{BuGa})_{12}(\mu_3\text{-O})_8(\mu\text{-O})_2(\mu\text{-OH})_4$.

Other examples among well defined galloxanes include $[(\text{MesGa})_6(\mu_3\text{-O}_4)(\mu\text{-OH})_4\cdot 4\text{THF}]$[40] and $[(\text{Me}_3\text{Si})_3\text{CGa}]_4(\mu\text{-O})_2(\mu\text{-OH})_4$.[34]

There are surprisingly few studies dealing with the heavier group 13 congeners of alumoxanes and galloxanes which was attributed to the reduced oxophilicity and lower Lewis acidity of In and Tl.[41]

The number of well-defined indoxane clusters is limited to only two. The first one is a tetranuclear oxygen-centered adamantane structure $[(\text{Me}_3\text{Si})_3\text{CIn}]_4(\mu_4\text{-O})(\mu\text{-OH})_6$[42] (Figure 19) with each indium pentacoordinated with three bridging hydroxy groups along the edges of a tetrahedron and the trimethylsilyl group on the exterior.

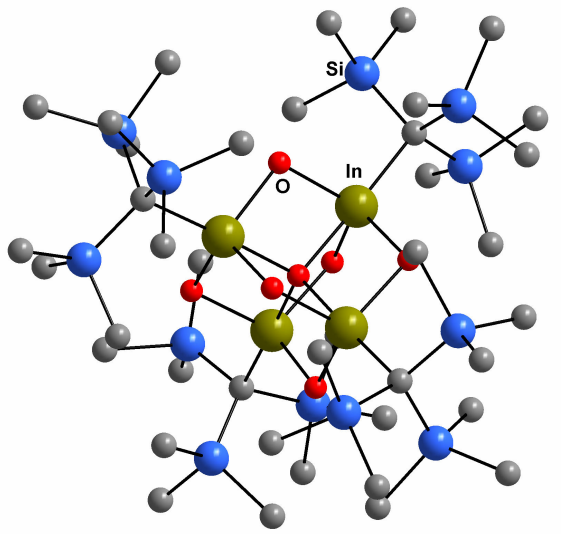

Figure 19: Molecular structure of indoxane $[(\text{Me}_3\text{Si})_3\text{CIn}]_4(\mu_4\text{-O})(\mu\text{-OH})_6$.

The second well defined indoxane $[(Me_3Si)_3CIn(\mu_3\text{-}O)]_4$[43] adopts a distorted In_4O_4 heterocubane structure with normal In-O bond lengths but short intercage In···In and O···O distances (Figure 20).

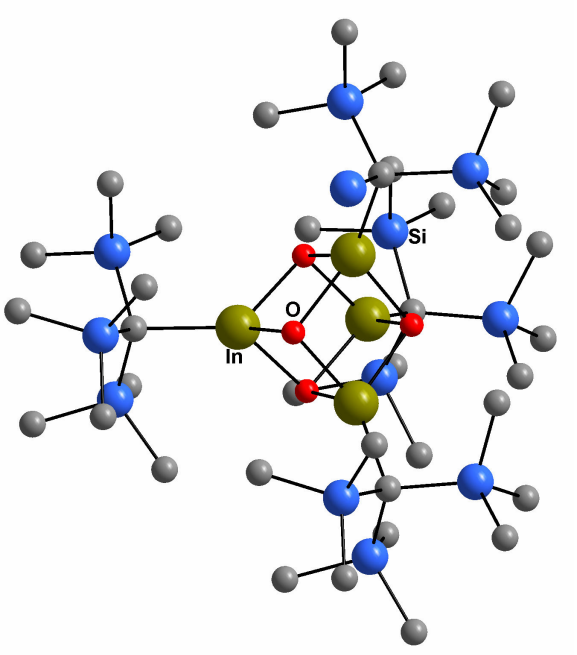

Figure 20: Molecular structure of indoxane $[(Me_3Si)_3CIn(\mu_3\text{-}O)]_4$.

During the course of this work two four-membered galloxane and indoxane rings, $[2,6\text{-}(2',6'\text{-}i Pr_2C_6H_3)_2C_6H_3E(\mu\text{-}O)]_2$ (E = Ga, In), were also reported in which further aggregation is prevented by a bulky *m*-terphenyl substituent.[44] The molecules contain almost perfectly square metal-oxygen cores (Figure 21).[44]

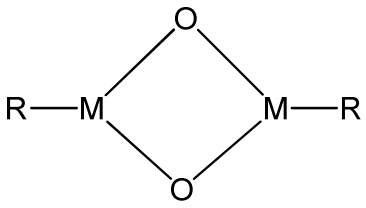

R = 2,6-(2',6'-*i*$Pr_2C_6H_3)_2C_6H_3$

Figure 21: Lewis structural representation of $[2,6\text{-}(2',6'\text{-}i Pr_2C_6H_3)_2C_6H_3M(\mu\text{-}O)]_2$ (M = Ga, In).

There is virtually no organothalloxane oxide $(RTlO)_n$ or dihydroxide $RTl(OH)_2$ reported to the best of our knowledge.

2. Scope

The goal of this work is the synthesis and characterization of well-defined stannoxanes, indoxanes and thalloxanes and by the basic hydrolysis of the appropriate aryltin(IV) trichloride, arylindium(III) dichloride and arylthallium(III) dichloride. The compounds produced as the hydrolysis products are structurally characterized and examined on the basis of their degree of aggregation. The degree of aggregation is associated with the tendency to realize hypercoordinate geometries. The focus of attention lie on the metal-oxygen bonds (where metal = Sn, In or Tl) and hypercoordination at the metal atoms. Therefore this work contributes to the bonding theory of heavy *p*-block elements.

The kinetic stabilization of the respective monoorganoelement (Sn, In, Tl) chlorides is to be achieved by the use of a bulky organic substituent, namely *m*-terphenyl group (2,6-dimesitylphenyl group) (Figure 22).

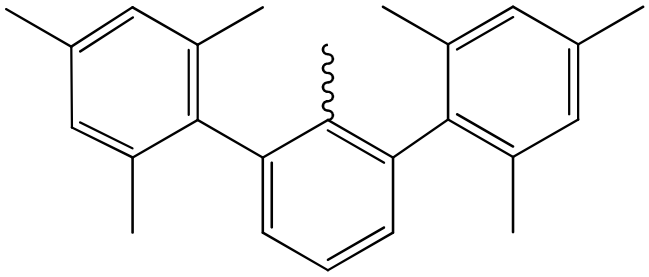

Figure 22: Structural representation of the 2,6-dimesitylphenyl substituent.

During the course of the basic hydrolysis of these sterically demanding monoorganoelement (Sn, In, Tl) chlorides a variety of products with varying hydrolysis grade can be isolated depending upon the number of chloride and the strength of base hydrolysis. The progression of hydrolysis involves at the same time condensation and aggregation processes. Therefore the exact determination of an individual hydrolysis product is difficult to predict and depends largely on the size of the sterically demanding organic rest.

The 2,6-dimesitylphenyl substituent has previously been used in our research group for the stabilization and isolation of a number of crucial main group element oxo compounds. The following results encouraged us to employ this substituent for the stabilization of the heavier element oxides and hydroxides of the 13^{th} and 14^{th} main group elements.

- The very first well-defined stibonic acid $[2,6\text{-}Mes_2C_6H_3Sb(O)(OH)_2]_2$ with asymmetric four-membered Sb_2O_2 ring structure possessing two exocyclic hydroxy groups.[45]
- Mixed-valent antimony oxo clusters $(2,6\text{-}Mes_2C_6H_3Sb^{V})_2(ClSb^{III})_4O_8$ and $(2,6\text{-}Mes_2C_6H_3Sb^{V})_4(ClSb^{III})_4(HOSb^{III})_2O_{14}$, that resulted from partial cleavage of Sb-C bonds.[46]
- The first well-defined tellurinic acid $[2,6\text{-}Mes_2C_6H_3Te(O)(OH)_2]_2$ with asymmetric four-membered Te_2O_2 ring structure with one exocyclic hydroxy group.[45]
- A well-defined dinuclear telluronic acid $[2,6\text{-}Mes_2C_6H_3Te(O)(OH)_3]_2$ comprised of an asymmetric four-membered Te_2O_2 ring structure that is completely shielded by two *m*-terphenyl groups.[47]
- An unprecedented tetranuclear $Na_4Te_4O_8$ cage structure, sodium *m*-terphenyltellurinate $Na_4(2,6\text{-}Mes_2C_6H_3Te)_4(\mu_3\text{-}O)_8$, that is completely shielded by four *m*-terphenyl groups.[47]

3. Results and discussion

3.1. Synthesis and controlled hydrolysis of *m*-terphenyltin trichloride

The treatment of 2,6-$Mes_2C_6H_3Li$[48] with $SnCl_4$ produced the *m*-terphenyltin trichloride 2,6-$Mes_2C_6H_3SnCl_3$ (**1**) as a crystalline solid in quantitative yield (Scheme 3).

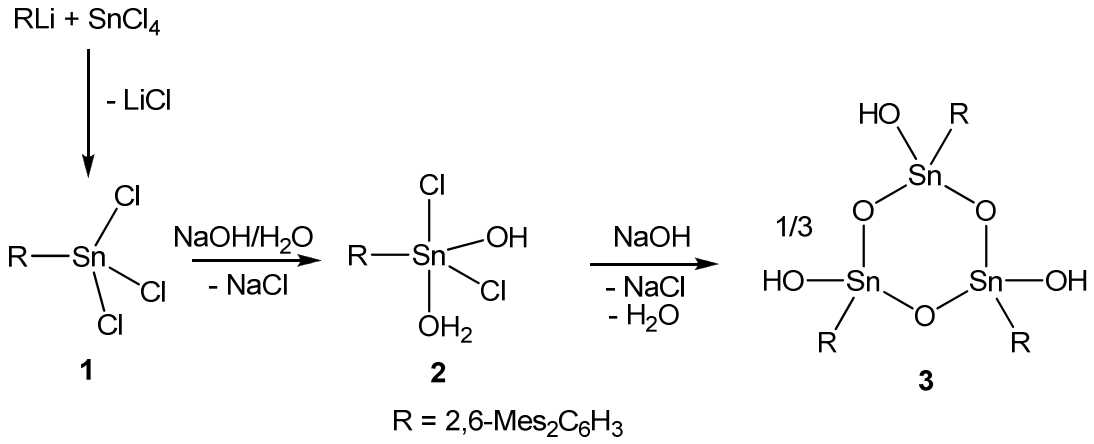

Scheme 3: Synthetic route of *trans*-[2,6-$Mes_2C_6H_3Sn(O)(OH)]_3$ (**3**).

The Sn atom of **1** is tetracoordinated with a slightly distorted tetrahedral geometry (Figure 23). In contrast to many other organotin(IV) halides, **1** does not have significant intermolecular Sn···Cl contacts. The chemical shift for the ^{119}Sn NMR ($CDCl_3$) is observed at δ = –113.9, and resembles that reported for the even bulkier terphenyltin trichloride 2,6-(2′,4′,6′-*i*$Pr_3C_6H_2)_2C_6H_3SnCl_3$ (δ = –116.8).[49]

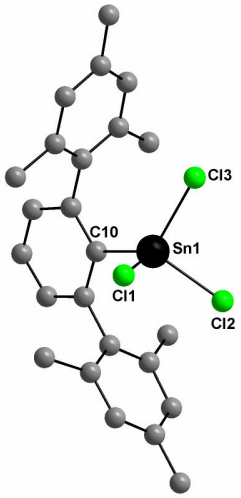

Figure 23: Molecular structure of 2,6-$Mes_2C_6H_3SnCl_3$ (**1**). Selected bond lengths (Å) and angles (º): Sn1-Cl1 2.303(2), Sn1-Cl2 2.312(2), Sn1-Cl3 2.331(2), Sn1-C10 2.128(6), Cl1-Sn1-Cl2 103.0(1), Cl1-Sn1-Cl3 101.8(1), Cl2-Sn1-Cl3 97.48(8), Cl1-Sn1-C10 112.9(2), Cl2-Sn1-C10 119.1(2), Cl3-Sn1-C10 119.8(2).

The intermediate hydrolysis product of the hydrolysis of **1** is a monochloro substituted 2,6-$Mes_2C_6H_3Sn(OH)Cl_2 \cdot H_2O$ (**2**). The compound has a dimeric structure with a trigonal bipyramidal arrangement around the Sn atom in which the C atom, one Cl atom, and the hydroxy group occupy the equatorial positions (Figure 24). The other Cl atom and the water molecule are situated in the axial positions. The previously known organotin hydroxide chlorides such as $[RSn(OH)Cl_2 \cdot H_2O]_2$ (R = *i*Pr, *i*Bu,[23] Et,[50] *n*Bu,[51] *trans*Myr[52]) differ in the regard that they posses hexacoordintated Sn atoms. The increase in the aggregation number is prevented because of the presence of the bulky *m*-terphenyl substituent.

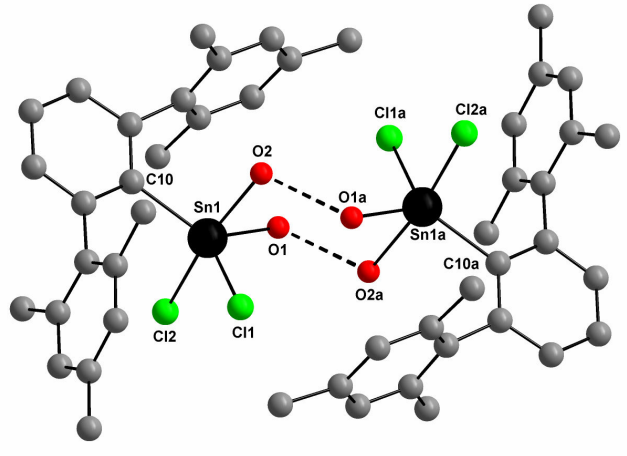

Figure 24: Molecular structure of 2,6-$Mes_2C_6H_3Sn(OH)Cl_2 \cdot H_2O$ (**2**). Selected bond lengths (Å) and angles (°): Sn1-O1 1.973(4), Sn1-O2 2.316(4), Sn1-Cl1 2.242(3), Sn1-Cl2 2.401(2), Sn1-C10 2.132(5), O1-Sn1-O2 81.5(2), O1-Sn1-Cl1 101.5(1), O1-Sn1-Cl2 92.2(1), O2-Sn1-Cl1 83.0(1), O2-Sn1-Cl2 171.7(1), O1-Sn1-C10 130.4(2), O2-Sn1-C10 87.9(2), Cl1-Sn1-Cl2 93.23(9), Cl1-Sn1-C10 125.1(2), Cl2-Sn1-C10 100.3(1); (Symmetry code: a = –x, 2–y, –z).

The coordinated water molecule gives rise to Sn-O bond length of 2.316(4) Å and compares well with other organotin water complexes, such as $(Me_3SiCH_2)_2SnCl_2 \cdot H_2O$ (2.404(8) Å) and 2,6-Mes_2-4-*t*Bu-$C_6H_2SnMe_2(O_3SCF_3) \cdot H_2O$ (2.273(3) Å)[53] and is considerably longer than the Sn-O bond length of the hydroxy group of 1.973(4) Å. In the crystal lattice, two molecules of **2** are associated as centrosymmetric dimers through hydrogen bonding (O···O distance 2.681(6) Å). Furthermore, the water molecules seem to be engaged in hydrogen bonding of the type O-H···π-aryl with one of the mesityl groups of the *m*-terphenyl substituent. The solid state ^{119}Sn NMR signal observed at δ_{iso} = –359, differs from the solution state NMR observed at δ = –171.5 in $CDCl_3$.

The water molecule is reversibly dissociated in solution that leads to the change in coordination number from 4 to 5 (Scheme 4). A similar observation was made for the water adduct $(Me_3SiCH_2)_2SnCl_2 \cdot H_2O$.[53]

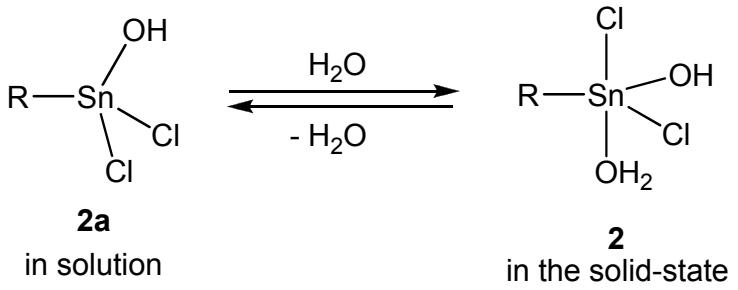

2a
in solution

2
in the solid-state

Scheme 4: Reversible dissociation of water molecule in **2**.

The final hydrolysis product of **1** is *trans*-[2,6-$Mes_2C_6H_3Sn(O)(OH)]_3$ (**3**). The molecular structure of **3** reveals puckered six-membered Sn_3O_3 ring structure (largest deviation from the ideal plane 0.525(2) Å) and the *trans*-configuration of the endocyclic substituents (Figure 25).

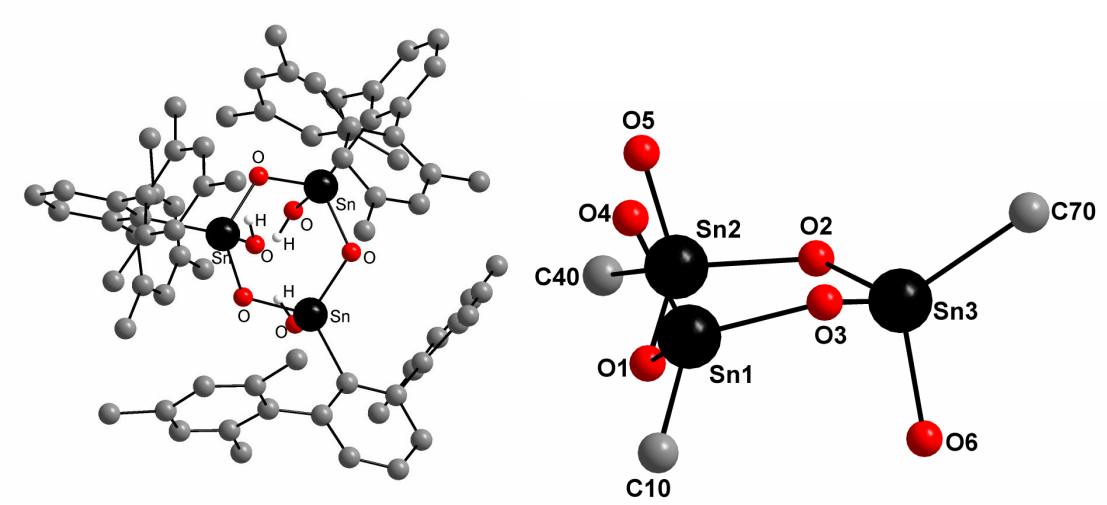

Figure 25: Molecular structure and inorganic core of *trans*-[2,6-$Mes_2C_6H_3Sn(O)(OH)]_3$ (**3**). Selected bond lengths (Å) and angles (°): Sn1-O1 1.962(6), Sn1-O3 1.960(7), Sn1-O4 1.956(7), Sn1-C10 2.16(1), Sn2-O1 1.962(6), Sn2-O2 1.955(7), Sn2-O5 1.966(7), Sn2-C40 2.166(9), Sn3-O2 1.971(6), Sn3-O3 1.940(6), Sn3-O6 1.959(7), Sn3-C70 2.171(9), O1-Sn1-O3 102.6(3), O1-Sn1-O4 111.0(3), O3-Sn1-O4 103.8(3), O1-Sn1-C10 113.4(3), O3-Sn1-C10 116.6(4), O4-Sn1-C10 108.9(4), O1-Sn2-O2 106.7(3), O1-Sn2-O5 96.8(3), O2-Sn2-O5 103.3(3), O1-Sn2-C40 118.8(3), O2-Sn2-C40 114.7(3), O5-Sn2-C40 114.0(3), O2-Sn3-O3 108.0(3), O2-Sn3-O6 107.4(3), O3-Sn3-O6 100.7(3), O2-Sn3-C70 108.9(3), O3-Sn3-C70 117.0(3), O6-Sn3-C70 114.1(3), Sn1-O1-Sn2 117.8(3), Sn2-O2-Sn3 121.8(3), Sn1-O3-Sn3 128.7(3).

Although all three Sn sites are crystallographically independent, the ^{119}Sn MAS NMR spectrum of **3** exhibits only two signals at δ_{iso} = –210 and –224 with an integral ratio

of 2:1. The ^{119}Sn NMR spectrum of **3** in dry C_6D_6 shows two signals at δ = –207.7 (integral 66%, $^2J(^{119}\text{Sn-O-}^{119/117}\text{Sn})$ = 538 Hz) and –222.5 (integral 33%; $^2J(^{119}\text{Sn-O-}^{119/117}\text{Sn})$ = 539 Hz), which reveals that the six-membered ring structure and the *trans*-configuration are retained in solution. However, in wet C_6D_6, the ^{119}Sn NMR spectrum reveals only one slightly broad signal at δ = –227.1 without tin satellites ($\omega_{1/2}$ = 220 Hz). Although the almost unchanged ^{119}Sn NMR chemical shift is indicative for the coordination number of 4, the lack of $^2J(^{119}\text{Sn-O-}^{119/117}\text{Sn})$ couplings discard multinuclear products, such as the *cis*-isomer of **3**. Together, these data suggest that **3** undergoes a reversible hydrolysis in wet C_6D_6 to give the monomeric organostannonic acid 2,6-$Mes_2C_6H_3Sn(OH)_3$ (**3a**, Scheme 5). The facile interconversion of **3** and **3a** is attributed to the lability of the Sn-O bonds within these compounds.

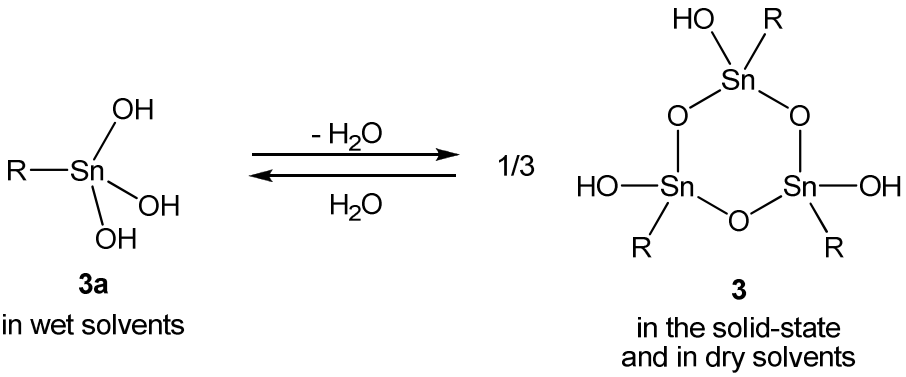

3a
in wet solvents

3
in the solid-state
and in dry solvents

Scheme 5: Interconversion of monomeric **3a** to trimeric **3**.

3.1.1. Reactivity of *m*-terphenylstannonic acid (3)

Despite the extensive research being done on the subject of stannoxanes,[22-29] still little is known about the reactivity of molecular organostannonic acids. To the best of our knowledge, only the reaction of $[(2,4,6\text{-}i\text{Pr}_3C_6H_2Sn(O)OH]_6$ with sulfonic acids has been described, which gave rise to new organostannoxy sulfonate cluster types.[54] The reactivity of the organostannonic acid **3**, kinetically stabilized by the bulky *m*-terphenyl substituent, towards a number of reagents has been carried out.

A redistribution reaction between *trans*-$[2,6\text{-}Mes_2C_6H_3Sn(O)OH]_3$ (**3**) and $(t\text{Bu}_2SnO)_3$ was performed for a deeper study on the lability of Sn-O bonds (Scheme 6). The reaction was studied by ^{119}Sn NMR spectroscopy in dry C_6D_6. The NMR data revealed the formation of just a single product 2,6-$Mes_2C_6H_3(OH)Sn(OSnt\text{Bu}_2)_2O$ (**4**)

and against all expectations no evidence was found for the existence of tBu$_2$Sn[OSn(2,6-Mes$_2$C$_6$H$_3$)OH]$_2$O in solution.

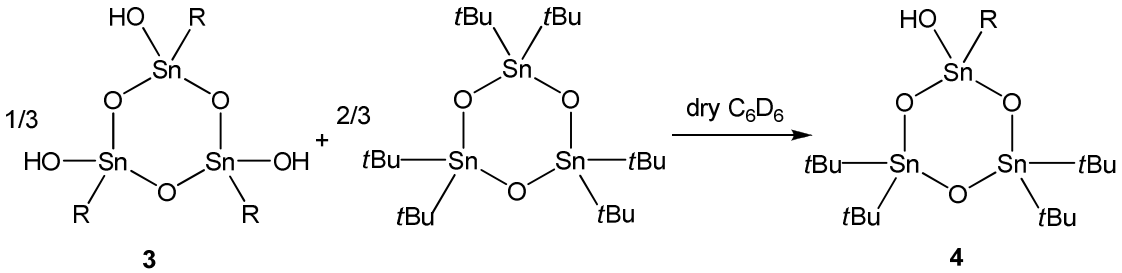

3 **4**

Scheme 6: NMR scale reaction of [2,6-Mes$_2$C$_6$H$_3$Sn(O)OH)]$_3$ (**3**) with (tBu$_2$SnO)$_3$.

This result is in marked contrast with the redistribution reaction of [(Me$_3$SiCH$_2$)$_2$SnO]$_3$ and (tBu$_2$SnO)$_3$, which give rise to an equilibrium mixture of both possible products (Me$_3$SiCH$_2$)$_2$Sn(OSntBu$_2$)$_2$O and tBu$_2$Sn[OSn(CH$_2$SiMe$_3$)$_2$]O.[55] Compound **4** is characterized by two ^{119}Sn NMR chemical shifts of δ = –68.0 (integral 66%, ^2J(^{119}Sn-O-$^{119/117}$Sn) = 437 Hz) and –222.4 (integral 33%; ^2J(^{119}Sn- O-$^{119/117}$Sn) = 425/417 Hz) and therefore consists also most likely of a six-membered ring structure.

3.1.2. *m*-Terphenylstannoxane carbonate

A number of *s*-, *d*- and *f*-block metals are able to bind and activate CO_2.[56] However *p*-block elements known to react with CO_2 are rarer. Extensive research on heavy *p*-block elements in this aspect has resulted in the isolation and full characterization of some interesting organotin intermediates[57,58,59] and very recently organobismuth carbonates.[60] Notably, carbon dioxide absorption is not unprecedented in organotin chemistry and has attracted considerable interest recently in the context of the C-O bond activation for the preparation of commodities such as diorgano carbonates.[61] Particularly noteworthy is the tendency of (tBu$_2$SnO)$_3$ to absorb CO_2 to produce the trinuclear organostannoxane carbonate cluster OC(OSntBu$_2$)$_2$OtBu$_2$Sn(OH)$_2$.[62]
During an attempt to obtain single crystals by air evaporation of a $CHCl_3$ solution of **4**, the decanuclear organostannoxane carbonate cluster [tBu$_2$Sn(OH)OSnR(OH)$_2$OC (OSntBu$_2$OH)$_2$(O)SnR(OH)(H$_2$O)]$_2$ (**5**, R = 2,6-Mes$_2$C$_6$H$_3$) was obtained as a single crystalline product in low yield (Scheme 7).

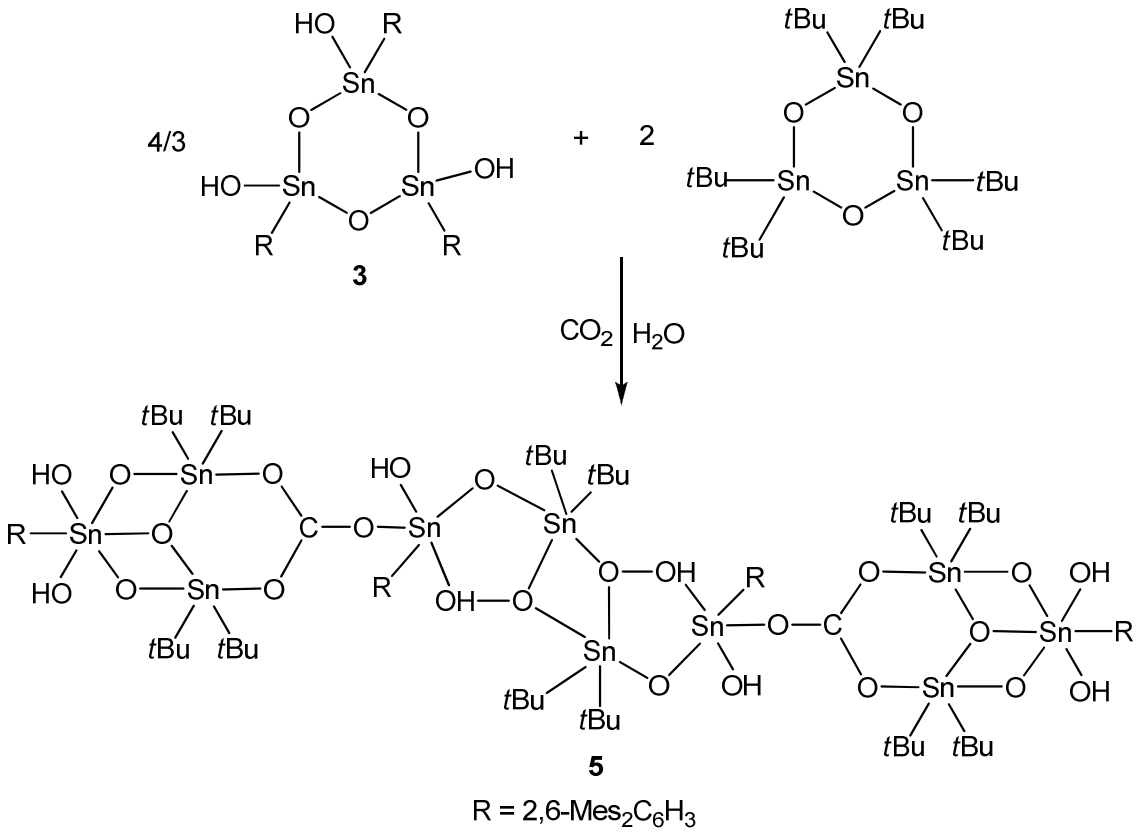

Scheme 7: Synthesis of $[t\text{Bu}_2\text{Sn(OH)OSnR(OH)}_2\text{OC(OSn}t\text{Bu}_2\text{OH)}_2\text{(O)SnR(OH)(H}_2\text{O)}]_2$ (**5**, R = 2,6-$\text{Mes}_2\text{C}_6\text{H}_3$)

Compound **5** is a unique assembly of six $t\text{Bu}_2\text{Sn}$ and four 2,6-$\text{Mes}_2\text{C}_6\text{H}_3\text{Sn}$ units as well as two carbonate moieties, which result from absorption of atmospheric CO_2. The same compound was obtained in nearly quantitative yield when a solution with the appropriate ratio of **3** and $(t\text{Bu}_2\text{SnO})_3$ was purged with an excess of CO_2 gas for 5 min. The molecular structure of **5** comprises of a central four-membered $(t\text{Bu}_2\text{SnOH})_2$ ring (Figure 26), reminiscent of those observed in $(t\text{Bu}_2\text{SnOH})_2\text{X}_2$ (X = F, Cl, Br, OH, NO_3, O_3SCF_3, $OOCCH_3$)[63] and two terminal tricyclic rings $\text{OC(OSn}t\text{Bu}_2)_2\text{O(2,6-Mes}_2\text{C}_6\text{H}_3\text{)(OH)Sn(OH)}_2$ similar to those found in $\text{E(OSn}t\text{Bu}_2)_2\text{O}t\text{Bu}_2\text{Sn(OH)}_2$ (E = OC,[62] Ph_2Si,[64] Ph_2P^+[65]), which are linked by two 2,6-$\text{Mes}_2\text{C}_6\text{H}_3\text{(OH)}_2\text{SnO}$ units. A key feature of the structure is the hypercoordination of every Sn atom, with all $t\text{Bu}_2\text{Sn}$ units and two of the 2,6-$\text{Mes}_2\text{C}_6\text{H}_3\text{Sn}$ units being pentacoordinated. The other two 2,6-$\text{Mes}_2\text{C}_6\text{H}_3\text{Sn}$ units have a hexacoordinate arrangement around the Sn atoms involving coordination of a water molecule, which can be distinguished from the hydroxy groups by comparison of the Sn-O bond lengths of 2.24(1) and 2.09(1) Å,

respectively. Some of the hydroxy groups are involved in intramolecular hydrogen bonding, as evidenced by the short O···O distances of 2.55(5) and 2.85(5) Å. The IR spectrum of **5** is consistent with the presence of five crystallographically independent hydroxy groups and one water molecule and reveals presumably overlapping absorptions at $\tilde{\nu}$ = 3649, 3588 and 3545 cm^{-1} that were assigned to OH stretching vibrations. Compound **5** is only slightly soluble in organic solvents.

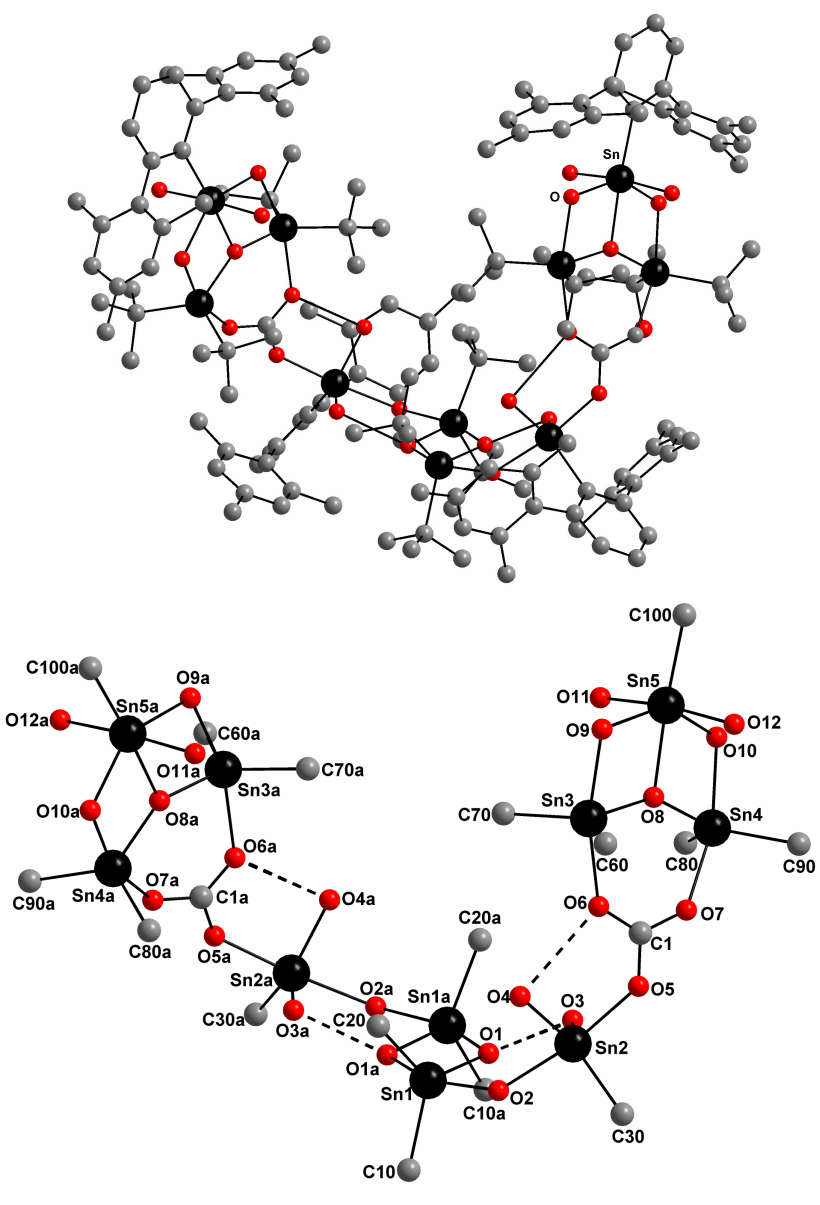

Figure 26. Molecular structure and inorganic core of [*t*Bu_2Sn(OH)OSnR(OH)$_2$OC(OSn*t*Bu_2OH)$_2$(O)SnR(OH)(H_2O)]$_2$ (**5**, R = 2,6-$Mes_2C_6H_3$). Selected bond lengths (Å) and angles (º): Sn1-O1 2.024(8), Sn1-O2 2.21(1), Sn1-C10 2.20(2), Sn2-O2 2.18(1), Sn2-O3 1.987(9), Sn2-O4 1.97(1), Sn2-O5 2.11(1), Sn2-C30 2.16(1), Sn3-O6 2.270(9), Sn3-O8 1.992(9), Sn3-O9 2.189(8), Sn3-C60 2.16(2), Sn3-C70 2.18(2), O1···O3 2.55(5), O4···O6 2.85(2), O1-Sn1-O1a 71.7(4), O1-Sn1-O2 84.1(3), O1-Sn1-O2 155.7(3), O1-Sn1-C10 114.2(5), O1a-Sn1-C10 96.3(5), O1-Sn1-C20 124.5(5), O1a-Sn1-C20

96.5(5), O2-Sn1-C10 95.7(6), O2-Sn1-C20 95.3(5), C10-Sn1-C20 121.0(6), O2-Sn2-O3 83.4(3), O2-Sn2-O4 84.6(4), O2-Sn2-O5 169.3(4), O3-Sn2-O4 109.2(5), O3-Sn2-O5 88.9(4), O4-Sn2-O5 91.0(4), O2-Sn2-C30 97.6(4), O3-Sn2-C30 121.6(5), (Symmetry code: a = –x, y, 0.5–z).

The carbonate coordination in previously known *p*-block element carbonates is classified in different coordination modes as shown in Scheme 8.[66] These modes depict the extent of metal coordination with the carbonate moiety. Maximum coordination is observed in mode E, as for example, in polymeric trialkyl tin carbonates $[(Me_3Sn)_2CO_3]_n$ and $[(iBu_3Sn)_2CO_3]_n$ which complies with the high tendency of tin to be hypercoordinated.[67] Whereas mode A depicts least involvement of metal coordination as for example in the cases of $O[(2\text{-}Me_2NCH_2C_6H_4)Sn]_2CO_3$[68] and $2,6\text{-}(Me_2NCH_2)_2C_6H_3)SbCO_3$[69] which is explained by the presence of the intramolecularly coordinated *N*-donor ligand thus reducing the Lewis acidity of the organotin and organoantimony atoms. Thus the stannoxane carbonate **5** displays maximum coordination for the Sn atoms from the carbonate and falls in the category of mode E (Scheme 8).

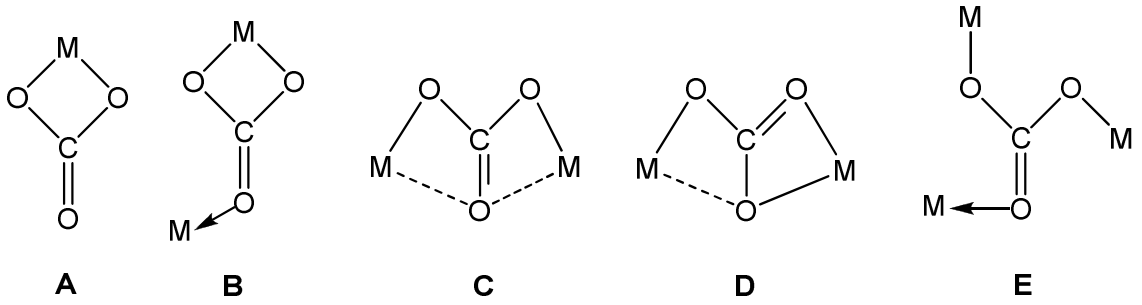

Scheme 8: Classification of different modes of carbonate coordination

3.1.3. Hexameric methylstannoxyl carbonate

The recent interest in the molecular organostannonic acids *cis*-$[(Me_3Si)_3CSn(O)OH]_3$,[26] *trans*-$[(2,6\text{-}Mes_2C_6H_3Sn(O)OH]_3$ (**3**), $[(2,4,6\text{-}iPr_3C_6H_2Sn(O)OH]_6$,[27] and $[2,6\text{-}(Me_2NCH_2)_2C_6H_3Sn(O)OH]_6$[29] as well as the carbon dioxide fixation and activation ability of organotin oxides and related species[70] (Scheme 7, synthesis of stannoxane carbonate **5**) prompted a structural investigation of the crystalline potassium methylstannoxyl carbonate cluster by ^{13}C and ^{119}Sn MAS NMR spectroscopy and X-ray crystallography. The study is an attempt to better understand

the structure of $[MeSn(O)OH]_n$ which is structurally still not completely characterized, as discussed earlier in introduction.

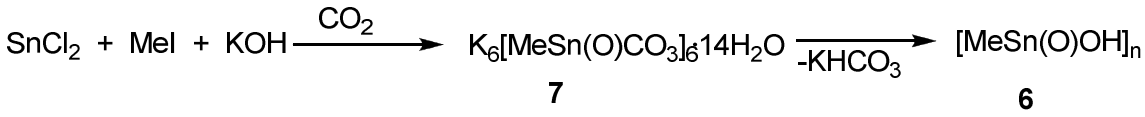

Scheme 9: Synthesis of potassiummethylstannoxyl carbonate (**7**).

A representative specimen of the potassium methylstannoxyl carbonate[71] turned out to have the exact composition $K_6[MeSn(O)CO_3]_6 \cdot 14H_2O$ (**7**) and contains hydrated potassium cations and $[MeSn(O)CO_3]_6^{6-}$ anions (Scheme 9). The molecular structure of the $[MeSn(O)CO_3]_6^{6-}$ ion comprises a prismatic or so-called hexameric drum structure and is shown in Figure 27. The perspective view on the crystal structure is shown in Figure 28. The hexameric drum is a commonly found structural motif in neutral organostannoxyl carboxylates $[RSn(O)CO_2R']_6$ (R, R′ = alkyl, aryl).[72] The faces of the drum may be described as two Sn_3O_3 six-membered rings that are linked in two complementary ways. Each O atom of each ring connects to a Sn atom of the second ring, of opposite orientation, leading to six μ_3-oxo atoms. The girth of the drum may be considered as six Sn_2O_2 four-membered rings arranged so as to form a tube. Six bidentate bridging carbonate ions diagonally span the Sn_2O_2 four-membered rings. The methyl groups are oriented above and below the faces of the drum. The centrosymmetric anion contains three crystallographically independent hexacoordinated Sn atoms and carbonate ions. Consistently, the ^{119}Sn MAS NMR spectrum of **7** shows three signals at δ_{iso} = –474, –481, and –486 having approximately equal intensities. The ^{13}C MAS NMR spectrum shows two sets of three signals at δ_{iso} = 164.2, 162.2, and 160.7 as well as 8.0, 5.7, and 5.2, which were assigned to the crystallographically independent carbonate ions and methyl groups. The spatial arrangement of the Sn atoms is distorted octahedral and defined by O_5C-donor sets. The Sn-(μ_3-O) bond lengths (Sn-O bonds within the hexameric cage) cover a range from 2.079(7) to 2.121(7) Å (average 2.102(7) Å), while the Sn-(μ_2-O) bond lengths (related to the bidentate carbonate ions) are slightly longer, ranging from 2.106(7) to 2.167(8) Å (average 2.129(9) Å). The spatial arrangement of the three independent carbonate ions is rather unsymmetric. Those O atoms involved in coordination to the Sn atoms show rather long C-O bond lengths, ranging from 1.28(2) to 1.32(2) Å, while the remaining C-O bond lengths are between 1.24(2) and

1.25(1) Å. The latter O atoms are involved in coordination to the K^+ ions, whose coordination sphere is completed by five or six water molecules, with K-O distances varying between 2.73(1) and 3.16(1) Å. Overall, the hydrated potassium ions fill the voids between the hexameric methylstannoxyl carbonate ions $[MeSn(O)CO_3]_6^{6-}$ in the crystal lattice.

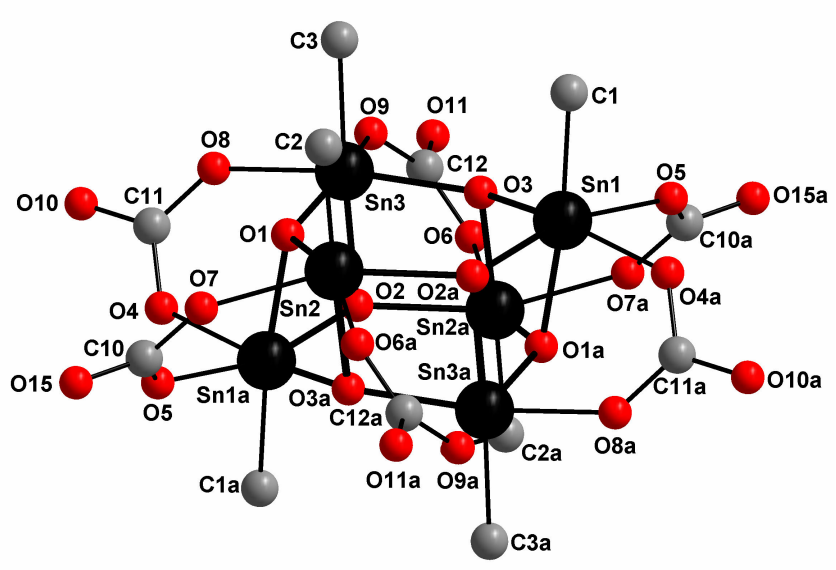

Figure 27: Molecular structure of **9** $K_6[MeSn(O)CO_3]_6 \cdot 14H_2O$ (**7**). Selected bond lengths (Å) and angles (º): Sn1-O1a 2.091(8), Sn1a-O2 2.110(7), Sn1a-O3a 2.110(8), Sn1a-O4 2.167(8), Sn1-O5 2.129(6), Sn1-C1 2.11(1), Sn2-O1 2.093(7), Sn2-O2 2.121(7), Sn2-O3a 2.079(7), Sn2-O6a 2.106(7), Sn2-O7 2.140(8), Sn2-C2 2.12(1), Sn3-O1 2.111(7), Sn3-O2 2.096(8), Sn3-O3 2.104(7), Sn3-O8 2.107(9), Sn3-O9 2.122(7), Sn3-C3 2.10(1), C10-O5 1.30(1), C10-O7 1.32(2), C10-O15 1.25(1), C11a-O4a 1.32(2), C11-O8 1.28(2), C11-O10 1.24(2), C12-O6 1.29(1), C12-O9 1.30(1), C12-O11 1.24(1).

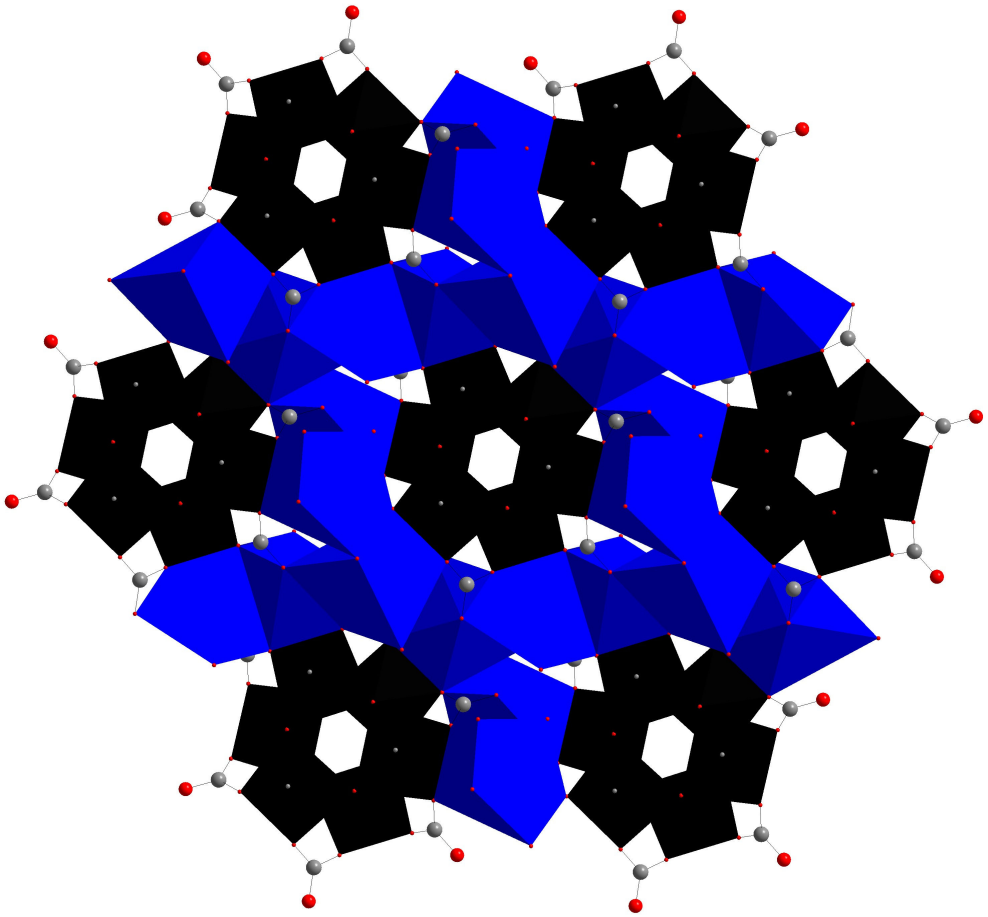

Figure 28: Perspective view on the crystal structure of $K_6[MeSn(O)CO_3]_6 \cdot 14H_2O$ (**7**). The polyhedra of the metals are drawn in black (Sn) and blue (K).

The ^{119}Sn MAS NMR of the amorphous methylstannonic acid $[MeSn(O)OH]_n$ (**6**) prepared from **7** by the published procedure[73] shows two signals at δ_{iso} = –448 and –470 of approximately the same intensity. Both chemical shifts are indicative for hexacoordinated Sn atoms. By contrast, for commercially available butylstannonic acid $[BuSn(O)OH]_n$, ^{119}Sn MAS NMR spectroscopy revealed approximately 80% hexacoordinated Sn and 20% pentacoordinated Sn atoms.[74] For the related well-defined dodecanuclear cluster $[(BuSn)_{12}O_{14}(OH)_6](OH)_2 \cdot 4i$PrOH ^{119}Sn MAS NMR spectroscopy independently confirmed the presence of 50% hexacoordinated Sn and 50% pentacoordinated Sn atoms.[75] While the precise structure of methylstannonic acid $[MeSn(O)OH]_n$ (**6**) remains elusive, pentacoordinated Sn atoms or a local symmetry similar to those of the well-established Sn_{12} oxo cluster family[76] can be clearly ruled out.

3.1.4. *m*-Terphenylstannoxane phosphinate

Previously known polymeric organostannonic acids containing small organic groups undergo condensation reactions with phosphinic and phosphonic acids to give well-defined multinuclear organostannoxane clusters, the chemistry of which has been comprehensively reviewed.[77] Reaction of **3** with $Ph_2P(O)OH$ provided the novel dinuclear cluster $[2,6\text{-}Mes_2C_6H_3Sn(OH)_2(O_2PPh_2)]_2$ (**8**) as a colourless crystalline solid in high yield (Scheme 10).

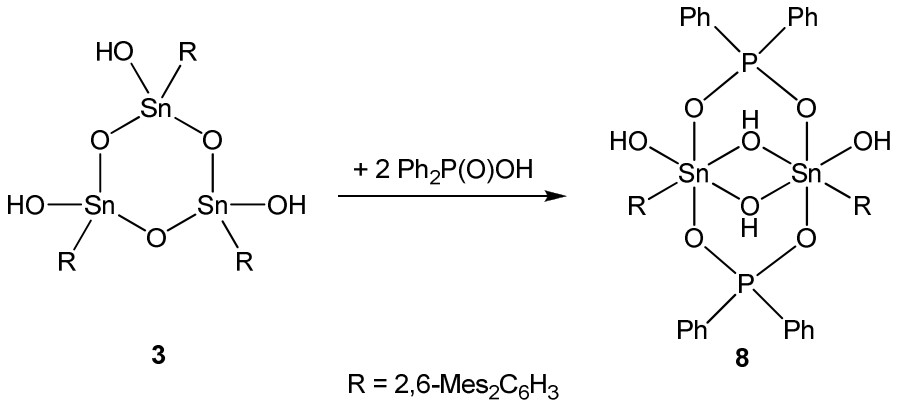

Scheme 10: Synthesis of $[2,6\text{-}Mes_2C_6H_3Sn(OH)_2(O_2PPh_2)]_2$ (**8**).

The compound $[2,6\text{-}Mes_2C_6H_3Sn(OH)_2(O_2PPh_2)]_2$ (**8**) is somewhat reminiscent of the so-called butterfly structure reported for $BuSn(OH)(O_2P\textit{c}Hex_2)_2]_2$, which was obtained by the condensation reaction of $[BuSn(O)OH]_n$ with $\textit{c}Hex_2P(O)OH$.[78] The centrosymmetric four-membered Sn_2O_2 ring possesses one crystallographically independent Sn atom situated in an octahedral environment, despite the presence of the bulky *m*-terphenyl substituent (Figure 29). The structure of **8** comprises two types of hydroxy groups, both of which are not involved in hydrogen bonding. In agreement with this, the IR spectrum of **8** shows two sharp absorptions at $\tilde{\nu}$ = 3634 and 3574 cm^{-1} that were assigned to OH stretching vibrations. The ^{119}Sn MAS NMR spectrum shows one signal at δ_{iso} = –582, which is indicative for hexacoordinated Sn atoms. Compound **8** is only sparingly soluble in most solvents, but was reasonably soluble in chloroform. The solution state ^{119}Sn NMR spectrum of **8** ($CDCl_3$) exhibits a signal at δ = –449.2, which is consistent with pentacoordinated Sn atoms.

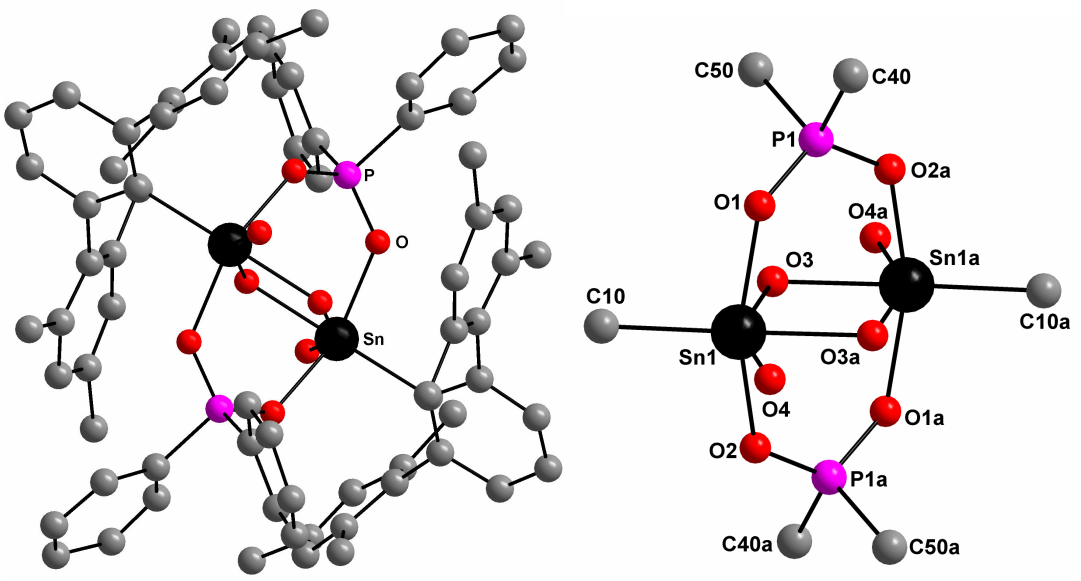

Figure 29: Molecular structure and inorganic core of $[2,6\text{-}Mes_2C_6H_3Sn(OH)_2(O_2PPh_2)]_2$ (**8**). Selected bond lengths (Å) and angles (°): Sn1-O1 2.147(4), Sn1-O2 2.142(4), Sn1-O3 2.071(4), Sn1-O3a 2.162(4), Sn1-O4 2.069(5), Sn1-C10 2.199(5), P1-O1 1.518(4), P1-O2a 1.526(4), P1-C40 1.798(6), O2-Sn1-O3a 80.1(2), O2-Sn1-O4 94.3(2), O3-Sn1-O3a 72.3(2), O3-Sn1-O4 151.2(2), O3a-Sn1-O4 79.0(2), O1-Sn1-C10 97.2(2), O2-Sn1-C10 99.3(2), (Symmetry code: a = 1–x, 2–y, 2–z).

The change of the coordination number is most likely caused by the partial dissociation of the diphenylphoshinate moiety associated with a P=O→Sn bond cleavage and which gives rise to the isomer **8a** (Scheme 11). The driving force for the P=O→Sn bond cleavage might be the competitive formation of P=O···H-CCl_3 hydrogen bonds in solution. Recent ab initio calculations have shown that one of these hydrogen bonds accounts for an energy gain of about 5-6 kcal·mol^{-1}.[79] The ^{31}P NMR spectrum of **8** ($CDCl_3$) shows one signal at δ = 30.0, which is only slightly shifted compared with the value of the parent compound $Ph_2P(O)OH$ (δ = 33.9).

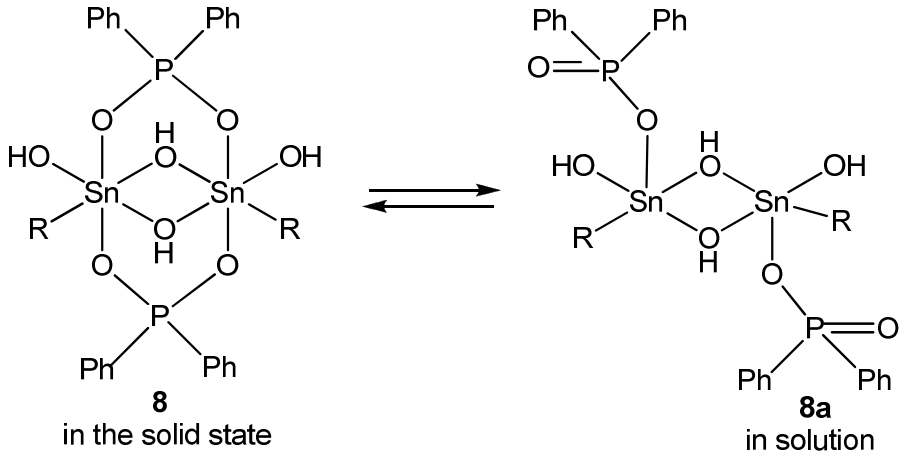

Scheme 11: Reversible change of coordination number in **8/8a**.

3.1.5. Sodium *m*-terphenylstannoxylate

Unlike previously known organostannonic acids, such as $[MeSn(O)OH]_n$,[20,80] compound **3** is virtually insoluble in aqueous NaOH solution and no reaction was observed when a toluene solution of **3** was treated with aqueous or solid NaOH. The reaction of **3** with a stoichiometric amount of NaH suspended in THF proceeds with H_2 evolution and afforded the novel tetranuclear sodium *m*-terphenylstannoxylate cluster $Na_3(2,6\text{-}Mes_2C_6H_3Sn)_4O_6(OH)_3$ (**9**) as a colorless crystalline solid in good yields (Scheme 12).

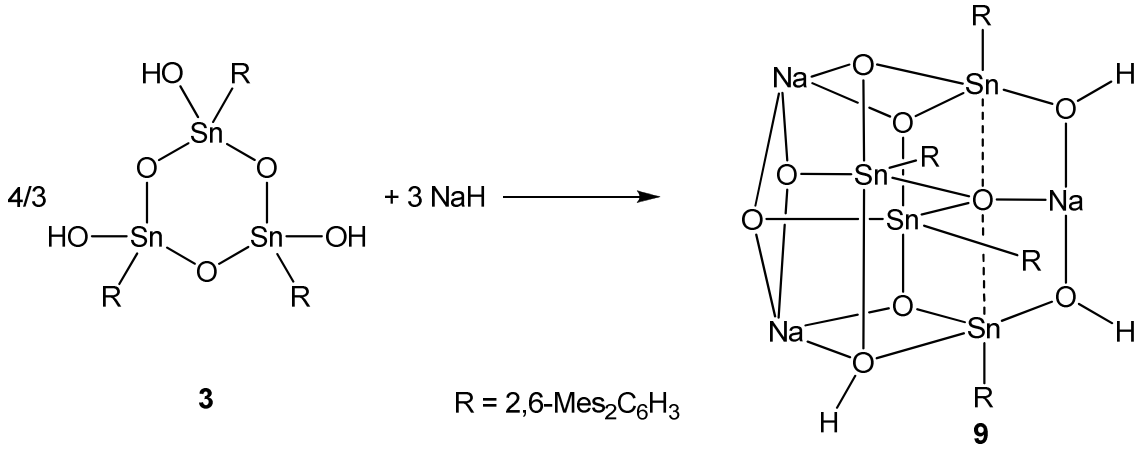

Scheme 12: Synthesis of $Na_3(2,6\text{-}Mes_2C_6H_3Sn)_4O_6(OH)_3$ (**9**).

Besides the dodecanuclear organostannoxane cation $[Na(i\text{PrSn})_{12}O_4(OH)_{24}]^{5+}$, compound **9** is only the second alkali organostannoxane cluster.[81] The molecular structure and selected bond parameters are shown in Figure 30. The centrosymmetric structure contains four pentacoordinated Sn atoms, two of which are crystallographically independent. Of the three Na atoms, two are crystallographically independent. Each Na atom is coordinated by three O atoms. In addition, the Na1 and Na2 atoms are involved in π interactions with one and two mesityl groups of the *m*-terphenyl substituent, respectively, as indicated by the bond distances Na1-C52 to C55 (3.030(8), 2.632(8), 2.522(8), and 2.843(9) Å) and Na2-C34 to C35 (2.812(6) and 3.089(6) Å). The key feature of the structure is the μ_5-O3 atom that is situated on an inversion center in a trigonal bipyramidal environment with four Sn atoms and one Na atom. Although cases involving μ_4-O and μ_6-O atoms are quite frequently observed in molecular oxide chemistry amongst the higher coordinated O atoms,[82] μ_5-O atoms are much rarer. Notable examples include $[Li_5Bi_3(\mu_5\text{-}O)_2(\mu_3\text{-}SiMe_3)_2(\mu_3\text{-}$

O*t*Bu)$_2$(μ-O*t*Bu)$_6$], [Mn$_8$Sb$_4$(μ_5-O)$_4$(μ_3-OEt)$_4$(μ-OEt)$_{16}$], and [(CpY)$_5$(μ_5-O)(μ_3-OMe)$_4$(μ_3-OMe)$_4$].[83]

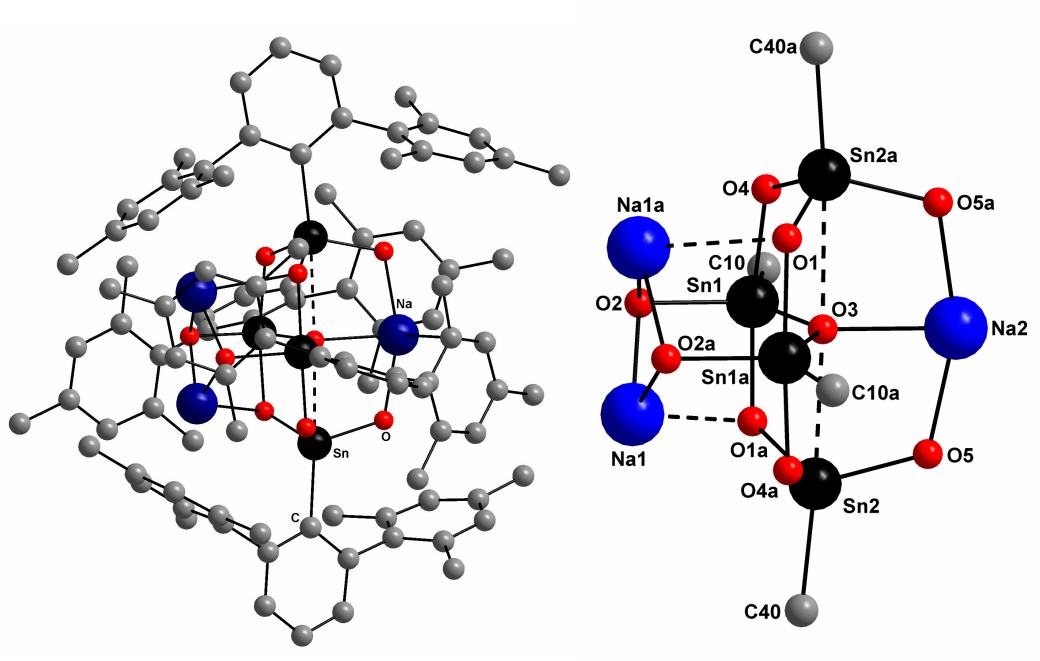

Figure 30: Molecular structure and inorganic core of Na$_3$(2,6-Mes$_2$C$_6$H$_3$Sn)$_4$O$_6$(OH)$_3$ (**9**). Selected bond lengths (Å) and angles (°): Sn1-O1a 2.043(4), Sn1-O2 1.996(3), Sn1-O3 2.084(2), Sn1a-O3 2.084(2), Sn1-O4 2.039(4), Sn1-C10 2.195(4), Sn2-O1a 1.943(4), Sn2···O3 2.702(3), Na2-O3 2.269(5), Na2-O5 2.283(4), Na2-O5a 2.283(4), O1a-Sn1-O2 91.6(2), O1a-Sn1-O3 83.5(1), O1a-Sn1-O4 166.4(1), O2-Sn1-O3 107.8(2), O2-Sn1-O4 91.3(2), O3-Sn1-O4 83.0(1), O1a-Sn1-C10 96.9(2), O2-Sn1-C10 111.9(2), O3-Sn1-C10 140.3(2), O4-Sn1-C10 94.3(2), (Symmetry code: a = –x, y, 0.5–z).

The IR spectrum of **9** shows absorptions at $\tilde{\nu}$ = 3716, 3595, 3563 cm^{-1}, which are assigned to hydroxy groups not being involved in hydrogen bonding. Although the location of related H atoms could not be established by X-ray diffraction, their positions might be disordered throughout all O atoms of the structure. Consistent with the crystallographic structure, the ^{119}Sn MAS NMR spectrum contains two signals at δ_{iso} = –371.5 and –451.2 in a 1:1 ratio. Once crystallized from the mother liquor, **9** is very poorly soluble in most common organic solvents. However the solubility in $CDCl_3$ was enough to get the ^{1}H NMR spectrum which confirms the presence of two sets of signals for the magnetically inequivalent *m*-terphenyl substituents. Electrospray ionization mass spectrometry (ESI-MS) was used to identify the organotin ions associated with **9** in solution. This MS technique was developed for the detection of (trace amounts of) charged species formed in solution by auto ionization. Neutral species remain unaccounted for as ESI-MS lacks an ionization source. The ESI-MS spectrum (positive mode, cone voltage 50 V) of **9** in MeCN

revealed mass clusters with the expected isotope patterns that were assigned to the organotin cations (R = 2,6-$Mes_2C_6H_3$): $[RSn(OH)_3 + Na]^+$ (507.1), $[RSn(OH)_4 + 2Na]^+$ (547.1), $[R_2Sn(OH)_2 + Na]^+$ (803.3), $[(RSn)_2O_2(OH)_2 + Na]^+$ (953.2), $[(RSn)_2O(OH)_4 + Na]^+$ (971.2), $[(RSn)_2(OH)_6 + Na]^+$ (989.2), $[(RSn)_2O_2(OH)_3 + 2\ Na]^+$ (993.2), $[(RSn)_3O_4(OH) + Na]^+$ (1399.3), $[(RSn)_3O_4(OH)_2 + 2\ Na]^+$ 1439.3), $[(RSn)_3O_4(OH)_3 + 3\ Na]^+$ (1479.3), $[(RSn)_4O_5(OH)_2 + Na]^+$ (1865.4), $[(RSn)_4O_6(OH) + 2\ Na]^+$ (1887.3), $[(RSn)_4O_4(OH)_5 + 2\ Na]^+$ (1923.4), $[(RSn)_4O_5(OH)_4 + 3\ Na]^+$ (1945.3), $[(RSn)_4O_7(OH) + 4\ Na]^+$ (1949.3). A number of smaller aggregates are observed in solution, however, the maximum degree of aggregation is 4 and therefore consistent with the molecular structure of **9**. The ESI-MS spectrum (negative mode, cone voltage 50 V) of **9** in MeCN showed mass clusters with the expected isotope patterns that were assigned to the organotin anions (R = 2,6-$Mes_2C_6H_3$): $[RSnO_2]^-$ (465.1), $[RSnO(OH)_2]^-$ (483.1), $[(RSn)_2O_3(OH)]^-$ (929.2), $[(RSn)_2O_2(OH)_3]^-$ (947.2), $[(RSn)_3O_4(OH)_2]^-$ (1393.3). It is interesting to note that no anions containing Na atoms were observed in the negative-detection mode.

3.2. Synthesis and controlled hydrolysis of *m*-terphenylindium dichloride

The arylindium dichloride (2,6-$Mes_2C_6H_3In)_2(\mu$-$Cl)_2Cl_2$ (**10**)[84] was obtained by the reaction of 2,6-$Mes_2C_6H_3Li$ with $InCl_3$ similar to a procedure already published by Robinson *et al*. (Scheme 13). While these authors used a benzene/toluene mixture for the extraction and isolated the solvate **10**·C_6H_6, the use of aromatic solvents was avoided and a solvent-free crystalline product **10** was obtained.

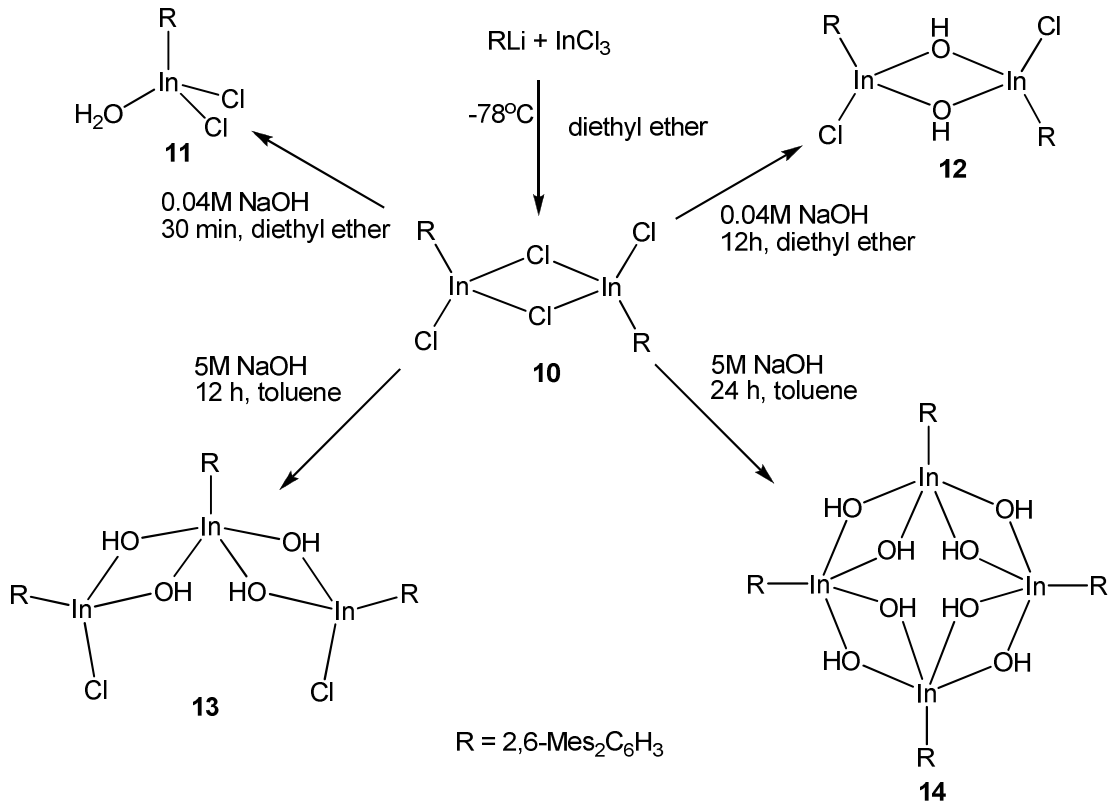

Scheme 13: Synthetic route of *m*-terphenylindium dihydroxide (**14**).

The solvent-free orthorhombic modification of **10** measured at 150 K adopts a four-membered $In_2(\mu\text{-}Cl)_2$ ring structure very similar to that of the monoclinic pseudo polymorph **10**·C_6H_6 measured at room temperature (Figure 31).[84] While the exocylic In-Cl bond lengths are identical within the experimental error (2.346(4) and 2.344(3) Å), the endocylic In-Cl bond lengths are slightly shorter in **10** (2.482(4) and 2.491 Å) than in **10**·C_6H_6 (2.519(2) and 2.514(2) Å).[84] The slightly shorter bond lengths can be attributed to the lower temperature during the X-ray data collection and is not due to the "contamination of the μ-Cl sites by μ-OH groups", as it was discussed for the related $[2,6\text{-}(2',6'\text{-}i\text{Pr}_2C_6H_3)C_6H_3In]_2(\mu\text{-}Cl)_2Cl_2$.[85]

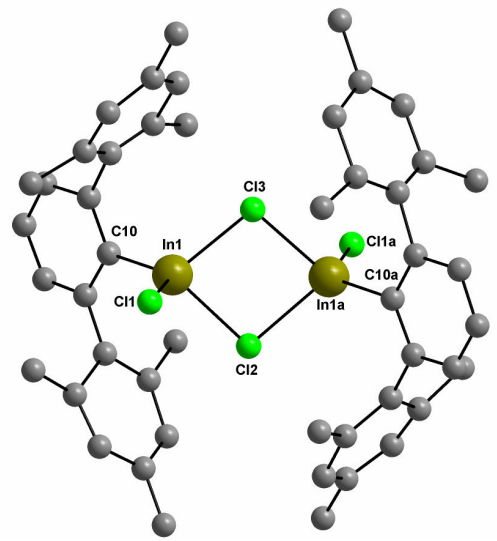

Figure 31: Molecular structure of (2,6-$Mes_2C_6H_3In)_2(\mu$-Cl)$_2Cl_2$ (**10**). Selected bond lengths (Å) and angles (°): In1-Cl1 2.346(4), In1-Cl2 2.482(4), In1-Cl3 2.491(4), In1-C10 2.118(8), Cl1-In1-Cl2 103.7(2), Cl1-In1-Cl3 100.0(2), Cl2-In1-Cl3 85.0(1), Cl1-In1-C10 121.7(3), Cl2-In1-C10 120.9(4), Cl3-In1-C10 118.2(4).

The base hydrolysis of (2,6-$Mes_2C_6H_3In)_2(\mu$-Cl)$_2Cl_2$ (**10**) in a two-layer system of aqueous NaOH/diethyl ether or toluene afforded 2,6-$Mes_2C_6H_3InCl_2\cdot H_2O$ (**11**), (2,6-$Mes_2C_6H_3In)_2(\mu$-OH)$_2Cl_2$ (**12**), (2,6-$Mes_2C_6H_3In)_3(\mu$-OH)$_4Cl_2$ (**13**), and (2,6-$Mes_2C_6H_3In)_4(\mu$-OH)$_8$ (**14**), depending on the reaction conditions (NaOH concentration and reaction time) applied (Scheme 13). Compounds **11**-**14** are isolated in high yields as single crystalline materials and can be distinguished easily by their melting points. The structure of 2,6-$Mes_2C_6H_3InCl_2\cdot H_2O$ (**11**) comprises a simple Lewis acid-base pair (Figure 32).

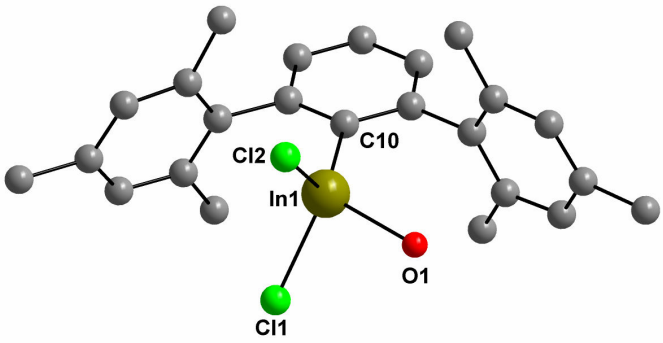

Figure 32: Molecular structure of 2,6-$Mes_2C_6H_3InCl_2\cdot H_2O$ (**11**). Selected bond lengths (Å) and angles (°): In1-O1 2.207(5), In1-Cl1 2.374(2), In1-Cl2 2.408(2), In1-C10 2.130(8), O1-In1-Cl1 91.4(2), O1-In1-Cl2 91.5(2), O1-In1-C10 117.4(3), Cl1-In1-Cl2 109.70(9), Cl1-In1-C10 117.3(2), Cl2-In1-C10 122.5(2).

The spatial arrangement of the In atom is distorted tetrahedral and defined by a CCl_2O donor set. The In-Cl bond lengths of **11** (2.374(2) and 2.408(2) Å) are somewhat longer than the exocyclic In-Cl bond lengths of **10**, and the In-O bond length of **11** (2.207(5) Å) falls within the range of In-(μ-OH) groups being observed for **12**-**14**. In the crystal lattice, the water molecule is involved in weak hydrogen bonding with chlorine atoms of adjacent molecules (O···Cl 3.173(6) and 3.256(6) Å). The IR spectrum of **11** shows two absorptions at $\tilde{\nu}$ = 3611 and 3587 cm^{-1} that were assigned to OH stretching vibrations.

The molecular structure of (2,6-$Mes_2C_6H_3In)_2(\mu$-$OH)_2Cl_2$ (**12**) consists of a four-membered $In_2(\mu$-$OH)_2$ ring featuring tetrahedral In atoms defined by CO_2Cl donor sets (Figure 33). It is noteworthy that similar four-membered $In_2(\mu$-$OR)_2$ ring structures were also observed in methylindium(III) alkoxides (R = alkyl, aryl).[86]

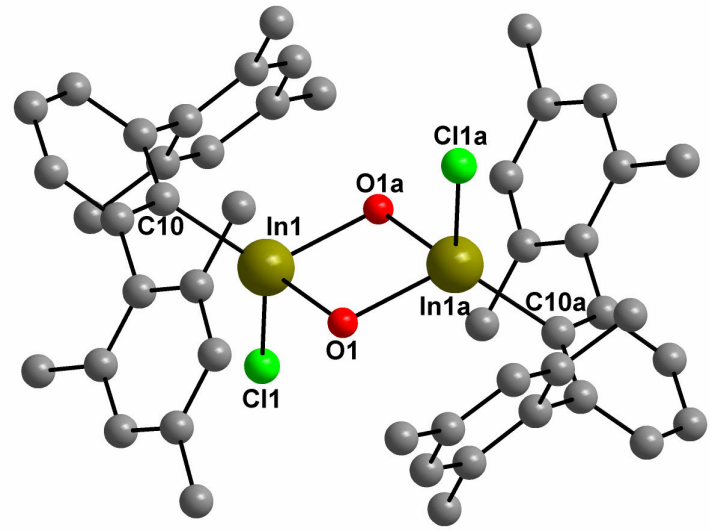

Figure 33: Molecular structure of (2,6-$Mes_2C_6H_3In)_2(\mu$-$OH)_2Cl_2$ (**12**). Selected bond lengths (Å) and angles (°): In1-O1 2.130(3), In1-O1a 2.131(3), In1-Cl1 2.368(2), In1-C10 2.138(4), O1-In1-O1a 76.6(1), O1-In1-Cl1 101.72(9), O1a-In1-Cl1 103.53(9), O1-In1-C10 122.5(2), O1a-In1-C10 120.3(1), C10-In1-Cl1 122.3(1), (Symmetry code: a = –x, –y, –z).

The molecular structure of (2,6-$Mes_2C_6H_3In)_3(\mu$-$OH)_4Cl_2$ (**13**) contains two $In_2(\mu$-$OH)_2$ rings that are linked by a central spirocylic In atom that adopts a square-pyramidal arrangement defined by a set of one C and four O atoms (Figure 34). The spatial arrangement of the two terminal In atoms resembles those of **12**.

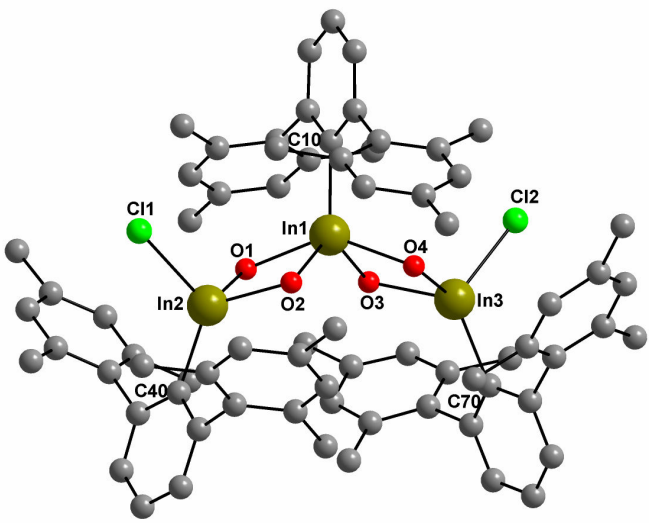

Figure 34: Molecular structure of (2,6-$Mes_2C_6H_3In)_3(\mu$-OH)$_4Cl_2$ (**13**). Selected bond lengths (Å) and angles (°): In1-O1 2.211(5), In1-O2 2.142(6), In1-O3 2.138(4), In1-O4 2.200(5), In1-C10 2.164(6), In2-O1 2.093(6), In2-O2 2.107(5), In2-Cl1 2.455(3), In2-C40 2.122(7), In3-O3 2.1152(5), In3-O4 2.0999(5), In3-Cl2 2.5207(3), In3-C70 2.1420(7), O1-In1-O2 72.5(2), O1-In1-O3 87.0(2), O1-In1-O4 140.2(2), O2-In1-O3 118.7(2), O2-In1-O4 87.3(2), O3-In1-O4 72.9(2), O1-In1-C10 111.1(2), O2-In1-C10 121.9(2), O3-In1-C10 119.5(2), O4-In1-C10 108.7(2), O1-In2-O2 75.6(2), O1-In2-Cl1 104.0(2), O1-In2-C40 124.4(2), O2-In2-Cl1 108.9(2), O2-In2-C40 120.6(3), Cl1-In2-C40 116.3(2), O3-In3-O4 75.4(2), O3-In3-Cl2 105.7(2), O3-In3-C70 121.4(2), O4-In3-Cl2 108.5(2), O4-In3-C70 121.3(2), Cl2-In3-C70 117.1(2), In1-O1-In2 104.6(2), In1-O2-In2 106.5(2), In1-O3-In3 106.0(2), In1-O4-In3 104.4(2).

The structure of (2,6-$Mes_2C_6H_3In)_4(\mu$-OH)$_8$ (**14**) possesses C_2 symmetry and contains four spirocylic In atoms that are involved in four $In_2(\mu$-OH)$_2$ rings, two of which are crystallographically independent (Figure 35). Compound **14** can be regarded as a heavier and aggregated analogue of arylboronic acids. It is worth mentioning that the central $(L_nM)_4(\mu$-O)$_8$ structural motif of **14** is unprecedented in metalloxane chemistry, whereas similar motifs, such as $(L_nM)_3(\mu$-O)$_6$ and $(L_nM)_6(\mu$-O)$_{12}$, are already known.[87]

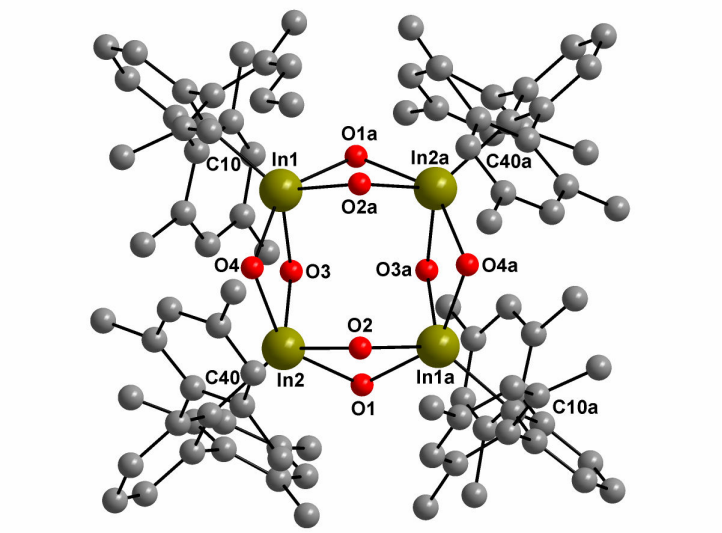

Figure 35: Molecular structure of $(2,6\text{-}Mes_2C_6H_3In)_4(\mu\text{-}OH)_8$ (**14**). Selected bond lengths (Å) and angles (°): In1-O1a 2.189(3), In1-O2a 2.137(3), In1-O3 2.163(3), In1-O4 2.190(3), In2-O1 2.198(3), In1-C10 2.198(5), In2-O2 2.141(3), In2-O3 2.136(3), In2-O4 2.224(3), In2a-O1a 2.198(3), In2a-O2a 2.141(3), In2-C40 2.192(4), O1a-In1-O2a 71.5(1), O1a-In1-O3 84.0(1), O1a-In1-O4 142.6(1), O2a-In1-O3 106.9(1), O2a-In1-O4 87.8(1), O3-In1-O4 72.3(1), O1a-In1-C10 108.7(2), O2a-In1-C10 127.0(2), O3-In1-C10 126.1(2), O4-In1-C10 108.6(2), O1-In2-O2 71.3(1), O1-In2-O3 86.1(1), O1-In2-O4 142.1(1), O2-In2-O3 107.4(1), O2-In2-O4 85.8(1), O3-In2-O4 72.2(1), O1-In2-C40 110.4(2), O2-In2-C40 125.2(2), O3-In2-C40 127.4(2), O4-In2-C40 107.4(2), In1a-O1a-In2a 102.1(1), In1a-O2a-In2a 105.8(1), In1-O3-In2 108.5(1), In1-O4-In2 104.4(1).

The In-O bond lengths of **12**-**14** vary within the range 2.093(6) to 2.224(3) Å (average 2.159(6) Å). None of the hydroxy groups of **12**-**14** are involved in hydrogen bonding. This is confirmed by the IR spectra, which show absorptions at $\tilde{\nu}$ = 3617 and 3534 cm^{-1} (**12**), 3633, 3598, 3568, 3529, and 3484 cm^{-1} (**13**), and 3646, 3632, and 3599 cm^{-1} (**14**), respectively, which were assigned to OH stretching vibrations. The endocyclic In-Cl bond lengths of **13** (2.455(3) and 2.5207(3) Å) are somewhat longer than the related values of **10** and **12**. In light of established molecular structures and bond parameters, the hypothesis of Twamley and Power is supported that the crystal of $[2,6\text{-}(2',6'\text{-}i\text{Pr}_2C_6H_3)C_6H_3In]_2(\mu\text{-}Cl)_2Cl_2$ originally investigated by Robinson *et al*. was in fact a mixture of the related hydrolysis products $[2,6\text{-}(2',6'\text{-}i\text{Pr}_2C_6H_3)C_6H_3In]_2(\mu\text{-}OH)_2Cl_2$ and $[2,6\text{-}(2',6'\text{-}i\text{PrC}_6H_3)C_6H_3In]_2(\mu\text{-}OH)_2(OH)_2$.[85] It is interesting to compare the (average) In···In separation, which is significantly larger in the chlorine bridged compounds **10** (3.896(9) Å) and $[2,6\text{-}(2',6'\text{-}i\text{Pr}_2C_6H_3)C_6H_3In]_2(\mu\text{-}Cl)_2Cl$ (3.7765(4) Å)[85] than in the hydroxy bridged compounds **12** (3.345(1) Å), **13** (3.401(2) Å), and **14** (3.350(2) Å). Notably, the latter values are also in good agreement with the In···In separation observed in the mixture of $[2,6\text{-}(2',6'\text{-}i\text{Pr}_2C_6H_3)C_6H_3In]_2(\mu\text{-}OH)_2Cl_2$ and $[2,6\text{-}(2',6'\text{-}i\text{Pr}_2C_6H_3)C_6H_3In]_2(\mu\text{-}OH)_2(OH)_2$ (3.38(2) Å)[85] and the four-membered

asymmetric indoxane ring [2,6-(2′,6′-*i*Pr$_2$C$_6$H$_3$)C$_6$H$_3$In(*μ*-O)]$_2$ (3.598 Å).[44] Compounds **10**-**14** are readily soluble in most organic solvents. The ^{1}H and ^{13}C NMR spectra show one (**10, 11, 12, 14**) and two sets (**13**) of signals for the *m*-terphenyl substituents.

3.2.1. *m*-Terphenylindoxane phosphinates

The chemistry of group 13 element phosphinates dating back to the pioneering work of Coates and Mukherjee in 1964[88] was comprehensively reviewed more than 10 years ago.[89] Amongst the very few indium phosphinates known, the most notable are the eight-membered heterocycles (R′$_2$InO$_2$PR$_2$)$_2$. These were obtained by the reaction of the phosphinic acids R$_2$PO$_2$H with the indium trialkyls R′$_3$In (R′ = Me, Et; R = Me, Ph).[88,90,91] The compound (Me$_2$InO$_2$PPh$_2$)$_2$, also obtained by the oxidation of (Me$_2$InPPh$_2$)$_2$ with pyridine oxide, was hydrolyzed in the presence of pyridine (py) to give the unique tetrameric heterocubane cluster [MeIn(OH)(O$_2$PPh$_2$)]$_4$·4py.[91]

The reactions of [2,6-Mes$_2$C$_6$H$_3$In(OH)$_2$]$_4$ (**14**) with dimethylphosphinic acid, diphenylphosphinic acid and 2,2,3,4,4-pentamethylphosphetanic acid,[92] give rise to the formation of the arylindium phosphinates [(2,6-Mes$_2$C$_6$H$_3$In)$_2$(OH)$_2$(O$_2$PMe$_2$)$_2$] (**15**), [(2,6-Mes$_2$C$_6$H$_3$In)$_2$(OH)(O$_2$PPh$_2$)$_3$] (**16**) and [(2,6-Mes$_2$C$_6$H$_3$In)(O$_2$PC$_3$HMe$_5$)$_2$(H$_2$O)$_2$] (**17**) as sole products regardless of the stoichiometric ratio of the reactants applied (Scheme 14). The In to P ratio is observed to be 1:1, 1:1.5, and 1:2 in the three cluster compounds respectively. The In center is found to be pentacoordinated in all the three compounds. The phosphinate group behaves as a bidentate bridge in **15** and **16** through the two O atoms leading to eight membered In$_2$P$_2$O$_4$ type central ring core structures.

The ^{31}P NMR spectra ($CDCl_3$) of **15**-**17** reveal signals at δ = 40.5 for **15**, 31.8, 28.0 (integral ratio 1:2) for **16** and 49.4 for **17**, which shifted significantly from those of the phosphinic acids Me$_2$P(O)OH (54.1) , Ph$_2$P(O)OH (38.7) and Me$_5$C$_3$HP(O)OH (60.2), respectively. The IR spectra of **15**-**17** show absorptions at $\tilde{\nu}$ = 3624 cm^{-1} for **15**, 3587 cm^{-1} for **16** and 3626 cm^{-1} for **17** that are indicative of OH stretching vibrations.

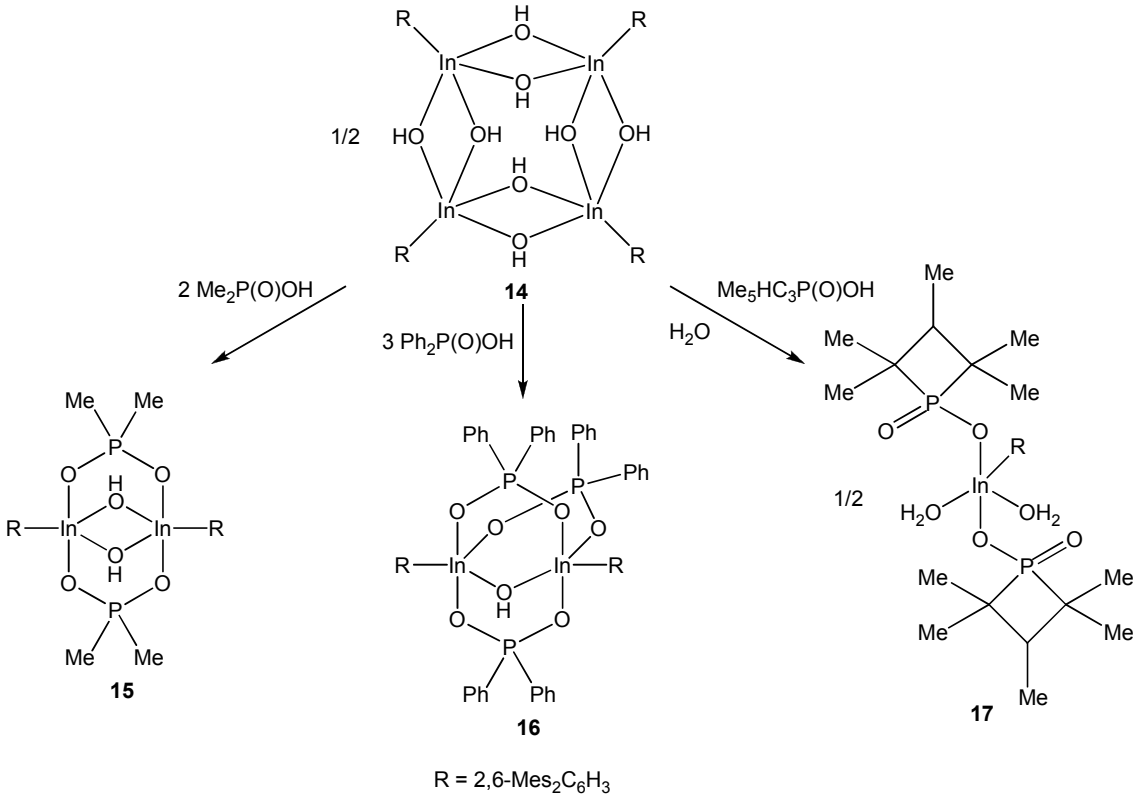

Scheme 14: Reaction of **14** with dimethylphosphinic acid, diphenylphosphinic acid and 2,2,3,4,4-pentamethylphosphetanic acid.

The core structure of **15** consists of two planar rings perpendicular to each other (Figure 36). An eight-membered $In_2P_2O_4$ ring and another four membered $In_2(\mu\text{-}OH)_2$ ring perpendicular to the $In_2P_2O_4$ plane. The P-O bond lengths are almost identical (1.504(2) and 1.478(2) Å) suggesting an equal charge distribution for O2 and O3. The In-O-In linkage is symmetric attributed by the identical In-(μ-OH) bond lengths (2.124(8) and 2.145(7) Å). The central cavity possessing the two ring systems is well protected by the two *m*-terphenyl substituents because of the less sterically demanding methyl moieties on the phosphinic group.

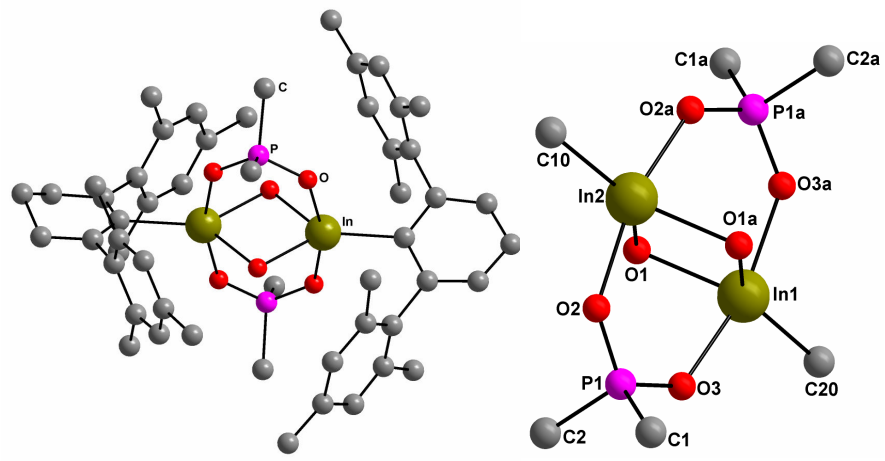

Figure 36: Molecular structure and inorganic core of $[(2,6\text{-}Mes_2C_6H_3In)_2(\mu\text{-}OH)_2(O_2PMe_2)_2]$ (**15**). Selected bond lengths [Å]: In1-O1 2.104(8), In1-O1a 2.104(8), In1-O3a 2.16(1), In2-O2a 2.16(1), In1-C20 2.134(3), In2-O1 2.145(7), In2-O2 2.145(7), In1-O3 2.14(1), In1-O3a 2.14(1), In2 -C10 2.14(2), P1-O2 1.51(2), P1-O3 1.48(2), P1-C1 1.75(2), P1-C2 1.79(2).

In comparison to **15**, the central core structure of **16** is also represented by two ring structures perpendicular to each other (Figure 37). The molecule possess an $In_2P_2O_4$ type ring analogous to **15**. Another In_2PO_3 type planar ring where the Indium atoms are connected through a bidentate phosphinate group and a μ-OH group completes the coordination sphere by bonding to the two In atoms.

^{31}P NMR ($CDCl_3$) spectrum of **16** displays two chemical shifts at 31.8 and 28.0 with the intensities in the ratio of 1:2 showing the presence of two different environments around the P atoms.

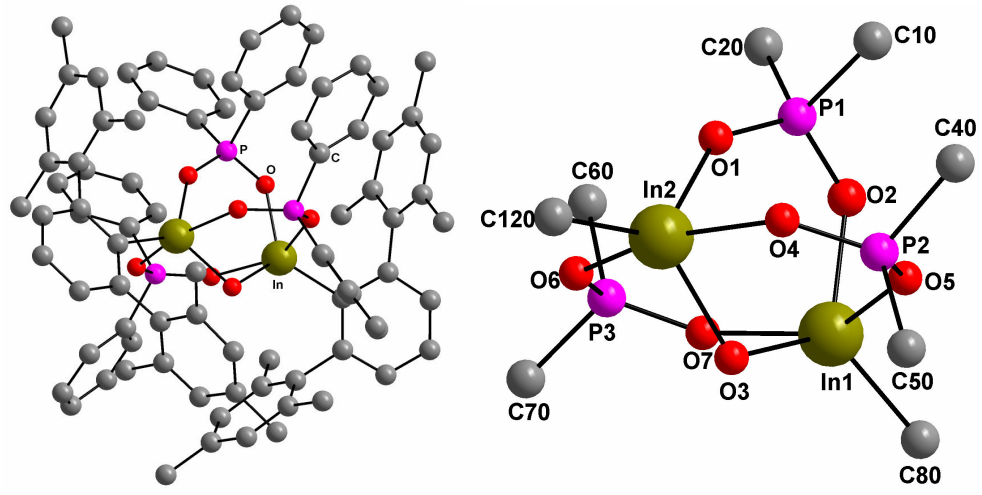

Figure 37: Molecular structure and inorganic core of $[(2,6\text{-}Mes_2C_6H_3In)_2(OH)(O_2PPh_2)_3]$ (**16**). Selected bond lengths (Å): In1-O2 2.121(4), In1-O3 2.140(3), In1-O5 2.207(4), In1-O7 2.247(4), In1-C80 2.137(6), In2-O1 2.118(3), In2-O3 2.121(4), In2-O4 2.197(4), In2-O6 2.232(4), In2-C120 2.167(5), P1-O1 1.521(3), P1-O2 1.499(4), P1-C10 1.800(6), P1-

C20 1.793(5), P2-O4 1.510(4), P2-O5 1.514(4), P2-C40 1.795(7), P2-C50 1.805(6), P3-O6 1.521(4), P3-O7 1.500(4), P3-C60 1.801(7), P3-C70 1.798(6).

The core structure of **17** is represented by a pentacoordinated In atom with distorted trigonal bipyramidal geometry (Figure 38), as observed in **15** and **16**. The coordination sphere around In is completed by two axial O atoms of the phosphinate groups, and two equatorially associated water molecules and a C of the *m*-terphenyl substituent.

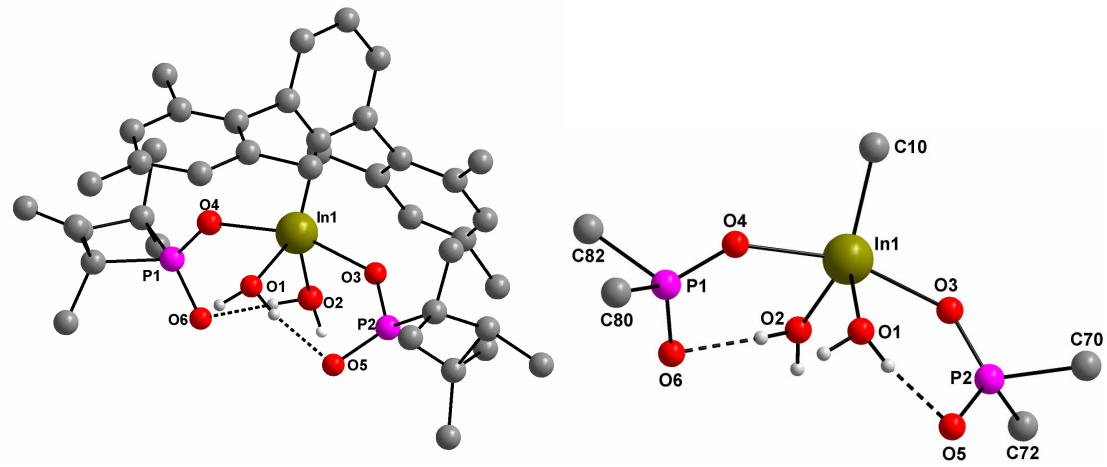

Figure 38: Molecular structure and inorganic core of [(2,6-$Mes_2C_6H_3In$)($O_2PMe_5C_3H$)$_2$ (H_2O)$_2$] (**17**). Selected bond lengths (Å): In1-O1 2.121(5), In1-O2 2.126(5), In1-O3 2.225(4), In1-O4 2.240(4), In1-C10 2.141(6), P1-O4 1.508(4), P1-O6 1.529(5), P1-C80 1.831(7), P1-C82 1.842(7), P2-O3 1.509(4), P2-O5 1.511(5), P2-C70 1.858(7), P2-C72 1.834(8), O1···O5 2.647(6), O2···O6 2.659(7).

The phosphinate group acts as a monodentate ligand towards the In center through an In-O-P type bond. Intramolecular hydrogen bonding is observed between an O atom of the phosphinate group and the water molecule bonded to the In center. In this regard **17** differ from **15** and **16** in that the molecule does not show an In_2O_2P type moiety. The O···O bond distance (2.647(6) and 2.659(7) Å) fall in the range of medium strength hydrogen bonding. The In-O bond length of the coordinated water molecules for **17** (2.121(5) and 2.126(5) Å) are comparatively shorter compared with that in **11** (2.207(5) Å).

3.2.2 Stannaindoxanes

Oxides of zinc, cadmium, indium and tin are well known for their unique combination of visible transparency and excellent *n*-type electrical conductivity. These materials are referred to as 'transparent conducting oxides' or TCOs, and find applications as low-emissivity coatings for windows and as transparent conductors in solar cells, flat panel displays, organic light-emitting diodes, etc. Among these indium-tin oxide (ITO) are the most commercially utilized TCOs.[93] Shannon *et al*. did the preliminary work on bulk TCOs.[94] There have been ongoing efforts to understand the fundamental structural and chemical factors underlying their transparent conductivity.[93] However, the number of crystallographically studied In-O-Sn clusters is limited. $In(OtBu)_3Sn$ was reported by Veith *et al*. and was further treated with $Cr(CO)_6$ and $Mo(CO)_6$ to give the diadducts $[(CO)_5MSn(OtBu)_3InM(CO)_5]$, (M = Cr, Mo).[95] The same group later also reported on the synthesis of two more related structures $Cl_2In(OtBu)_3Sn\cdot THF$ and $Br_2In(OtBu)_3Sn\cdot THF$.[96]

The treatment of 2,6-$Mes_2C_6H_3InCl_2$ with $(tBu_2SnO)_3$ resulted in (2,6-$Mes_2C_6H_3In$)$(tBu_2Sn)_2O(OH)_2Cl_2$ (**18**), a mixed indium-tin oxide cluster in high yield (Scheme 15).

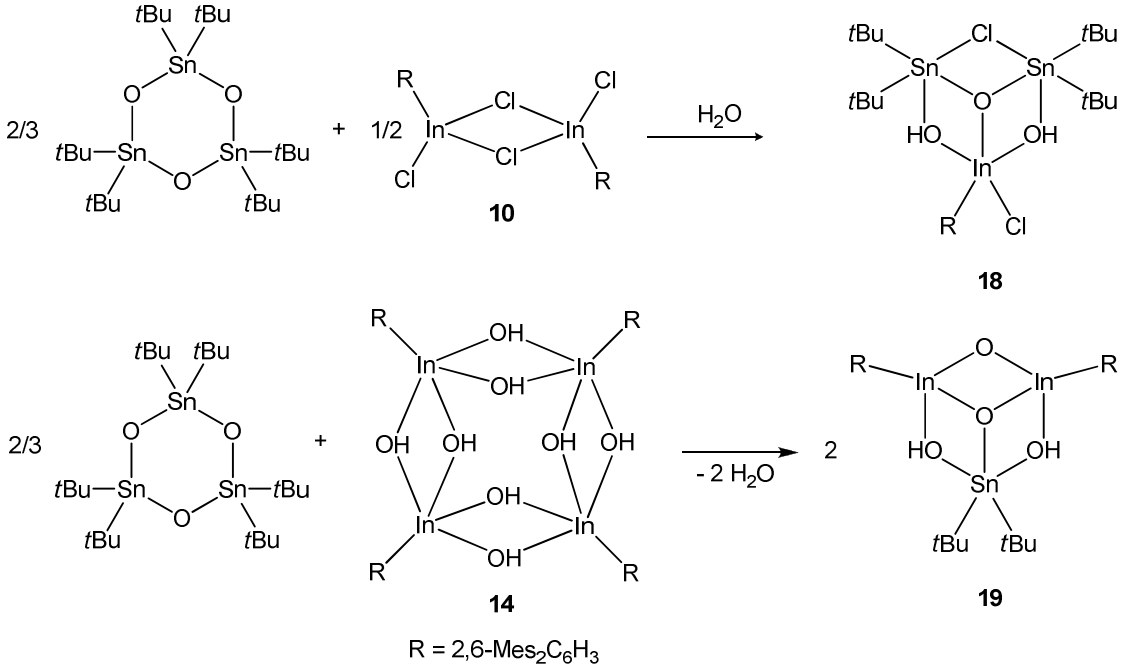

Scheme 15: Treatment of **10** and **14** with $(tBu_2SnO)_3$.

The atomic ratio of In:Sn in **18** is 1:2. Both tin atoms and the indium atom are pentacoordinated with distorted trigonal bipyramidal geometries with the C atom, the Cl and O at the equatorial positions and the two hydroxy groups at the equatorial positions. ^{119}Sn NMR reveals a single shift at δ = –202 suggesting a penta-coordinated environment for the Sn atoms. The ^{1}H NMR spectrum reveals two shifts for *t*butyl protons. An interesting feature of the structure is the breaking of an In-Cl bond and a Cl atom being shared by the two Sn atoms (Figure 39).

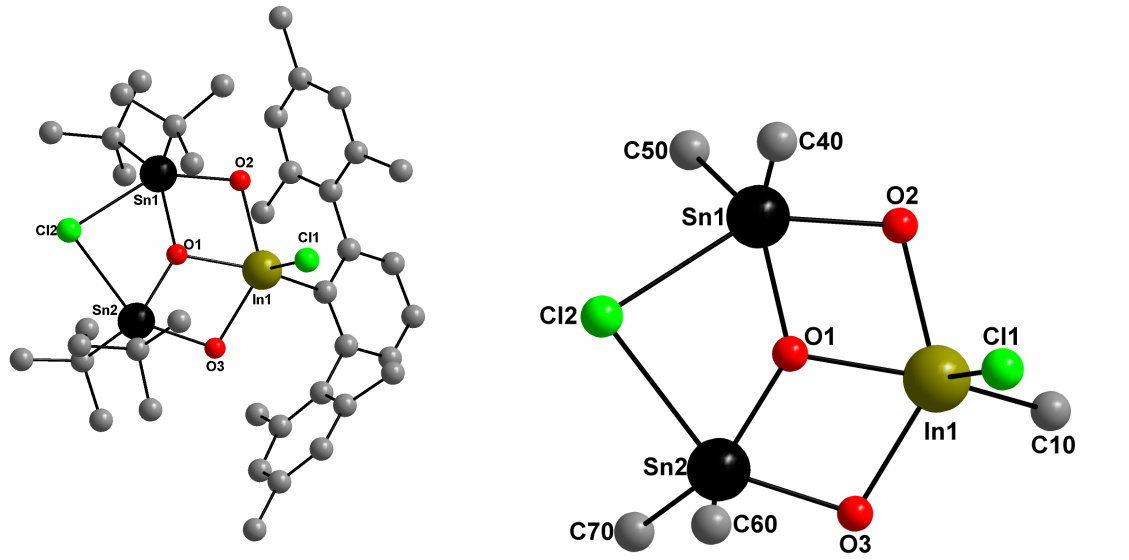

Figure 39: Molecular structure and inorganic core of (2,6-$Mes_2C_6H_3In$)(*t*Bu_2Sn)$_2$O$(OH)_2Cl_2$ (**18**). Selected bond lengths (Å): In1-O1 2.131(5), In1-O2 2.233(5), In1-O3 2.252(5), In1-Cl1 2.417(3), In1-C10 2.204(8), Sn1-O1 1.996(5), Sn1-O2 2.103(5), Sn1-Cl2 2.756(3), Sn1-C40 2.180(9), Sn1-C50 2.18(1), Sn2-O1 1.990(5), Sn2-O3 2.094(6), Sn2-Cl2 2.765(3), Sn2-C60 2.172(9), Sn2-C70 2.188(9).

An attempt to synthesize a halogen free In-O-Sn type cluster by treating **14** with (*t*$Bu_2SnO)_3$ resulted in (2,6-$Mes_2C_6H_3In)_2$(*t*$Bu_2Sn)O(OH)_2$ (**19**) in the ratio of In:Sn 2:1. The compound **19** is characterized by multinuclear NMR, FT-IR and elemental analysis. In contrast to **18**, just a single shift for protons belonging to *t*butyl groups is observed for **19**. The recrystallization of the bulk compound **19** in $CHCl_3$/hexane at air revealed in X-ray analysis the formation of a new bicarbonate cluster (2,6-$Mes_2C_6H_3In)_3(HCO_3)_2(OH)_4$ (**20**). The compound **20** is produced during the process of crystallization by taking up of atmospheric CO_2 and possible splitting of In-O-Sn bond. A deliberate attempt to synthesize **20** by passing CO_2 through a solution of **14** in chloroform resulted in **20** with high yield (Scheme 16).

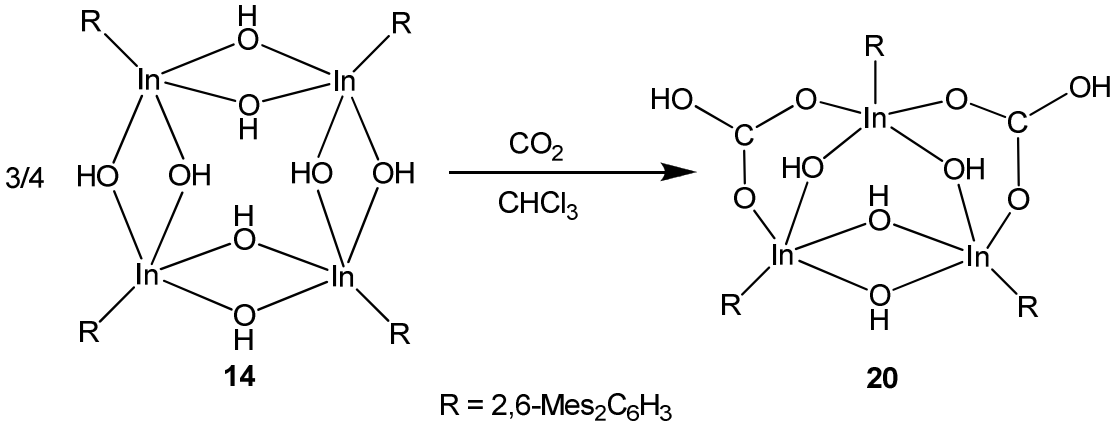

Scheme 16: Treatment of **14** with CO_2 in $CHCl_3$.

Compounds **19** and **20** are distinguished from each other on the basis of IR. A sharp signal for OH at 3630 cm^{-1} with two shoulder signals at 3646 and 3586 cm^{-1} are observed for **19** whereas two sharp OH shifts of equal intensity at 3570 and 3636 cm^{-1} are observed for **20**. ^{13}C NMR shows a characteristic shift for bicarbonate moiety **20** at δ = 176 which is otherwise absent for the bulk compound **19**. The ^{119}Sn NMR ($CDCl_3$) shift is observed at δ = –278 for **19** suggesting a pentacoordinated Sn center.

The molecular structure for **20** reveals all the three In atoms to be pentacoordinated (Figure 40). The three In atoms have two different environments in the molecular structure that are retained in the solution state, as revealed by the solution NMR. In ^1H NMR ($CDCl_3$) two sets of signals are observed for the *m*-terphenyl substituents in the ratio of 1:2 illustrating two environments around the In atoms. Characteristic feature of the crystal structure is a $In_2(\mu\text{-}OH)_2$ type ring linking In1 and In2. The three C-O bond lengths of the bicarbonate group are unequal, a longer C-O bond (1.541(9) Å, represents the OH group of the bicarbonate moiety) compared to the other two C-O bonds of the bicarbonate group (1.237(7) and 1.260(7) Å).

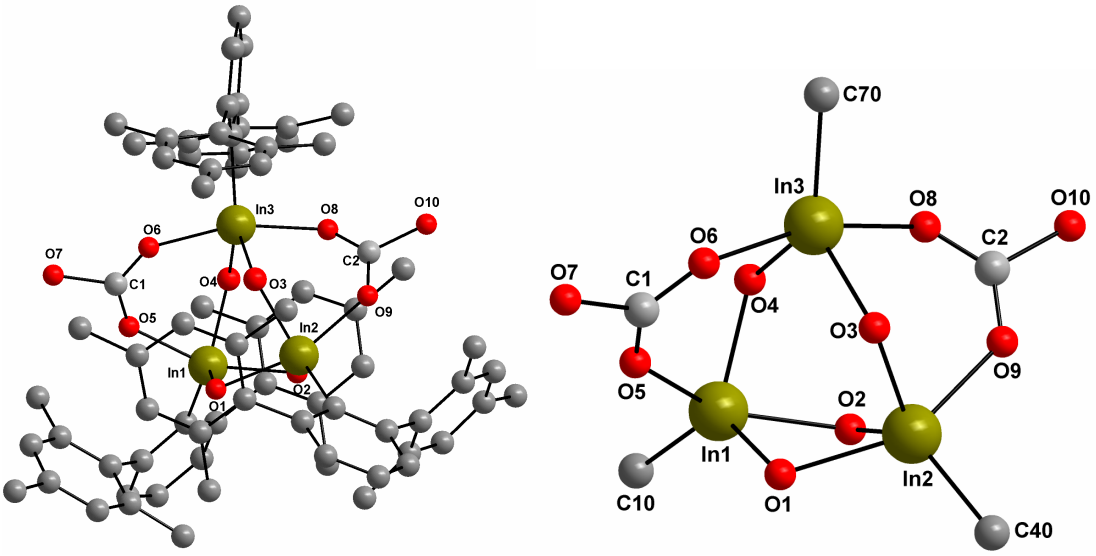

Figure 40: Molecular structure and inorganic core of $(2,6\text{-}Mes_2C_6H_3In)_3(HCO_3)_2(OH)_4$ (**20**). Selected bond lengths (Å): In1-O1 2.097(4), In1-O2 2.203(4), In1-O4 2.167(4), In1-O5 2.206(5), In1-C10 2.155(5), In2-O1 2.217(4), In2-O2 2.097(4), In2-O3 2.132(4), In2-O9 2.222(4), In2-C40 2.151(6), In3-O3 2.121(5), In3-O4 2.104(4), In3-O6 2.216(4), In3-O8 2.248(4), In3-C70 2.145(6), C1-O5 1.237(7), C1-O6 1.260(7), C1-O7 1.541(9), C2-O9 1.250(7), C2-O8 1.265(7), C2-O10 1.549(8).

Each of the In atoms have the C atom of the *m*-terphenyl group and the hydroxy groups at the equatorial positions whereas one In is bonded to two O atoms of the bicarbonate groups at the axial positions and the other two In atoms with one O atom and a μ-OH group at the axial positions.

3.2.3. *m*-Terphenylindoxane carbonates

The reactivity of stannonic acid **3** towards CO_2 has already been discussed in detail (synthesis of stannoxane carbonate **5**, Scheme 7). The motivation behind the investigation of the behaviour of the *m*-terphenylindium dihydroxide (**14**) towards CO_2 was the results obtained by treating the stannonic acid **3** with CO_2.

Synthesis of dimethyl carbonate (DMC) from CO_2 is of importance for a number of reasons. CO_2 is a naturally abundant carbon resource and a green house gas. DMC is a non-toxic substitute for dimethyl sulfate and phosgene,[97] which are otherwise toxic and corrosive methylating or carbonylating agents.[98]

Much attention has been given to the synthesis of DMC involving ethylene carbonate or cyclic carbonates as intermediates in the previous years.[99] The alternate method is the oxidative carbonylation or phosgenation of methanol that involves use of poisonous or corrosive gases like phosgene, chlorine, and carbon monooxide.[100]

The objective behind treating **14** with CO_2 and ethylene glycol was the utilization of CO_2 to obtain cyclic ethylene carbonate. The catalytic behaviour of **14** towards recycling of CO_2 was to be determined.

The reaction of **14** with CO_2 and ethylene glycol resulted in the indoxane carbonate cluster $(2,6\text{-}Mes_2C_6H_3In)_4(CO_3)_2(OH)_4(H_2O)_2$ (**21**) and the glycol indoxane cluster $(2,6\text{-}Mes_2C_6H_3In)_4(OCH_2CH_2O)_2(OH)_4$ (**22**), respectively. The successful incorporation of CO_2 and ethylene glycol in the indoxane **14** resulted in the unique cluster $(2,6\text{-}Mes_2C_6H_3In)_4(CO_3)_2(OCH_2CH_2OH)_2(OH)_2$ (**23**) as shown in Scheme 17.

All the three compounds **21**-**23** are tetrameric and have centrosymmetric structures with pentacoordinated indium atoms.

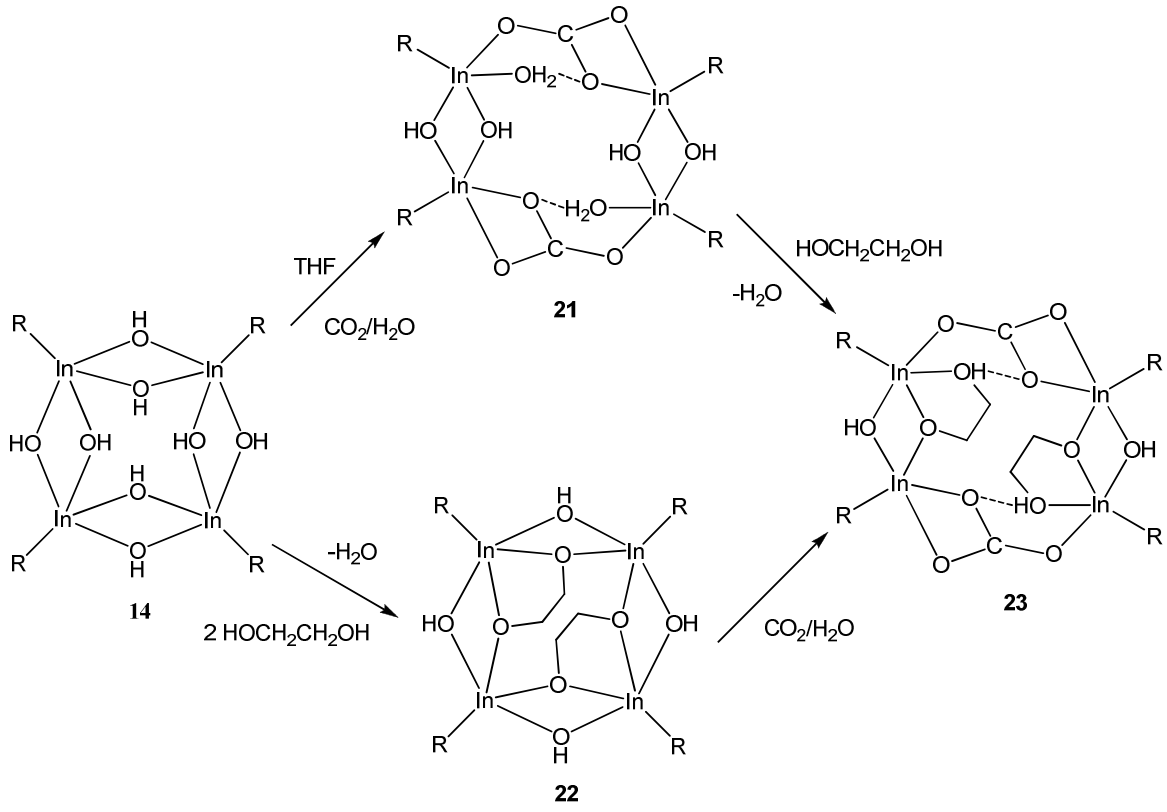

Scheme 17: Synthetic route for $(2,6\text{-}Mes_2C_6H_3In)_4(CO_3)_2(OCH_2CH_2OH)_2(OH)_2$ (**23**).

The treatment of **14** with CO_2 in THF resulted in a dihydrated tetranuclear carbonate cluster **21** obtained as colorless crystals. It is important to note that the same procedure using chloroform produced the bicarbonate cluster **20**.

Subsequent treatment of **21** with ethylene glycol resulted in $(2,6\text{-}Mes_2C_6H_3In)_4(CO_3)_2(OCH_2CH_2OH)_2(OH)_2$ (**23**), a unique cluster containing carbonate and ethylene glycol

moieties. The fixation of CO_2 and simultaneous recycling through the involvement of cheap raw materials is an active field of research. The attempt to recycle CO_2 from **23** in the form of ethylene carbonate, however did not meet with success. The compound **23** was heated upto 200 ^oC and tested for the evolution of ethylene carbonate. The absence of a chemical shift at δ = 165.8 in the ^{13}C NMR spectrum confirmed the removal of carbonate moiety from **23** and the presence of two signals at δ = 59.0, 58.8 in ^{13}C NMR spectrum indicated the formation of **22**. Another route to obtain **23** from **14** is by treating the indoxane with ethylene glycol. This lead to the formation of another tetrameric indium glycol cluster **22**. Further treatment of **22** with CO_2 again resulted in the formation of **23**.

Whereas the stannoxane carbonate **5** displays hypercoordination at the Sn centre and showed maximum coordination with the carbonate group, the organoindium carbonates **21** and **23** are intermediates of the modes displayed in Scheme 8 and show less involvement in metal coordination. Both **21** and **23** fall in the category of mode B (Scheme 8).

The molecular structure of **21** contains four pentacoordinated Indium atoms with a distorted trigonal bipyramidal arrangement around the In atoms (Figure 41). The two $In_2(\mu\text{-}OH)_2$ rings are facing each other and two carbonate moieties are adjacent to the $In_2(\mu\text{-}OH)_2$. The shortest In-O bond length (2.111(3) Å) is observed for the (μ-OH) O atoms whereas longest In-O bond length (2.236(3) Å) is associated with the carbonate substituent. The In-O-In linkage is symmetric with a relatively small variation in the In-O bond lengths, the shortest In-μ-OH bond length being 2.111(3) Å and longest 2.150(3) Å. The two water molecules (O4 and O4a) and two oxygen atoms from each of the carbonate moiety (O5 and O5a) are involved in hydrogen bonding. The O···O distance (2.552 Å) suggest strong hydrogen bonding (O4···O5). The bond lengths of three C-O bonds of the carbonate group do not vary much (1.277(5), 1.282(5), and 1.264(4) Å).The compound displays a characteristic ^{13}C NMR shift at δ = 165.8 for the carbonate moiety. The IR spectrum of **21** show absorptions at $\tilde{\nu}$ = 3646 and 3629 cm^{-1} that are indicative of OH stretching vibrations.

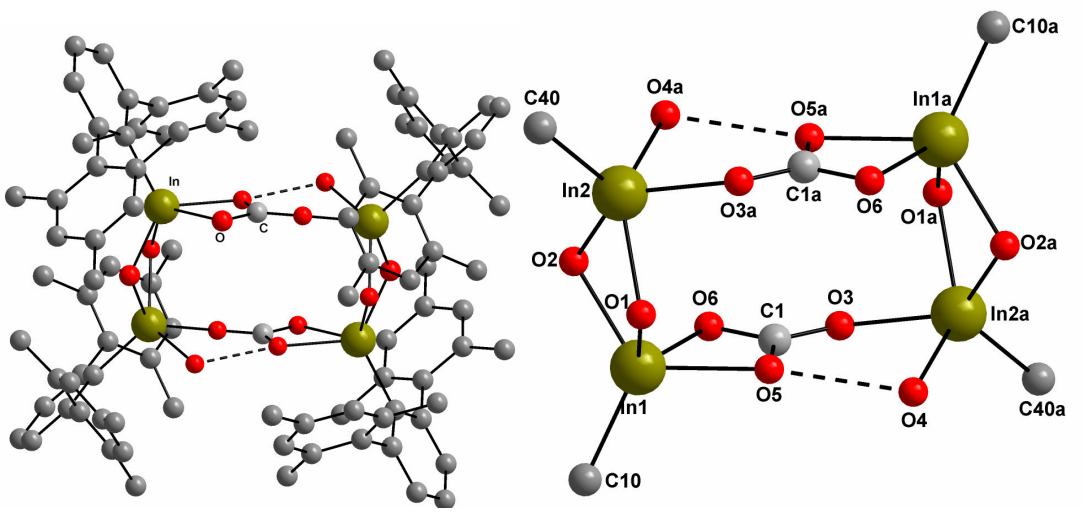

Figure 41: Molecular structure and inorganic core of (2,6-$Mes_2C_6H_3In)_4(CO_3)_2(OH)_4(H_2O)_2$ (**21**). Selected bond lengths (Å): In1-O1 2.111(3), In1-O2 2.119(3), In1-O5 2.236(3), In1-O6 2.211(3), In1-C10 2.149(3), In2-O1 2.144(3), In2-O2 2.150(3), In2-O3a 2.150(3), In2-O4a 2.228(3), In2-C40 2.158(3), C1-O5 1.277(5), C1-O6 1.282(5), C1-O3 1.264(4).

The centrosymmetric molecule **22** resembles the adduct **14** in that it has also four spirocyclic In atoms involved in four $In_2(\mu_2\text{-}OH)_2$ rings (Figure 42). The In-O bond lengths in these rings vary from 2.139(4) to 2.215(3) Å. The C-O bond lengths in **22** (1.433(5) and 1.408(6) Å) and **23** (1.430(1) and 1.434(1) Å) as well as the C-C bond lengths associated with the glycol motif (1.54(6) Å for **22** and 1.56(1) Å for **23**) are analogous to each other. A sharp absorption in the IR spectrum of **22** at $\tilde{\nu}$ = 3631 cm^{-1} represents the OH stretching vibration.

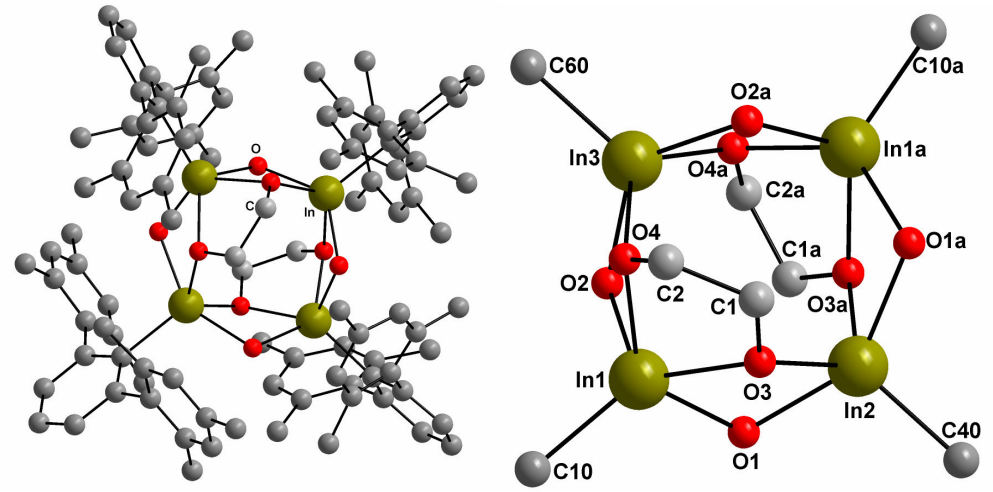

Figure 42: Molecular structure and inorganic core of (2,6-$Mes_2C_6H_3In)_4(OCH_2CH_2O)_2(OH)_4$ (**22**). Selected bond lengths (Å): In1-O1 2.160(3), In1-O2 2.149(4), In1-O3 2.215(3), In1-O4 2.144(4), In1-C10 2.195(3), In2-O1 2.194(3), In3-O2 2.139(4), In3-O2a 2.139(4), In2-O3 2.156(3), In3-O4 2.197(4), In3-O4a 2.197(4), In2-C40 2.189(5), In3-C60 2.196(5), C1-O3 1.433(5), C2-O4 1.408(6), C1-C2 1.540(6).

Molecular structure of **23** features pentacoordinated In atoms with four spirocyclic In atoms involved in two $In_2(\mu_2\text{-}OH)_2$ rings (Figure 43). The most interesting feature of the molecule is the presence of two carbonate and two glycol moieties in the molecule. The O···O distances for both **21** and **23** are much similar (2.552 and 2.561 Å). However, the three C-O distances in the carbonate moiety in **23** (1.26(1), 1.27(1) and 1.33(1) Å) are different as compared to **21** (1.277(5), 1.282(5), and 1.264(4) Å). The O with the longer C-O bond belonging to the carbonate moiety is also involved in hydrogen bonding with the OH group of the glycol motif. The In-O bond lengths vary from 2.129(7) to 2.307(6) Å. The IR shift at $\tilde{\nu}$ = 3623 cm^{-1} is indicative of OH stretching vibrations.

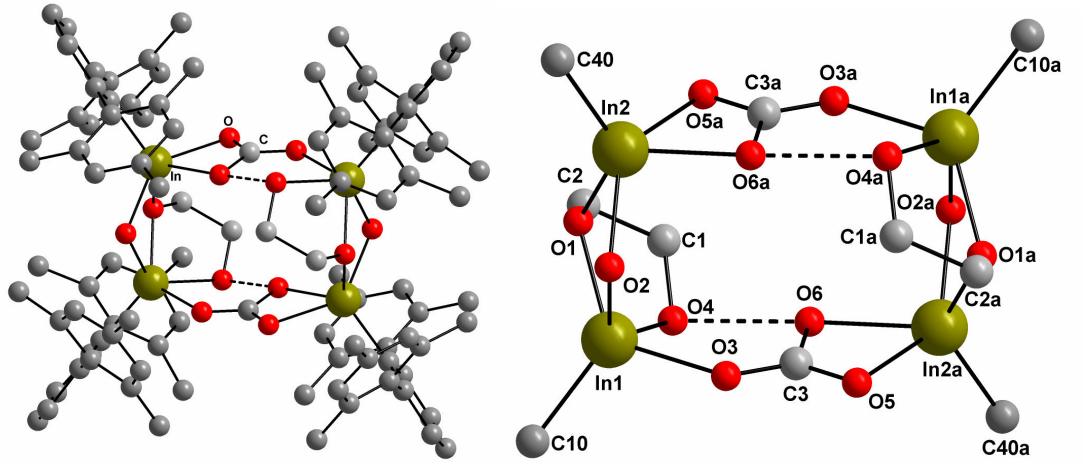

Figure 43: Molecular structure and inorganic core of $(2,6\text{-}Mes_2C_6H_3In)_4(CO_3)_2(OCH_2CH_2OH)_2(OH)_2$ (**23**). Selected bond lengths (Å): In1-O1 2.142(6), In1-O2 2.161(7), In1-O3 2.140(7), In1-O4 2.307(6), In1-C10 2.144(8), In2-O1 2.129(7), In2-O2 2.131(6), In2-O5a 2.208(6), In2-O6a 2.217(7), In2-C40 2.11(1), C1-O4 1.43(1), C2-O1 1.43(1), C1-C2 1.56(1), C3-O3 1.26(1), C3-O5 1.27(1), C3-O6 1.33(1).

3.3. Synthesis of *m*-terphenylthallium hydroxide chloride and its controlled hydrolysis

The *m*-terphenyllithium $2,6\text{-}Mes_2C_6H_3Li$ was reacted with TlCl to produce $2,6\text{-}Mes_2C_6H_3Tl$ in analogy with a procedure published for similar *m*-terphenylthallium(I) compounds.[101] It is noted that the structure of these compounds is very sensitive to the steric demand of the organic substituent; for example, $2,6\text{-}(2',4',6'\text{-}i\text{Pr}_3C_6H_2)_2C_6H_3Tl$ is a monomer, while $2,6\text{-}(2',6'\text{-}i\text{Pr}_2C_6H_3)_2C_6H_3Tl$ is a dimer, and $2,6\text{-}(2',6'\text{-}Me_2C_6H_3)_2C_6H_3Tl$ is a trimer, respectively. Any attempt to separate $2,6\text{-}Mes_2C_6H_3Tl$ from the byproduct LiCl by recrystallization from

inert solvents, such as toluene or diethyl ether did not meet with success. Consequently, the crude mixture of 2,6-$Mes_2C_6H_3Tl$ and LiCl was chlorinated using SO_2Cl_2, upon which the color changed from purple to yellow. Surprisingly, the extraction of the crude reaction mixture with $CHCl_3$ did not afford the expected $(2,6\text{-}Mes_2C_6H_3Tl)_2(\mu\text{-}Cl)_2Cl_2$ (**24**), but the isomeric diorganothallium cation containing $[(2,6\text{-}Mes_2C_6H_3)_2Tl]TlCl_4$ (**25**) as a colorless crystalline solid in good yield (Scheme 18), which implies that a migration of *m*-terphenyl groups occurred.

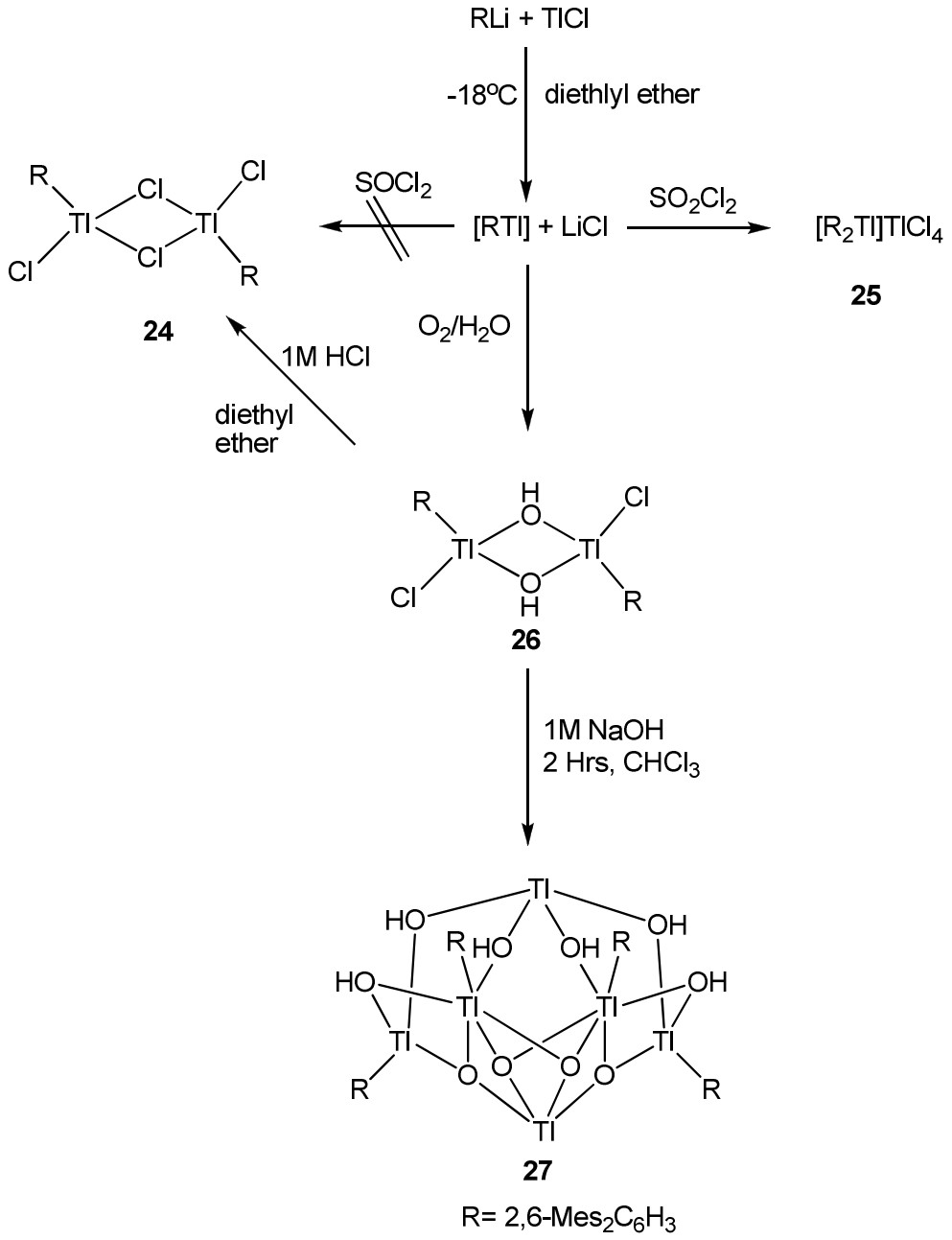

Scheme 18: Synthetic route of $(2,6\text{-}Mes_2C_6H_3Tl)_4Tl_2(\mu_3\text{-}O)_4(\mu\text{-}OH)_6$ (**27**).

Crystals of **25** contain essentially separated $[(2,6\text{-}Mes_2C_6H_3)_2Tl]^+$ cations and $TlCl_4^-$ anions (Figure 44). By contrast, the closely related compounds $[Mes_2Tl][MesTlCl_3]$[102] and $[Mes_2Tl]BF_4$[103] comprise organothallium cations that are involved in significant secondary Tl···Cl (3.046(3) and (3.119(3) Å) and Tl···F (2.796(8) Å) interactions, which can be attributed to the smaller size of the mesityl groups.

Like the isoelectronic $(2,6\text{-}Mes_2C_6H_3)_2Hg$[104] and the cation of $[(2,6\text{-}Mes_2C_6H_3)_2Ga]Li\{Al[OCH(CF_3)_2]_4\}_2$,[105] the $[(2,6\text{-}Mes_2C_6H_3)_2Tl]^+$ cation of **25** possesses an almost linear C-M-C linkage (178.6(3)°, M = Hg; 175.69(7)°, M = Ga; 177.4(3)°, M = Tl). By contrast, the more Lewis acidic cation of $[(2,6\text{-}Mes_2C_6H_3)_2Al][B(C_6F_5)_4]$[106] reveals an C-Al-C angle (159.17(5)°) that is distorted from linearity, due to significant Al···π interaction with the *ipso*-C atoms of the *o*-mesityl groups. Similar M···π interactions appear to be absent in the heavier compounds with M = Hg, Ga, Tl. The Tl-Cl bond lengths (average 2.404(4) Å) of the tetrahedral $TlCl_4^-$ anion of **25** resemble those with other counterions (e.g., Bu_4N^+).[107] The electrospray ionization time-of-flight mass (ESI-TOF-MS) spectrum of **25** (MeOH, positive mode) shows only one mass cluster at m/z = 831.4 g mol^{-1}, which was assigned to the $[(2,6\text{-}Mes_2C_6H_3)_2Tl]^+$ cation.

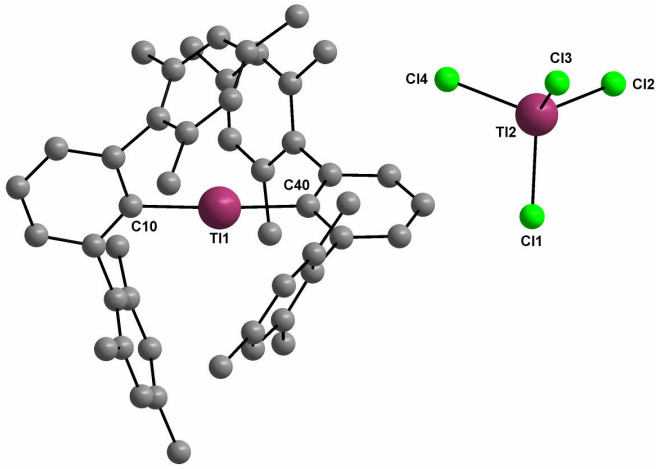

Figure 44: Molecular structure of $[(2,6\text{-}Mes_2C_6H_3)_2Tl]TlCl_4$ (**25**). Selected bond lengths (Å) and angles (°): Tl1-C10 2.126(9), Tl1-C40 2.127(9), Tl2-Cl1 2.412(4), Tl2-Cl2 2.394(4), Tl2-Cl3 2.413(6), Tl2-Cl4 2.398(5), C10-Tl1-C40 177.4(3), Cl1-Tl2-Cl2 108.2(2), Cl1-Tl2-Cl3 111.0(2), Cl1-Tl2-Cl4 107.1(2), Cl2-Tl2-Cl3 106.9(2), Cl2-Tl2-Cl4 112.7(2), Cl3-Tl2-Cl4 110.9(2).

When a crude reaction mixture consisting of $2,6\text{-}Mes_2C_6H_3Tl$ and LiCl was exposed to moist air, the color faded immediately. Extraction with $CHCl_3$ surprisingly afforded $(2,6\text{-}Mes_2C_6H_3Tl)_2Cl_2(\mu\text{-}OH)_2$ (**26**), (Figure 45) the Tl analogue of **12**, in reasonable yields (Scheme 18).

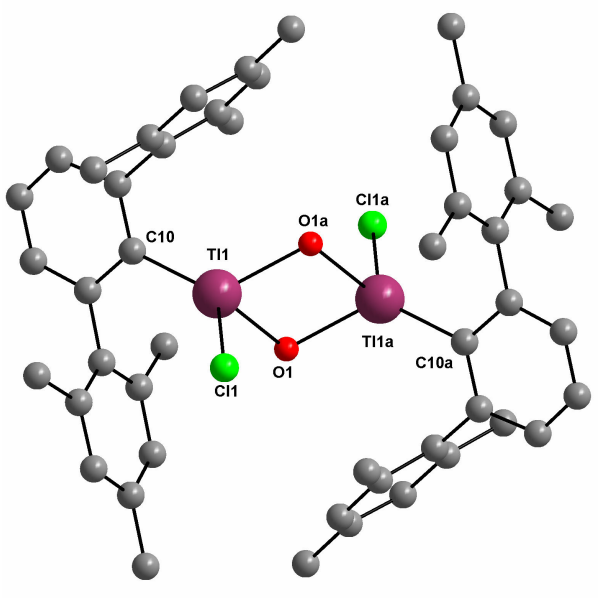

Figure 45: Molecular structure of (2,6-$Mes_2C_6H_3Tl)_2Cl_2(\mu$-OH)$_2$ (**26**). Selected bond lengths (Å) and angles (°): Tl1-O1 2.202(9), Tl1-O1a 2.25(1), Tl1-Cl1 2.546(4), Tl1-C10 2.10(1), O1-Tl1-O1a 76.1(3), O1-Tl1-Cl1 96.6(3), O1a-Tl1-Cl1 97.2(3), O1-Tl1-C10 125.4(4), O1a-Tl1-C10 121.4(4), Cl1-Tl1-C10 126.8(3); (Symmetry code: a = –x, –y, –z)

Treatment of **26** with hydrochloric acid provided (2,6-$Mes_2C_6H_3Tl)_2(\mu$-Cl)$_2Cl_2$ (**24**), the elusive analogue of **10** (Figure 46). Not surprising, the structures of **24** and **26** closely resemble those of the lighter homologues **10** and **12**. The spatial arrangement of the Tl atoms is tetrahedral and defined by two donor sets, with one C and three Cl atoms and the second set composed of two O, one C and one Cl atom, respectively. The endocyclic Tl-Cl bond lengths (2.681(2) and 2.633(2) Å for **24** and 2.546(4) Å for **26**) are slightly longer than the related exocyclic value (2.427(3) Å for **24**). Interestingly, the Tl-O bond lengths of **26** (2.202(9) and 2.25(1) Å) are only marginally longer than the In-O bond lengths of **12**-**14** (average 2.159(6) Å), which is presumably due to the fact that Tl is only marginally larger than In (as the result of the lanthanide contraction). The IR spectrum of **26** shows two absorptions at $\tilde{\nu}$ = 3574 and 3551 cm^{-1}, which were unambiguously assigned to OH stretching vibrations of hydroxy groups that are not involved in hydrogen bonding. Similarly to the In···In separation of **10** (3.896(9) Å) and **12** (3.345(1) Å), the Tl···Tl separation of **24** (3.937(2) Å) and **26** (3.502(4) Å) is distinctively different.

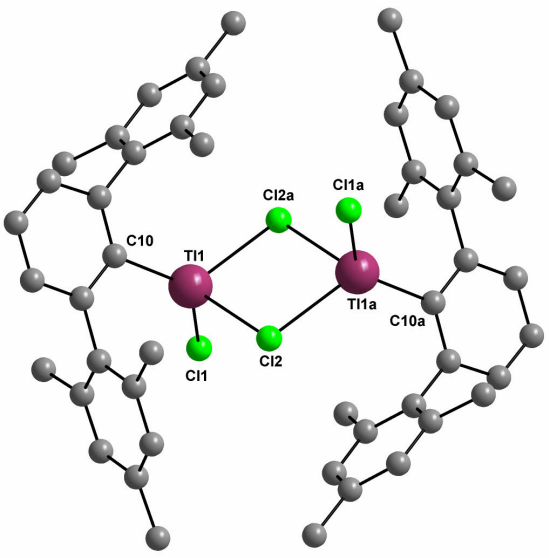

Figure 46: Molecular structure of (2,6-$Mes_2C_6H_3Tl)_2(\mu$-Cl)$_2Cl_2$ (**24**). Selected bond lengths (Å) and angles (°): Tl1-Cl1 2.427(3), Tl1-Cl2 2.633(2), Tl1-Cl2a 2.681(2), Tl1-C10 2.159(7), Cl1-Tl1-Cl2 93.08(7), Cl1-Tl1-Cl2a 99.05(8), Cl2-Tl1-Cl2a 84.37(7), Cl1-Tl1-C10 130.7(2), Cl2-Tl1-C10 124.6(2), Cl2a-Tl1-C10 113.8(2), (Symmetry code: a = –x, –y, –z).

The base hydrolysis of (2,6-$Mes_2C_6H_3Tl)_2(\mu$-OH)$_2Cl_2$ (**26**) in a two-layer system of aqueous NaOH/$CHCl_3$ afforded only a single product, the thalloxane cluster (2,6-$Mes_2C_6H_3Tl)_4Tl_2(\mu_3$-O)$_4(\mu$-OH)$_6$ (**27**), which is isolated as colorless crystals in moderate yield (Scheme 18). The formation of **27** can be rationalized by the partial hydrolytic cleavage of Tl-C bonds. All attempts to prepare a chlorine free thalloxane without the concomitant cleavage of Tl-C bonds failed. It is critically noted that with the exception of Tl1 and Tl2 all atoms of the inorganic core are disordered over two positions (Figure 48 in crystallography section), which can be attributed to the shielding of the *m*-terphenyl substituents dominating the crystal packing. Already a similar observation has been made for the molecular structure of the mixed-valent antimony oxo cluster (2,6-$Mes_2C_6H_3Sb)_2(ClSb)_4(\mu_3$-O)$_8$, which contains the same *m*-terphenyl substituent.[45] The spatial arrangement of the organometallic Tl atoms of **27** is distorted tetrahedral, whereas the inorganic Tl atoms are best described as distorted square pyramidal (Figure 47). The Tl-O bond lengths of **27** vary between 2.00(2) and 2.69(2) Å and are not discussed in more detail due to the disorder (crystallography section). The hydroxy groups were tentatively assigned on the basis of the coordination numbers of the O atoms. The presence of hydroxy groups is confirmed by IR spectroscopy. The IR spectrum of **27** shows only one absorption at $\tilde{\nu}$ = 3596 cm^{-1} that arose from OH stretching vibrations. Attempts to independently

confirm the molecular mass of **27** using electrospray mass spectrometry (ESI-MS) at ambient conditions failed, as no reasonable spectrum could be obtained. At 200 ºC, the only mass cluster observed was at m/z = 831.4 g mol^{-1} and unambiguously assigned to the $[(2,6\text{-}Mes_2C_6H_3)_2Tl]^+$ cation, which apparently formed by migration of the *m*-terphenyl substituent under MS conditions. Compounds **24**-**27** are readily soluble in most organic solvents. The ^1H and ^{13}C NMR spectra show one set of signals for the *m*-terphenyl substituents.

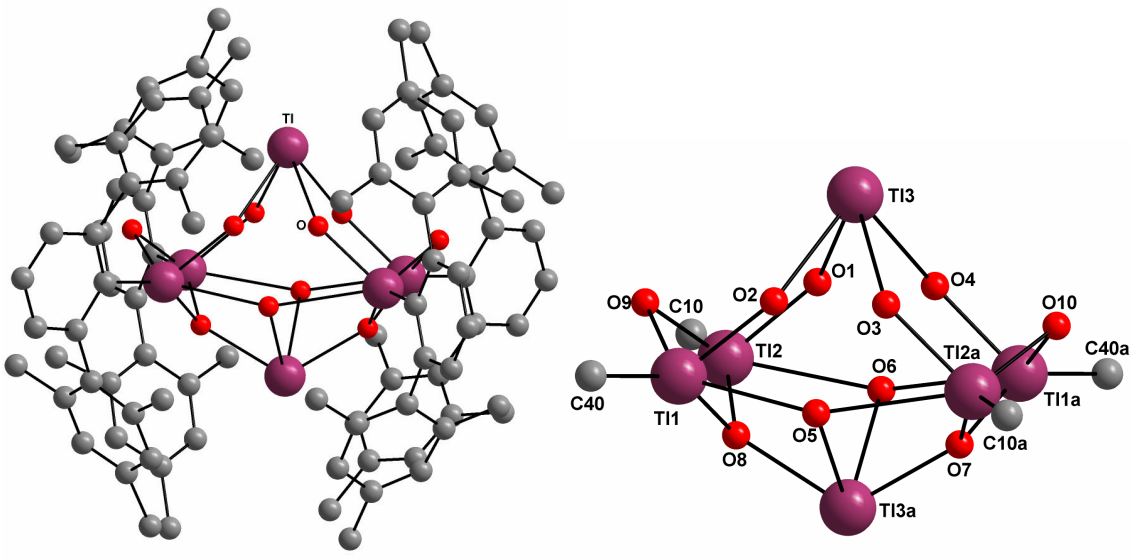

Figure 47: Molecular structure and inorganic core of $(2,6\text{-}Mes_2C_6H_3Tl)_4Tl_2(\mu_3\text{-}O)_4(\mu\text{-}OH)_6$ (**27**). Selected bond lengths (Å): Tl1-O2 2.242(2), Tl1a-O4 2.188(2), Tl1a-O7 2.146(2), Tl1-O8 2.111(2), Tl1-O9 2.248(2), Tl1a-O10 2.284(2), Tl1-C40 2.140(1), Tl2-O1 2.266(2), Tl2a-O3 2.210(2), Tl2a-O7 2.075(2), Tl2-O8 2.181(2), Tl2-O9 2.289(2), Tl2a-O10 2.243(1), Tl2-C10 2.138(1), Tl3-O1 2.664(2), Tl3-O2 2.585(2), Tl3-O3 2.690(2), Tl3-O4 2.592(2), (Symmetry code: a = –x, –y, –z).

4. Summary

In the present work the chemistry of group 14 and 13 element oxide hydroxides has been extended to a new series of well-defined stannoxanes, indoxanes and thalloxanes that are kinetically stabilized by a bulky *m*-terphenyl substituent.

The controlled base hydrolysis of appropriate *m*-terphenyltin trichloride (**1**) and *m*-terphenylindium dichloride (**10**) produced along with intermediate products, the trinuclear organostannonic acid [2,6-$Mes_2C_6H_3SnO(OH)]_3$ (**3**) and the tetranuclear indium dihydroxide [2,6-$Mes_2C_6H_3In(OH)_2]_4$ (**14**). Whereas the exposure to air of a mixture of *m*-terphenyl thallium and lithium chloride resulted in (2,6-$Mes_2C_6H_3Tl)_2(\mu$-$OH)_2Cl_2$ (**26**), base hydrolysis of which proceeded with partial cleavage of the *m*-terphenyl substituent and yielded the thalloxane cluster (2,6-$Mes_2C_6H_3Tl)_4Tl_2(\mu_3$-$O)_4(\mu$-$OH)_6$ (**27**).

In moist C_6D_6, **3** reversibly react with water to give the monomeric organostannonic acid 2,6-$Mes_2C_6H_3Sn(OH)_3$ (**3a**).

The reaction of (t-$Bu_2SnO)_3$ with **3** proceeded with the absorption of atmospheric CO_2 and give rise to the multinuclear hypercoordinated organostannoxane carbonate [t-$Bu_2Sn(OH)OSnR(OH)_2OC(OSnt$-$Bu_2OH)_2(O)SnR(OH)(H_2O)]_2$ (R = 2,6-$Mes_2C_6H_3$) (**5**). Whereas the treatment of (2,6-$Mes_2C_6H_3In)_2(\mu$-$Cl)_2Cl_2$ (**10**) and **14** with (t-$Bu_2SnO)_3$ resulted in the synthesis of stannaindoxane clusters (2,6-$Mes_2C_6H_3In)(t$-$Bu_2Sn)_2O(OH)_2Cl_2$ (**18**) and (2,6-$Mes_2C_6H_3In)_2(t$-$Bu_2Sn)O(OH)_2$ (**19**). Bubbling CO_2 through a solution of **3** did not have any reaction however **14** reacted with CO_2 to produce a bicarbonate cluster (2,6-$Mes_2C_6H_3In)_3(HCO_3)_2(OH)_4$ (**20**) in chloroform and a carbonate cluster (2,6-$Mes_2C_6H_3In)_4(CO_3)_2(OH)_4(H_2O)_2$ (**21**) in THF. The treatment of diphenylphosphinic acid with **3** resulted in [2,6-$Mes_2C_6H_3Sn(OH)_2$ $(O_2PPh_2)]_2$ (**8**) whereas **14** reacted with diphenylphosphinic acid to produce [(2,6-$Mes_2C_6H_3In)_2(OH)(O_2PPh_2)_3$] (**16**). **14** also reacted with $Me_2P(O)OH$ and $Me_5C_3HP(O)OH$ resulting in the formation of novel multinuclear organoindoxane phosphinate clusters (2,6-$Mes_2C_6H_3In)_2(OH)_2(O_2PMe_2)_2$ (**15**) and (2,6-$Mes_2C_6H_3In)$ $(Me_5C_3HPO)_2(H_2O)_2$ (**17**). The versatile reactivity of **14** towards CO_2 is further elaborated by its treatment with ethylene glycol and CO_2. The treatment of **14** with ethylene glycol in the absence of CO_2 produced the carbonate free cluster (2,6-$Mes_2C_6H_3In)_4(OCH_2CH_2O)_2(OH)_4$ (**22**) whereas the same in the presence of CO_2 resulted in the carbonate cluster (2,6-$Mes_2C_6H_3In)_4(CO_3)_2(OCH_2CH_2OH)_2(OH)_2$ (**23**).

The reaction of **3** with NaH afforded the novel tetranuclear sodium *m*-terphenylstannoxylate cluster $Na_3(2,6\text{-}Mes_2C_6H_3Sn)_4O_6(OH)_3$ (**9**).

An attempt at preparing $(2,6\text{-}Mes_2C_6H_3Tl)_2(\mu\text{-}Cl)_2Cl_2$ (**24**) by the chlorination of $2,6\text{-}Mes_2C_6H_3Tl$ (prepared in situ from $2,6\text{-}Mes_2C_6H_3Li$ and TlCl) using SO_2Cl_2 provided the isomeric diorganothallium cation containing compound $[(2,6\text{-}Mes_2C_6H_3)_2Tl]TlCl_4$ (**25**). $(2,6\text{-}Mes_2C_6H_3Tl)_2(\mu\text{-}OH)_2Cl_2$ (**26**) reacted with hydrochloric acid to give $(2,6\text{-}Mes_2C_6H_3Tl)_2(\mu\text{-}Cl)_2Cl_2$ (**24**). Any attempts to obtain a halogen free thalloxane without the partial cleavage of Tl-C bond did not meet with success.

Zusammenfassung

Im Rahmen dieser Arbeit wurde eine Reihe von neuen wohl definierten Stannoxanen, Indoxanen und Thalloxanen dargestellt und vollständig charakterisiert. Diese luftstabilen Verbindungen werden durch sperrige *m*-Terphenyl-substituenten kinetisch stabilisiert. Durch kontrollierte basische Hydrolyse des Monoorganozinntrichlorids **1** und des Monoorganoindiumdichlorids **10** werden zusammen mit Zwischenprodukten eine dreikernige Organostannonsäure $[2,6\text{-}Mes_2C_6H_3SnO(OH)]_3$ (**3**) bzw. ein aggregiertes Indiumdihydroxid $[2,6\text{-}Mes_2C_6H_3In(OH)_2]_4$ (**14**) gebildet. Durch Reaktion eines Gemisches aus $2,6\text{-}Mes_2C_6H_3Tl$ und LiCl mit Luftfeuchtigkeit entsteht $(2,6\text{-}Mes_2C_6H_3Tl)_2(\mu\text{-}OH)_2Cl_2$ (**26**), welches unter teilweiser Abspaltung der *m*-Terphenyl-Substituenten den Thalloxancluster $(2,6\text{-}Mes_2C_6H_3Tl)_4Tl_2(\mu_3\text{-}O)_4(\mu\text{-}OH)_6$ (**27**) liefert.
In feuchtem deuteriertem Benzol reagiert die dreikernige Stannonsäure **3** reversibel mit Wasser zu der monomeren Organostannonsäure $2,6\text{-}Mes_2C_6H_3Sn(OH)_3$ (**3a**).
Die Reaktion von $(t\text{Bu}_2SnO)_3$ mit **3** führt in Gegenwart von atmosphärischem CO_2 zum multikern-hyperkoordinierten Organostannoxancarbonat $[t\text{Bu}_2Sn(OH)OSnR(OH)_2$ $OC(OSnt\text{Bu}_2OH)_2(O)SnR(OH)(H_2O)]_2$ (**5**), (R = $2,6\text{-}Mes_2C_6H_3$). Die Behandlung von $(2,6\text{-}Mes_2C_6H_3In)_2(\mu\text{-}Cl)_2Cl_2$ (**10**) und **14** mit $(t\text{Bu}_2SnO)_3$ ergibt die Stannaindoxan-Clusterstrukturen $(2,6\text{-}Mes_2C_6H_3In)(t\text{Bu}_2Sn)_2O(OH)_2Cl_2$ (**18**) und $(2,6\text{-}Mes_2C_6H_3In)_2$ $(t\text{Bu}_2Sn)O(OH)_2$ (**19**). Die jeweilige Reaktion von Ph_2PO_2H mit **3** oder **14** liefert die multikern-hyperkoordinierten Phosphinate $[Mes_2C_6H_3Sn(OH)_2(O_2PPh_2)]_2$ (**8**) bzw. $[(2,6\text{-}Mes_2C_6H_3In)_2(OH)(O_2PPh_2)_3]$ (**16**). **14** reagiert weiterhin mit $Me_2P(O)OH$ und $Me_5C_3HP(O)OH$ und liefert die neuartigen Organoindophosphinate $[(2,6\text{-}Mes_2C_6H_3In)_2(OH)_2(O_2PMe_2)_2]$ (**15**) und $[(2,6\text{-}Mes_2C_6H_3In)(Me_5C_3HPO)_2(H_2O)_2]$ (**17**). Die vielseitige Reaktivität von **14** gegenüber CO_2 wurde weiter durch die Behandlung mit Ethylenglykol und CO_2 untersucht. Die Behandlung von **14** mit Ethylenglykol in Abwesenheit von CO_2 produziert den Carbonat-freien Cluster $(2,6\text{-}Mes_2C_6H_3In)_4(OCH_2CH_2O)_2(OH)_4$ (**22**), während in Gegenwart von CO_2 der Carbonat-haltige Cluster $(2,6\text{-}Mes_2C_6H_3In)_4(CO_3)_2(OCH_2CH_2OH)_2(OH)_2$ (**23**) erhalten wird. Die Behandlung von **3** mit NaH ergibt $Na_3(2,6\text{-}Mes_2C_6H_3Sn)_4O_6(OH)_3$ (**9**). Beim Versuch $(2,6\text{-}Mes_2C_6H_3Tl)_2(\mu\text{-}Cl)_2Cl_2$ (**24**) durch Chlorierung von $2,6\text{-}Mes_2C_6H_3Tl$ (in situ aus $2,6\text{-}Mes_2C_6H_3Li$ und TlCl hergestellt) mit SO_2Cl_2 zu erhalten, wird stattdessen das isomere Diorganothallium-Kation-haltige $[(2,6\text{-}Mes_2C_6H_3)_2Tl]TlCl_4$ (**25**) gebildet.

Alle Versuche ein halogenfreies Thalloxan ohne die partielle Spaltung der Tl-C-Bindung zu erhalten schlugen fehl.

5. Experimental

The handling of air and moisture sensitive compounds was carried out under Argon atmosphere. The starting materials *m*-terphenyl lithium 2,6-$Mes_2C_6H_3Li$[48] and $(tBu_2SnO)_3$[108] were prepared according to the literature procedures.

The starting materials $InCl_3$, TlCl and SO_2Cl_2, $Me_2P(O)OH$, $Ph_2P(O)OH$, $C_2H_4(OH)_2$ were obtained from commercial sources and used as received. 2,2,3,4,4-pentamethylphosphetanic acid was obtained as a gift from Dr. Vadapalli Chandrasekhar of the Indian Institute of Technology Kanpur. The ^{1}H, ^{13}C, ^{31}P and ^{119}Sn NMR spectra were recorded using Jeol JL400 FT-NMR-Spectrometer and are referenced to $SiMe_4$ (^{1}H, ^{13}C) and H_3PO_4 (^{31}P), Me_4Sn (^{119}Sn). The ^{13}C and ^{119}Sn CP MAS NMR spectra were obtained using a JEOL Eclipse Plus 400 MHz NMR spectrometer. The electrospray ionization time-of-flight mass (ESI-TOF MS) spectrum was obtained using an Agilent 6210 ESI-TOF mass spectrometer. The MAS NMR spectra as well as the ESI-TOF MS were obtained at the School of Life and Environmental Sciences, Deakin University, Australia. Electron impact mass (EI-MS) spectra were measured using a Varian MAT 711 mass spectrometer. The electron energy was set to 80 eV. The solvent flow rate was adjusted to 4 μL min^{-1} and the spray voltage set to 4 kV. Microanalyses were obtained from a Vario EL elemental analyzer. Infrared spectra were recorded using Nexus FT-IR spectrometer with a Smart DuraSamp IR. Melting points were recorded on the Electrothermal Thermo Scientific melting point instrument IA9200.

Synthesis of 2,6-$Mes_2C_6H_3SnCl_3$ (1)

A suspension of 2,6-$Mes_2C_6H_3Li$ (1.5 g, 4.6 mmol) in THF (30 mL) was added to a stirred suspension of $SnCl_4$ (1.22 g, 4.6 mmol) in THF (20 mL) at 0 ºC. The reaction mixture was stirred for 2 h at 0 ºC and then overnight at room temperature. The solvent was removed under reduced pressure and the crude product extracted with CH_2Cl_2, filtered and recrystallized from CH_2Cl_2 / hexane (1:3) to give colorless crystals of **1**.

Yield: 1.6 g (3.0 mmol, 64 %)

m.p.: 216 - 218 °C

^{1}H NMR ($CDCl_3$): δ = 7.73 (t, 1H; *p*-C_6H_3), 7.28 (d, 2H; *m*-C_6H_3), 7.00 (s, 4H; *m*-Mes), 2.36 (s, 6H; p-CH_3), 2.10(s, 12H; *o*-CH_3)

^{13}C NMR ($CDCl_3$): δ = 148.7, 139.1, 138.7, 135.8, 133.3, 130.2, 130.0, 129.0, 128.0, 128.0, 127.7, 127.5 (Ar), 21.2, 21.0, 20.7, 20.2 (Me)

^{119}Sn NMR ($CDCl_3$): δ = –113.9

EA: $C_{24}H_{25}Cl_3Sn$ (538.52 g/mol) Calcd.: C, 53.53; H, 4.68
Found: C, 53.67; H, 4.34

Synthesis of 2,6-$Mes_2C_6H_3Sn(OH)Cl_2 \cdot H_2O$ (2)

A solution of **1** (200 mg, 0.37 mmol) in diethyl ether (30 mL) was hydrolysed with a solution of NaOH (15 mg, 0.37 mmol) in water (30 ml). The mixture was stirred vigorously for 12 h at room temperature before the layers were separated. The organic layer was dried over Na_2SO_4 and the solvent removed in vacuum. Crystallization from diethyl ether afforded colourless crystals of **2**.

Yield: 160 mg (0.30 mmol, 82 %)

m.p.: 104 ºC (dec.)

^{1}H NMR ($CDCl_3$): δ = 7.63 (t, 1H; *p*-C_6H_3), 7.22 (d, 2H; *m*-C_6H_3), 6.99 (s, 4H; *m*-Mes), 2.38 (s, 6H; *p*-CH_3), 2.06 (s, 12H; *o*-CH_3)

^{13}C NMR ($CDCl_3$): δ = 147.6, 137.7, 136.5, 136.0, 135.2, 131.6, 128.6, 128.1, 127.5, 127.4, 127.2, 126.9 (Ar), 20.6, 20.5, 20.2, 19.6 (Me)

^{119}Sn NMR ($CDCl_3$): δ = –171.5
^{119}Sn MAS NMR: δ = –359

IR: $\tilde{\nu}$ (OH) = 3609 (m), 3576 (s), 3514 (m)

EA: $C_{24}H_{28}Cl_2O_2Sn$ (538.09 g/mol) Calcd.: C, 53.57; H, 5.24
Found: C, 53.54; H, 5.49

Synthesis of *trans*-[2,6-$Mes_2C_6H_3Sn(O)(OH)]_3$ (3)

A solution of **1** (200 mg, 0.37 mmol) in diethyl ether (30 mL) was hydrolysed with a solution of NaOH (44 mg, 1.11 mmol) in water (30 ml). The mixture was vigorously stirred for 12 h at room temperature before the layers were separated. The organic layer was dried over Na_2SO_4 and the solvent removed in vacuum. Recrystallisation from CH_2Cl_2/hexane (1:3) furnished colourless crystals of **3**.

Yield: 150 mg (0.10 mmol, 87%)

m.p.: 268 - 272 ºC

^{1}H NMR ($CDCl_3$): δ = 7.48 (t, 1H; *p*-C_6H_3), 7.04 (d, 2H; *m*-C_6H_3), 6.81 (s, 4H; *m*-Mes), 2.24 (s, 6H; *p*-CH_3), 1.93 (s, 12H; *o*-CH_3)

^{13}C NMR ($CDCl_3$) δ = 161.9, 137.2, 136.8, 136.7, 136.6, 130.9, 128.3, 128.1, 128.0, 127.8 (Ar), 21.2, 21.0, 20.9 (Me)

^{119}Sn NMR (C_6D_6): δ = –207.2 (integral 66%, $^2J(^{119}Sn\text{-}O\text{-}^{119/117}Sn)$ = 538 Hz), –222.5 (integral 33%; $^2J(^{119}Sn\text{-}O\text{-}^{119/117}Sn)$ = 539 Hz)

^{119}Sn MAS NMR: δ = –210 (integral 66%), –224 (integral 33%)

IR: $\tilde{\nu}$ (OH) = 3603 (s)

EA: $C_{72}H_{78}O_6Sn_3$ (1395.51 g/mol) Calcd.: C, 61.97; H, 5.63
Found: C, 62.27; H, 5.85

NMR scale reaction of *trans*-[2,6-$Mes_2C_6H_3Sn(O)(OH)]_3$ (3) and ($tBu_2SnO)_3$

A NMR tube was charged with **3** (60.0 mg, 0.04 mmol) and ($tBu_2SnO)_3$ (64.0 mg, 0.08 mmol). Dry $CDCl_3$ (400 μL) was added and the NMR tube flame sealed under vacuum. The mixture was heated at 40°C for 2 h to give a clear solution of **4**.

^{119}Sn NMR ($CDCl_3$): δ = –68.0 (integral 66%, $^2J(^{119}Sn\text{-}O\text{-}^{119/117}Sn)$ = 437 Hz), – 222 (integral 33%; $^2J(^{119}Sn\text{-}O\text{-}^{119/117}Sn)$ = 425/417 Hz)

Synthesis of [$tBu_2Sn(OH)OSnR(OH)_2OC(OSnt\text{-}Bu_2OH)_2(O)SnR(OH)(H_2O)]_2$ (5, R = 2,6-$Mes_2C_6H_3$)

A mixture of **3** (250 g, 0.17 mmol) and ($tBu_2SnO)_3$ (200 mg, 0.26 mmol) placed in a Schlenk tube and dissolved in THF (20 mL). This solution was variously purged with CO_2 for 10 min at room temperature. The solvent was removed in vacuum and the solid residue recrystallized from THF / hexane (1:3) to give **5**.

Yield: 285 mg (0.08 mmol, 62 %)

m.p.: 205 - 210 °C

^{1}H NMR ($CDCl_3$): δ = 7.45, 7.44, 7.35, 7.33 (t, 1H; *p*-C_6H_3), 7.18, 7.16, 7.10, 7.08 (d, 2H; *m*-C_6H_3), 6.95, 6.93, 6.91, 6.90 (s, 4H, *m*-Mes) 2.32, 2.28, 2.27, 2.21 (s, 6H; *p*-CH_3) 2.07, 2.06, 2.04, 1.98 (s,12H; *o*-CH_3) 1.22, 1.21, 1.18, 1.16, 1.14, 1.10 (*t*Bu)

IR: $\tilde{\nu}$(OH) = 3649 (m), 3588 (s), 3545 (m)

EA: $C_{146}H_{218}O_{24}Sn_{10}$ (3544.0 g/mol) Calcd.: C, 49.40; H, 6.15
Found: C, 49.19; H, 6.19

Synthesis of $K_6[MeSn(O)CO_3]_6 \cdot 14\ H_2O$ (7)

A solution of stannous chloride (10 g) in 20 ml water was cooled to 0 ^oC. 10 g KOH dissolved in 100 ml water was added slowly to the cooled solution. The solution was filtered afterwards from the black residue formed after the completion of reaction. To the filtered solution methyl iodide (8 g) and sufficient ethyl alcohol (65 mL) were added to make the solution homogeneous. CO_2 was afterwards bubbled through the solution and continued for two more hours once precipitation of product from the solution starts. The product was afterwards filtered off from the solution as heavy white precipitate.

^{13}C MAS NMR	δ = 164.2, 162.2, 160.7 (*CO_3*-C) 8.0, 5.7, 5.2 (*Me*-C)	
^{119}Sn MAS NMR	δ = – 474, – 481 and – 486	
EA:	$C_{12}H_{46}K_6O_{38}Sn_6$ (1745.23 g/mol)	Calcd.: C, 8.25; H, 2.63
		Found: C, 8.24; H, 2.61

Synthesis of $[2,6\text{-}Mes_2C_6H_3Sn(OH)_2(O_2PPh_2)]_2$ (8)

A mixture of **3** (230 mg, 0.16 mmol) and $Ph_2P(O)OH$ (110 mg, 0.77 mmol) in dry THF (20 ml) was stirred overnight. The solvent was removed in vacuum and the residue recrystallized from $CHCl_3$ / hexane (1:3) to give **8**.

Yield: 220 mg (0.16 mmol, 68%)

m.p.: 283 - 285 ^oC

^1H NMR ($CDCl_3$): δ = 7.56 (*o*-C_6H_5), 7.51, 7.48 (t, 1H; *p*-C_6H_3) 7.33 (*m*-C_6H_5), 7.20, 7.15 (d, 2H; *m*-C_6H_3) 6.98, 6.80 (s, 4H; *m*-Mes) 6.59 (*p*-C_6H_5), 2.31, 2.27 (s, 6H; *p*-CH_3) 2.03, 2.02 (s, 12H; *o*-CH_3)

^{13}C NMR ($CDCl_3$): δ = 147.1, 146.7, 142.0, 141.1, 138.9, 138.5, 137.9, 137.4, 137.2, 137.1, 136.9, 135.8, 135.3, 134.3, 131.3, 131.2, 130.9, 130.7, 130.2, 129.2, 128.7, 128.0, 127.8, 127.7, 127.4 (Ar), 22.1, 21.9, 21.8, 21.6, 21.4, 21.2, 21.1, 20.2 (Me)

^{31}P NMR ($CDCl_3$): δ = 30.0

^{119}Sn NMR ($CDCl_3$): δ = – 449.2

^{119}Sn MAS NMR: δ = – 582

IR: $\tilde{\nu}$ (OH) = 3634 (s), 3574 (s)

EA: $C_{72}H_{74}O_8P_2Sn_2$ (1366.72 g/mol) Calcd.: C, 63.27; H, 5.46
Found: C, 63.36; H, 5.51

Synthesis of $Na_3(2,6\text{-}Mes_2C_6H_3Sn)_4O_6(OH)_3$ (9)

A solution of **3** (200 mg, 0.14 mmol) dissolved in dry THF (10 ml) was added by a syringe to suspension of NaH (11 mg, 0.42 mmol) in dry THF (10 ml). The reaction mixture was stirred overnight before removing the solvent in vacuum and extracting the residue with wet toluene (20 mL). The solution was filtered and the volume reduced to about one third. Crystallization at 6 °C provided colorless crystals of **9**.

Yield: 110 mg (0.06 mmol, 57 %)

m.p.: 245 - 247 °C

^{1}H NMR ($CDCl_3$): δ = 7.50, 7.49, 7.45, 7.43 (t, 1H; *p*-C_6H_3) 7.17, 7.16, 7.02, 6.98 (d, 2H; *m*-C_6H_3) 6.86, 6.85, 6.78, 6.73 (s, 4H; *m*-Mes) 2.34, 2.29, 2.24, 2.16 (s, 6H; *p*-CH_3) 1.98, 1.93, 1.87, 1.85 (s, 12H; *o*-CH_3)

IR: $\tilde{\nu}$ (OH) = 3616 (s), 3595 (s), 3563 (m)

EA: $C_{96}H_{103}Na_3O_9Sn_4$ (1942.80 g/mol) Calcd.: C, 59.30; H, 5.34
Found: C, 59.92; H, 5.52

Synthesis of (2,6-$Mes_2C_6H_3In)_2(\mu$-$Cl)_2Cl_2$ (10)

To a suspension of $InCl_3$ (1.50 g, 6.77 mmol) in Et_2O (20 mL) cooled to –78 °C was slowly added a solution of 2,6-$Mes_2C_6H_3Li$ (2.16 g, 6.77 mmol) in Et_2O (40 mL). The reaction mixture was allowed to warm to room temperature and stirred overnight. The solvent was removed under reduced pressure, and the product was extracted with warm hexane (100 mL) and filtered. The solvent was reduced in vacuum to almost one third, and the precipitates were redissolved by heating. Crystallization afforded **10** as colorless crystals.

Yield: 2.57 g (2.57 mmol, 76 %)

m.p.: 270 °C (dec)

^{1}H NMR ($CDCl_3$): δ = 7.51 (t, 1H; *p*-C_6H_3), 7.14 (d, 2H; *m*-C_6H_3), 6.94 (s, 4H; *m*-Mes), 2.34 (s, 6H; *p*-CH_3), 2.03 (s, 12H; *o*-CH_3)

^{13}C NMR ($CDCl_3$): δ = 148.7, 146.5, 140.2, 137.6, 136.6, 130.4, 128.7, 127.3, (Ar) 21.2, 20.9 (Me)

EA: $C_{48}H_{50}Cl_4In_2$ (998.30 g/mol) Calcd.: C, 57.75; H, 5.05
Found: C, 57.77; H, 5.21

Synthesis of 2,6-$Mes_2C_6H_3InCl_2\cdot H_2O$ (11)

A solution of **10** (300 mg, 0.3 mmol) in diethyl ether (30 mL) was hydrolyzed with a solution of NaOH (48 mg, 1.20 mmol) in water (30 mL). The mixture was vigorously stirred for 30 min at room temperature before the layers were separated. The solvent was dried over Na_2SO_4 and removed under vacuum. Recrystallization of the solid residue from CH_2Cl_2/hexane (1:3) provided **11** as colorless crystals.

Yield: 280 mg (0.275 mmol, 92 %)

m.p.: 300 °C (dec)

^{1}H NMR ($CDCl_3$): δ = 7.49 (t, 1H; *p*-C_6H_3), 7.12 (d, 2H; *m*-C_6H_3), 6.93 (s, 4H; *m*-Mes), 2.33 (s, 6H; *p*-CH_3), 2.02 (s, 12H; *o*-CH_3)

^{13}C NMR ($CDCl_3$): δ = 148.3, 140.5, 138.0, 136.6, 130.3, 28.7, 128.0, 127.1 (Ar), 21.2, 20.8 (Me)

IR $\tilde{\nu}$ (OH) = 3611, 3587 cm^{-1}

EA: $C_{24}H_{27}Cl_2InO$ (517.19 g/mol) Calcd.: C, 55.73; H, 5.26
Found: C, 55.30; H, 5.43

Synthesis of (2,6-$Mes_2C_6H_3In)_2(\mu$-$OH)_2Cl_2$ (12)

A solution of **10** (300 mg, 0.3 mmol) in diethyl ether (30 mL) was hydrolyzed with a solution of NaOH (48mg, 1.2 mmol) in water (30 mL). The mixture was vigorously stirred for 12 h at room temperature before the layers were separated. The solvent was dried over Na_2SO_4 and removed under vacuum. Recrystallization of the solid residue from CH_2Cl_2/hexane (1:3) provided **12** as colorless crystals.

Yield: 230 mg (0.25 mmol, 83 %)

m.p.: 300 - 302 °C

^{1}H NMR ($CDCl_3$): δ = 7.30 (t, 1H; *p*-C_6H_3), 7.02 (d, 2H; *m*-C_6H_3), 6.86 (s, 4H; *m*-Mes), 2.43 (s, 6H; *p*-CH_3), 1.91 (s, 12H; *o*-CH_3)

^{13}C NMR ($CDCl_3$): δ = 149.2, 142.5, 136.3, 136.2, 135.5, 128.2, 127.8, 126.8 (Ar), 21.5, 21.4 (Me)

IR: $\tilde{\nu}$ (OH) = 3617, 3534 cm^{-1}

EA: $C_{48}H_{52}Cl_2In_2O_2$ (961.46 g/mol) Calcd.: C, 59.96; H, 5.45
Found: C, 60.13; H, 5.32

Synthesis of (2,6-$Mes_2C_6H_3In)_3(\mu$-OH)$_4Cl_2$ (13)

A solution of **10** (500 mg, 0.5 mmol) in toluene (35 mL) was hydrolyzed with a solution of NaOH (7.0 g, 175 mmol) in water (35 mL). The mixture was vigorously stirred overnight at room temperature before the layers were separated. The solvent was dried over Na_2SO_4 and removed under vacuum. Recrystallization of the solid residue from $CHCl_3$/hexane (1:3) provided **13** as colorless crystals.

Yield: 380 mg (0.27 mmol; 80 %)

m.p.: 342 - 348 °C

^{1}H NMR ($CDCl_3$): δ = 7.46, 7.40 (t, 1H; *p*-C_6H_3) 7.10, 7.00 (d, 2H; *m*-C_6H_3) 6.93, 6.88 (s, 4H; *m*-Mes) 2.45, 2.41 (s, 6H; *p*-CH_3) 1.94, 1.92 (s, 12H; *o*-CH_3)

^{13}C NMR ($CDCl_3$): δ = 148.6, 148.5, 141.3, 141.0, 137.3, 137.2, 136.8, 136.7, 136.6, 136.5, 128.5, 128.4, 128.2, 128.1, 126.6 126.5 (Ar) 21.5, 21.0, 20.9, 20.7 (Me)

IR: $\tilde{\nu}$ (OH) = 3633, 3598, 3568, 3529, 3484 cm^{-1}

EA: $C_{72}H_{79}Cl_2In_3O_4$ (1423.75 g/mol) Calcd.: C, 60.74; H, 5.59
Found: C, 60.79; H, 5.41

Synthesis of (2,6-$Mes_2C_6H_3In)_4(\mu$-OH)$_8$ (14)

A solution of **10** (500 mg, 0.5 mmol) in toluene (35 mL) was hydrolyzed with a solution of NaOH (7.0 g, 175 mmol) in water (35 mL). The mixture was vigorously stirred for 12 h at room temperature before the layers were separated. A fresh solution of NaOH (7.0 g, 175 mmol) in water (35 mL) was added, and the mixture stirred again for 12 h. The solvent was dried over Na_2SO_4 and removed under

vacuum. Recrystallization of the solid residue from $CHCl_3$/hexane (1:3) provided **14** as colorless crystals.

Yield: 340 mg (0.18 mmol, 74%)

m.p.: 354 - 360 °C

^{1}H NMR ($CDCl_3$): δ = 7.30 (t, 1H; *p*-C_6H_3), 6.87 (d, 2H; *m*-C_6H_3), 6.85 (s, 4H; *m*-Mes), 2.43(s, 6H; *p*-CH_3), 1.90 (s, 12H; *o*-CH_3)

^{13}C NMR ($CDCl_3$): δ = 149.1, 142.5, 136.3, 135.8, 135.4, 128.2, 127.8, 126.8 (Ar) 21.5, 21.4 (Me)

IR: $\tilde{\nu}$ (OH) = 3646, 3632, 3599 cm^{-1}

EA: $C_{96}H_{108}In_4O_8$ (1849.2 g/mol) Calcd.: C, 62.35; H, 5.89
Found: C, 62.29; H, 5.87

Synthesis of [(2,6-$Mes_2C_6H_3In)_2(OH)_2(O_2PMe_2)_2$] (15)

A mixture of [2,6-$Mes_2C_6H_3In(OH)_2]_4$ (**14**) (200 mg, 0.11 mmol) and dimethyl phosphinic acid (40 mg, 0.4 mmol) in THF (25 mL) was stirred overnight at rt. The solvent was completely removed in vacuum and the solid residue recrystallized from THF to give **15.**

Yield: 53 mg (0.14 mmol, 64 %)

m.p.: 290 - 292 ºC

^{1}H NMR ($CDCl_3$): δ = 7.36 - 7.32 (m, 2H; *p*-C_6H_3), 7.02, 6.97 (d, 4H; *m*-C_6H_3), 6.89, 6.87 (s, 8H, *m*-Mes), 2.54, 2.39 (s, 12H; *p*-CH_3), 2.00, 1.98 (s, 24H; *o*-CH_3), 0.90 (d, 12H; Me).

^{13}C NMR ($CDCl_3$): δ = 148.5, 148.3, 142.8, 142.1, 137.9, 136.9, 136.2, 136.0, 135.5, 135.3, 128.4, 128.2, 128.0, 127.8, 127.3, 126.4 (Ar) 21.8, 21.7, 21.4, 21.3, 21.2, 20.9, 18.3, 17.3 (Me)

^{31}P NMR: δ = 40.5

IR: $\tilde{\nu}$ (OH) = 3624 cm^{-1}

EA: $C_{52}H_{80}In_2O_6P_2$ (1092.74 g/mol): Calc.: C, 57.14; H, 7.32
Found: C, 57.15; H 7.35

Synthesis of [(2,6-$Mes_2C_6H_3In)_2(OH)(O_2PPh_2)_3$] (16)

A mixture of **14** (190 mg, 0.10 mmol) and diphenylphosphinic acid (140 mg, 0.64 mmol) in THF (25 mL) was stirred overnight at rt. The solvent was completely removed in vacuum and the solid residue recrystallized from CH_2Cl_2 / hexane (1:3) to give **16**.

Yield: 0.27 mg (0.17 mmol, 87 %)

m.p.: 330 ºC (dec.)

^{1}H NMR ($CDCl_3$): δ = 7.50 - 7.44 (m, 6H; C_6H_5), 7.39 - 7.27 (m, 24H; C_6H_5 + 2H; *p*-C_6H_3), 6.93 (d, 4H; *m*-C_6H_3), 6.47 (s, 8H; *m*-Mes) 2.33 (s, 12H; *p*-CH_3), 1.73 (s, 24H; *o*-CH_3).

^{13}C NMR ($CDCl_3$): δ = 149.2, 147.7, 142.3, 142.2, 137.3, 136.8, 136.5, 135.9, 135.7, 131.7, 131.6, 130.9, 130.2, 130.1, 129.4, 128.5, 128.3, 128.1, 127.7, 127.6, 127.2, 127.1, 127.0, 125.7 (Ar), 21.5, 21.4 (Me)

^{31}P NMR($CDCl_3$): δ = 31.8 (s, 1P), 28.0 (s, 2P).

IR: $\tilde{\nu}$ (OH) = 3587 cm^{-1}

EA: $C_{84}H_{80}In_2O_7P_3$ (1524.03g/mol): Calcd.: C, 66.14; H 5.24
Found: C, 65.35; H 5.10

Synthesis of [(2,6-$Mes_2C_6H_3In$)($Me_5C_3HPO_2$)$_2$(H_2O)$_2$] (17)

A mixture of [2,6-$Mes_2C_6H_3In(OH)_2]_4$ (**14**) (110 mg, 0.06 mmol) and 2,2,3,4,4-pentamethylphosphetanic acid (PMTA) (100 mg, 0.47 mmol) in THF (25 mL) was stirred overnight at rt. The solvent was completely removed in vacuum and the solid residue recrystallized from CH_2Cl_2 / hexane (1:3) to give **17**.

Yield: 167 mg (0.20 mmol, 86 %)

m.p.: 263 - 265 ºC

^{1}H NMR ($CDCl_3$): δ = 7.33 (t, 1H; *p*-C_6H_3), 6.94 (d, 2H; *m*-C_6H_3), 6.89 (s, 4H; *m*-Mes), 2.39 (s, 6H; *p*-CH_3), 1.99 (s, 12H; *o*-CH_3), 1.00 - 0.70 (m, 32H; Me + CH, PMTA).

^{13}C NMR ($CDCl_3$): δ = 148.8, 142.0, 136.6, 135.8, 128.8, 128.5, 128.2, 126.6 (Ar) 49.8, 49.0(*C*-PMTA) 41.9 (*CH*-PMTA) 24.2, 22.6 (*Me*-PMTA) 21.2, 21.1 (*Me*-Ter) 19.1 (*Me*-PMTA)

^{31}P NMR ($CDCl_3$): δ = 49.4

IR: $\tilde{\nu}$ (OH) = 3626 cm^{-1}

EA: $C_{40}H_{62}InO_6P_2$ (815.66 g/mol): Calcd.: C, 58.84; H, 7.60
Found: C, 58.91; H, 7.55

Synthesis of (2,6-$Mes_2C_6H_3In$)(*t*Bu_2Sn)$_2$O$(OH)_2Cl_2$ (18)

A solution of **10** (200 mg, 0.40 mmol) in 30 mL THF was treated with (*t*$Bu_2SnO)_3$ (200 mg, 0.26 mmol). The solution was vigorously stirred at rt in a schlenk tube. After over

night stirring the reaction mixture was extracted from the solvent. The product was recrystallized in $CHCl_3$/hexane.

Yield: 0.3 g (0.29 mmol, 74 %)

m.p.: 188 ºC sweats, 276 ^{o}C decomposes

^{1}H NMR ($CDCl_3$): δ = 7.41 (t, 1H, *p*-CH_3), 7.00 (d, 2H, *m*-C_6H_3), 6.95 (s, 4H, *m*-Mes), 2.27 (s, 6H, *p*-CH_3), 2.12 (s,12H, *o*-CH_3), 1.27 (s, 18H, Me) 1.24 (s, 18H, Me)

^{13}C NMR ($CDCl_3$): δ = 149.6, 142.6, 137.1, 136.3, 129.0, 128.2, 128.0 (Ar), 44.0, 41.0, 30.0, 29.9, 21.3, 20.1 (Me).

^{119}Sn NMR ($CDCl_3$): δ = –202

IR $\tilde{\nu}$ (OH) = 3599 (w), 3450 (s)

EA: $C_{40}H_{61}Cl_2InO_3Sn_2$ (1013.05 g/mol): Calcd.: C, 47.42; H, 6.07
Found: C, 47.53; H 6.10

Synthesis of (2,6-$Mes_2C_6H_3In)_2$(*t*$Bu_2Sn)O(OH)_2$ (19)

A solution of [2,6-$Mes_2C_6H_3In(OH)_2]_4$ (180 mg, 0.10 mmol) in chloroform was treated with (*t*$Bu_2SnO)_3$ (50 mg, 0.07 mmol) in a test tube and subjected to ultrasonic bath for two hours. Afterwards the reaction mixture was extracted from the solvent.

Yield: 134 mg (0.12 mmol, 53 %)

m.p.: starts sweating at 230 ^{o}C

^{1}H NMR ($CDCl_3$): δ = 7.35, 7.34 (t, 2H; *p*-CH_3), 6.97-6.88 (m, 4H; *m*-C_6H_3, 8H; *m*-Mes), 2.45, 2.42 (s, 12H, *p*-CH_3), 2.04, 2.00 (s, 24H; *o*-CH_3), 0.84 (s, 18H, *t*Bu)

^{13}C NMR ($CDCl_3$) δ = 149.5, 149.0, 142.8, 142.5, 136.4, 136.2, 135.8, 135.4, 135.3, 128.3, 128.1, 128.0, 127.8, 126.7, 126.6, (Ar) 30.5, 30.3, 21.6, 21.5, 21.4, 21.2 (Me).

^{119}Sn NMR ($CDCl_3$): δ = –278

IR: $\tilde{\nu}$ (OH) = 3646, 3630, 3586 cm^{-1}.

EA: $C_{56}H_{70}In_2O_3Sn$ (1137.48 g/mol): Calcd.: C 59.13; H, 6.03
Found: C 59.30; H 6.10

Synthesis of (2,6-$Mes_2C_6H_3In)_3(HCO_3)_2(OH)_4$ (20)

250 mg (0.14 mmol) of **14** were dissolved in 35 mL of $CHCl_3$ and CO_2 is bubbled through the solvent for approx 8 - 10 hr (approx. 700 g dry ice is used) in order to keep the compound in dissolved state the volume of chloroform is kept constant by adding the solvent as the rate of evaporation is much higher during the process of bubbling CO_2 through the solution. After the process has been completed the solvent is subjected to evaporation in open atmosphere until crystalline product (2,6-$Mes_2C_6H_3In)_2(OH)_4(HCO_3)_2$ (**20**) is obtained.

Yield: 120 mg (0.08 mmol, 60 %)

m.p.: 265 - 267 ºC

^{1}H NMR ($CDCl_3$): δ = 7.42, 7.37 (t, 1H; *p*-CH_3), 7.07, 6.98 (d, 2H; *m*-C_6H_3), 6.89, 6.81 (s, 4H; *m*-Mes), 2.36, 2.27 (s, 6H; *p*-CH_3), 1.97, 1.90 (s, 12H; *o*-CH_3).

^{13}C NMR ($CDCl_3$): δ = 176.3, 149.2, 148.9, 141.70, 141.2, 136.8, 136.5, 129.3, 128.6, 128.0, 127.5, 126.0 (Ar) 23.2, 21.2, 20.1, 20.5 (Me).

IR: $\tilde{\nu}$ (OH) = 3636, 3570 cm^{-1}

EA: $C_{74}H_{81}In_3O_{10}$ (1474.85 g/mol): Calcd.: C, 60.24; H, 5.48
Found: C, 51.77; H, 5.07.

Synthesis of (2,6-$Mes_2C_6H_3In)_4(CO_3)_2(OH)_4 \cdot 2\ H_2O$ (21)

A solution of **14** (250 mg, 0.14 mmol) in THF (35 mL) was purged with a slow stream of CO_2. Approx. within 2 h, the precipitation of the crude product starts. After 5 h, the precipitate was collected and recrystallized from $CHCl_3$/hexane to give **21**.

Yield: 168 mg (0.09 mmol, 64 %)

m.p.: 240 - 242 ºC

^{1}H NMR ($CDCl_3$): δ = 7.40 (t, 1H; *p*-CH_3), 7.03(d, 2H; *m*-C_6H_3), 6.87 (s, 4H; *m*-Mes), 2.42 (s, 6H; *p*-CH_3), 1.94 (s, 12H; *o*-CH_3)

^{13}C NMR ($CDCl_3$): δ = 165.8, 149.4, 141.1, 137.2, 136.2, 129.3, 128.0, 127.5, 126.3 (Ar) 21.3, 20.9 (Me).

IR: $\tilde{\nu}$ (OH) = 3646, 3629 cm^{-1}

EA: $C_{98}H_{102}In_4O_{12}$ (1931.08 g/mol): Calcd.: C, 60.90; H, 5.28
Found: C, 57.67; H, 5.20.

Synthesis of (2,6-$Mes_2C_6H_3In)_4(OCH_2CH_2O)_2(OH)_4$ (22)

300 mg (0.16 mmol) of **14** were dissolved in 35 mL of THF in a schlenk tube. 4-6 drops (stoichiometric excess) of ethylene glycol are added to the solution. After overnight stirring at room temperature the solvent is removed and the solid residue redissolved in 50 mL THF. The volume is reduced to almost half. After standing at room temperature for 72 hours, X-ray quality crystals of **22** appear in the Schlenk tube.

Yield: 173 mg (0.09 mmol, 56 %)

m.p.: 274 - 276 ºC

^{1}H NMR ($CDCl_3$): δ = 7.31, 7.29, 7.27, 7.25 (t, 1H; *p*-CH_3), 6.98, 6.95, 6.90, 6.87 (d, 2H; *m*-C_6H_3), 6.85, 6.84, 6.81, 6.75 (s, 4H; *m*-Mes), 2.39, 2.38 (s, 4H; CH_2), 1.98, 1.97, 1.96, 1.95 (s, 6H; *p*-CH_3), 1.94, 1.89, 1.86, 1.85 (s, 12H; *o*-CH_3).

^{13}C NMR ($CDCl_3$): δ = 149.8, 149.7, 149.6, 149.4, 143.1, 143.0, 142.9, 142.7, 137.2, 136.9, 136.8, 136.40, 136.3, 136.1, 136.0, 135.8, 135.7, 135.6, 135.5, 135.2, 128.4, 128.3, 128.2, 128.1, 128.0, 127.8, 127.7, 127.5, 127.4, 127.3, 127.2, 127.1, 126.8 (Ar), 22.3, 22.1, 21.9, 21.8, 21.7, 21.6, 21.5, 21.4, 21.3, 21.2, 21.1, 21.0 (Me).

IR: $\tilde{\nu}$(OH) = 3641, 3631 cm^{-1}

EA: $C_{108}H_{132}In_4O_{10}$ (2049.42 g/mol): Calcd.: C, 63.25; H, 6.44
Found: C, 59.82; H, 5.28.

Synthesis of (2,6-$Mes_2C_6H_3In)_4(CO_3)_2(OCH_2CH_2OH)_2(OH)_2$ (23)

200 mg (0.10 mmol) of **14** were dissolved in 25 mL of THF. 2-3 drops (stochiometric excess) of ethylene glycol are added to the solution. After overnight stirring at room temperature the solvent is removed and solid residue redissolved in chloroform. The compound is recrystallized in CH_2Cl_2/hexane.

Yield: 154 mg (0.08 mmol, 71 %)

m.p.: 260 - 262 ºC

^{1}H NMR ($CDCl_3$): δ = 7.41-7.33 (m, 4H; *p*-CH_3), 7.02-6.79 (m, 24H; *m*-C_6H_3 + *m*-Mes), 2.52-2.24 (m, 32H; *p*-CH_3 + CH_2), 1.98-1.95 (m, 48H; *o*-CH_3).

^{13}C NMR ($CDCl_3$): δ = 167.6, 150.2, 150.1, 149.9, 149.7, 149.4, 149.3, 149.1, 142.2, 142.1, 142.0, 141.5, 141.4, 141.3, 141.2, 136.7, 136.5, 135.7, 132.5, 130.8, 129.5, 129.3, 129.0, 128.8, 128.0, 127.7, 127.6, 127.4, 126.9, 126.3 (Ar) 38.7, 30.3, 28.9, 23.7, 22.9, 21.4, 21.2, 21.1, 21.0, 20.9, 20.8, 20.7 (Me).

IR: $\tilde{\nu}$ (OH) = 3623 cm^{-1}

EA: $C_{102}H_{110}In_4O_{12}$ (1987.18 g/mol): Calcd.: C, 61.60; H, 5.53
Found: C, 61.34; H, 5.32

Synthesis of (2,6-$Mes_2C_6H_3Tl)_2(\mu$-$Cl)_2Cl_2$ (24)

A solution of (2,6-$Mes_2C_6H_3Tl)_2(\mu$-$OH)_2Cl_2$ (**26**) (500 mg, 0.43 mmol) in diethyl ether was treated with 1 M HCl (10 mL). The mixture was stirred for 2 h before the layers were separated. The organic layer was dried over Na_2SO_4 and the solvent removed under vacuum. Recrystallization from $CHCl_3$/ hexane (1:3) furnished **24** as colorless crystals.

Yield: 470 mg (0.37 mmol, 92 %)

m.p: 132 - 134 °C

^{1}H NMR ($CDCl_3$): δ = 7.45 (t, 1H, *p*-C_6H_3), 7.11 (d, 2H, *m*-C_6H_3), 6.94 (s, 4H, *m*-Mes), 2.32 (s, 6H, *p*-CH_3), 2.05 (s, 12H; *o*-CH_3)

^{13}C NMR ($CDCl_3$): δ = 141.1, 139.0, 136.4, 135.8, 130.2, 128.4, 128.0, 127.5 (Ar) 21.0, 20.7 (Me)

EA: $C_{48}H_{50}Cl_4Tl_2$ (1177.48 g/mol) Calcd.: C, 48.96; H, 4.28
Found: C, 48.92; H, 4.59

Synthesis of [(2,6-$Mes_2C_6H_3$)$_2$Tl]$TlCl_4$ (25)

In the absence of light, a stirred suspension of TlCl (1.55 g, 6.46 mmol) in Et_2O (75 mL) was cooled to –18 °C, and a solution of 2,6-$Mes_2C_6H_3Li$ (2.07 g, 6.46 mmol) in Et_2O (30 mL) was added dropwise. The reaction mixture was then allowed to warm to room temperature and stirred for 4 h. Then, the solution was cooled to 0 °C, and SO_2Cl_2 (2.11 g, 15.65 mmol) was slowly added via syringe. The reaction mixture was stirred at room temperature for 2 h before the precipitate of LiCl was filtered off. The solvent was removed under reduced pressure and the crude solid recrystallized from $CHCl_3$/hexane to give colorless crystals of **25**·2 $CHCl_3$. The crystals were dried at 50 °C under high vacuum to give an analytical sample of **25**.

Yield: 2.58 g (2.20 mmol, 68 %)

m.p.: 120 -124 °C

^{1}H NMR ($CDCl_3$): δ = 7.46 (t, 3H; *p*-C_6H_3), 7.09 (d, 2H, *m*-C_6H_3), 6.94 (s, 8H; Ar), 2.33 (s, 12H; CH_3), 2.05 (s, 24H; CH_3)

^{13}C NMR ($CDCl_3$): δ = 141.0, 138.9, 136.4, 135.8, 130.2, 128.3, 127.9, 127.4 (Ar), 21.0, 20.7 (Me)

EA: $C_{48}H_{50}Cl_4Tl_2$ (1177.48 g/mol) Calcd.: C, 48.96; H, 4.28
Found: C, 48.73; H, 4.15

ESI-TOF MS (MeOH, positive mode): m/z 831.4 ($[C_{48}H_{50}Tl]^+$)

Synthesis of (2,6-$Mes_2C_6H_3Tl)_2$ (*μ*-$OH)_2Cl_2$ (26)

In the absence of light, a stirred suspension of TlCl (1.55 g, 6.46 mmol) in 75 mL of Et_2O was cooled to –18 °C, and a solution of 2,6-$Mes_2C_6H_3Li$ (2.07 g, 6.46 mmol) in 25 mL of Et_2O was added dropwise to the suspension. The reaction mixture was then allowed to warm to room temperature and stirred for over 4 h. The solvent was removed under vacuum. The solid residue was extracted with $CHCl_3$ in the air. After

filtration the solvent was again removed under vacuum. Recrystallization of the colorless residue from $CHCl_3$/hexane (1:3) yielded **26** as colorless crystals.

Yield: 2.57 g (2.25 mmol, 69.8%)

m.p.: dec at 270 °C

^{1}H NMR ($CDCl_3$): δ = 7.46 (t, 1H; *p*-C_6H_3), 7.11 (d, 2H; *m*-C_6H_3), 6.95 (s, 4H; *m*-Mes), 2.33 (s, 6H; *p*-CH_3), 2.05 (s, 12H; *o*-CH_3)

^{13}C NMR ($CDCl_3$): δ = 141.2, 139.1, 136.6, 136.0, 130.3, 128.5, 128.2, 127.6 (Ar) 21.2, 21.0 (Me)

IR: $\tilde{\nu}$ (OH) = 3574, 3551 cm^{-1}

EA: $C_{48}H_{52}Cl_2O_2Tl_2$ (1140.59 g/mol) Calcd.: C, 50.54; H, 4.60 Found: C, 50.50; H, 4.48

Synthesis of (2,6-$Mes_2C_6H_3Tl)_4Tl_2(\mu_3$-O)$_4(\mu$-OH)$_6$ (27)

A solution of **26** (500 mg, 0.43 mmol) in $CHCl_3$ (30 mL) was hydrolyzed with a solution of NaOH (1.2 g, 30 mmol) in water (30 mL). The mixture was vigorously stirred for 2 h at room temperature before the layers were separated. The solvent was dried over Na_2SO_4 and removed under vacuum. Recrystallization of the solid residue from $CHCl_3$/hexane (1:3) provided **27** as colorless crystals.

Yield: 300 mg (0.11 mmol, 79%)

m.p.: 120 -124 ºC

^{1}H NMR ($CDCl_3$): δ = 7.45 (t, 1H; *p*-C_6H_3), 7.11 (d, 2H; *m*-C_6H_3), 6.94 (s, 4H; *m*-Mes), 2.33 (s, 6H; *p*-CH_3), 2.05 (s, 12H; *o*-CH_3)

^{13}C NMR ($CDCl_3$): δ = 141.1, 139.0, 136.4, 135.8, 130.2, 128.4, 128.0, 127.5 (Ar), 21.0, 20.7 (Me)

IR: $\tilde{\nu}$ (OH) = 3596 cm^{-1}

EA: $C_{96}H_{106}Tl_6O_{10}$ (2644.2 g/mol) Calcd.: C, 43.56; H, 4.00
Found: C, 43.49; H, 4.06

6. Annex

Crystallography

Data collection and refinement

The X-ray data collection was performed by Dr. Jens Beckmann and Dr. Malte Hesse. Intensity data were collected on a STOE IPDS 2T area detector with graphite-monochromated Mo-Kα (0.7107 Å) radiation at the Institute of Chemistry and Biochemistry, Inorganic Chemistry at the Freie University, Berlin.
Data were reduced and corrected for absorption using the program Stoe X-Area.[109] The structures were solved by direct methods and difference Fourier synthesis using SHELXS-97 implemented in the program WinGX 2002.[110] Full-matrix least-squares refinements on F^2, using all data. All non-hydrogen atoms were refined using anisotropic displacement parameters. Carbon bonded hydrogen atoms were included in geometrically calculated positions using a riding model and were refined isotropically. Figures were created using program DIAMOND.[111]

Disorder in molecular structures

Disorder was resolved for the In atom of **10** and refined with split occupancies of 0.9 (In1) and 0.1 (In1′). Disorder was also resolved for one Tl atom and five O atoms of **27** and refined with split occupancies of 0.45 (Tl3), 0.05 (Tl3′) and 0.5 (Tl4) as well as 0.5 (O1 - O10), respectively. The absolute structures of **10** and **11** are determined by refinement of the Flack parameters 0.0(4) and 0.0(3) and comparison of the R-values of the enantiomeric space groups.

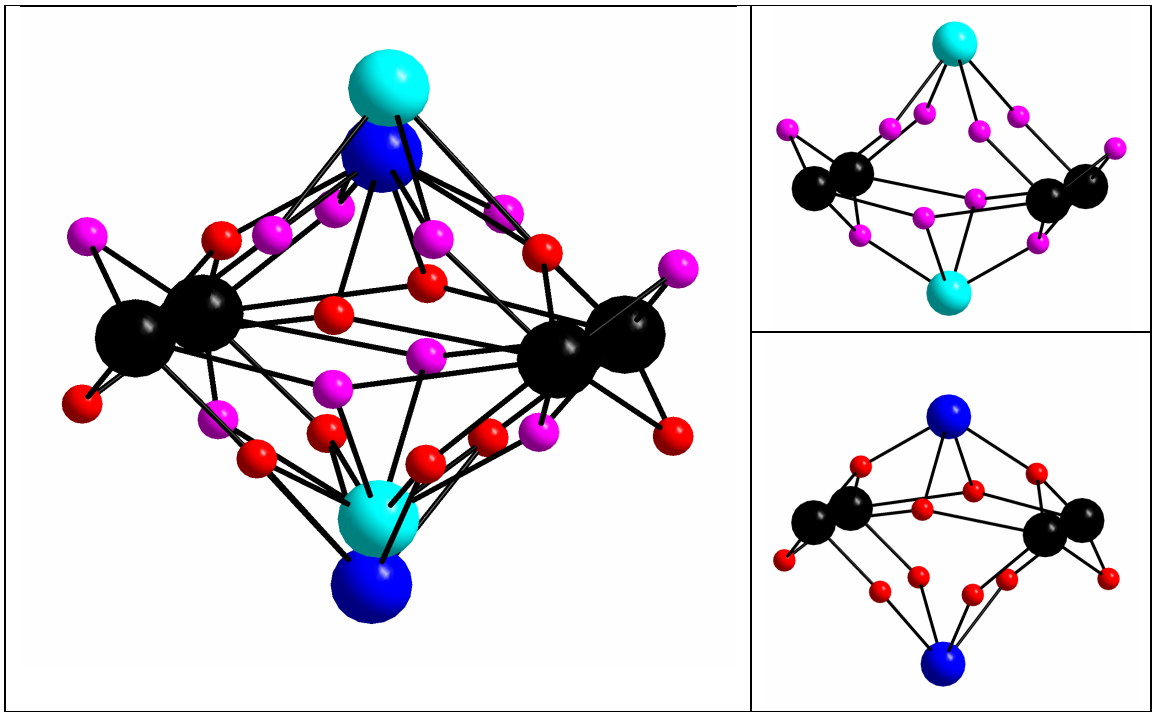

Figure 48: Illustration of the disordered fragments of **27**. Disordered Tl atoms are colored in blue and turquoise and the O atoms are colored in red and pink. The black Tl atoms are not disordered.

2,6-$Mes_2C_6H_3SnCl_3$ (1)

Formula	$C_{24}H_{25}Cl_3Sn$
Formula weight, g mol^{-1}	538.48
Crystal system	Monoclinic
Crystal size, mm	0.40 × 0.14 × 0.08
Space group	$P2_1/c$
Cell constants a, b, c (Å)	9.288(1), 17.339(2), 15.672(2)
Angle α,β,γ, (º)	90, 105.729(9), 90
Cell volume ($Å^3$)	2429.4(5)
Z	4
Density, (g/cm^3)	1.472
Absorption coefficient (mm^{-1})	1.389
F(000)	1080
θ range, deg	1.79 to 26.00
Collected / independent reflections	11421 / 4745
Observed reflections with ($I>2\sigma(I)$)	3224
Completeness to θ_{max}	99.3 %
parameter	253
GooF	0.989
R_1 (F) ($I > 2\sigma(I)$)	0.0462
wR_2 (F^2) (all data)	0.1542
$(\Delta/\sigma)_{max}$	< 0.001
Largest diff peak / hole, e $Å^{-3}$	0.771 / –1.500
CCDC- Number	749947

2,6-$Mes_2C_6H_3Sn(OH)Cl_2 \cdot H_2O$ (2)

Formula	$C_{24}H_{28}Cl_2O_2Sn$
Formula weight, g mol $^{-1}$	538.05
Crystal system	Monoclinic
Crystal size, mm	0.47 × 0.12 × 0.10
Space group	$P2_1/n$
Cell constants a, b, c (Å)	8.1715(5), 18.003(2), 15.718(1)
Angle α, β, γ (º)	90, 94.206(5), 90
Cell volume (Å^3)	2306.2(3)
Z	4
Density, (g/cm^3)	1.550
Absorption coefficient (mm^{-1})	1.357
F(000)	1088
θ range, deg	1.72 to 26.00
Collected / independent reflections	12355 / 4485
Observed reflections with ($I>2\sigma(I)$)	3025
Completeness to θ_{max}	99.0 %
parameter	262
GooF	0.928
R_1 (F) ($I > 2\sigma(I)$)	0.0425
wR_2 (F^2) (all data)	0.1163
$(\Delta/\sigma)_{max}$	< 0.001
Largest diff peak / hole, e Å^{-3}	0.680 / –1.331
CCDC- Number	749948

***trans*-[2,6-$Mes_2C_6H_3Sn(O)(OH)]_3$·½ Hexane (3)**

Formula	$C_{75}H_{85}O_6Sn_3$
Formula weight, g mol^{-1}	1438.63
Crystal system	Triclinic
Crystal size, mm	0.18 × 0.10 × 0.09
Space group	*P*-1
Cell constants a, b, c (Å)	12.247(9), 14.135(1), 21.963(1)
Angle α, β, γ (º)	81.47(6), 77.24(6), 67.73(5)
Cell volume ($Å^3$)	3423(4)
Z	2
Density, (g/cm^3)	1.396
Absorption coefficient (mm^{-1})	1.136
F(000)	1466
θ range, deg	1.83 to 26.00
Collected / independent reflections	27988 / 13335
Observed reflections with ($I>2\sigma(I)$)	5691
Completeness to θ max	99.1%
Parameter	757
GooF	0.714
R1 (F) ($I > 2\sigma(I)$)	0.0431
wR2 (F2) (all data)	0.1531
(Δ/σ)max	< 0.001
Largest diff peak / hole, e $Å^{-3}$	0.972 / –1.214
CCDC- Number	749949

[*t*Bu$_2$Sn(OH)OSnR(OH)$_2$OC(OSn*t*Bu$_2$OH)$_2$(O)SnR(OH)(H$_2$O)]$_2$ (5, R = 2,6-Mes$_2$C$_6$H$_3$).

Formula	$C_{146}H_{218}O_{24}Sn_{10}$
Formula weight, g mol^{-1}	3544.10
Crystal system	Monoclinic
Crystal size, mm	0.35 × 0.32 × 0.05
Space group	*C*2/*c*
Cell constants a, b, c (Å)	34.649(2), 17.583(9), 26.205(2)
Angle α, β, γ (º)	90, 99.01(4), 90
Cell volume (Å^3)	15768(14)
Z	4
Density, (g/cm^3)	1.489
Absorption coefficient (mm^{-1})	1.616
F(000)	7104
θ range, deg	4
Collected / independent reflections	1.82 to 26.00
Observed reflections with ($I>2\sigma(I)$)	39158 / 14201
Completeness to θ_{max}	99.5 %
Parameter	811
GooF	0.827
R_1 (F) ($I > 2\sigma(I)$)	0.0591
wR_2 (F^2) (all data)	0.1979
$(\Delta/\sigma)_{max}$	< 0.001
Largest diff peak / hole, e Å^{-3}	1.087 / –1.800
CCDC- Number	749950

$K_6[MeSn(O)CO_3]_6 \cdot 14\ H_2O$ (7)

Formula	$C_{12}H_{46}K_6O_{38}Sn_6$
Formula weight, g mol^{-1}	1745.23
Crystal system	Triclinic
Crystal size, mm	0.25 × 0.20 × 0.17
Space group	*P*-1
Cell constants a, b, c (Å)	9.572(2), 11.724(2), 11.838(2)
Angle α, β, γ (º)	62.77(1), 76.19(2), 87.76(2)
Cell volume ($Å^3$)	1143.4(4)
Z	1
Density, (g/cm^3)	2.494
Absorption coefficient (mm^{-1})	3.878
F(000)	808
θ range, deg	0.71073 to 26.00
Collected / independent reflections	8284 / 2961
Observed reflections with ($I>2\sigma(I)$)	4223
Completeness to θ max	93.9 %
Parameter	280
GooF	0.995
R1 (F) ($I > 2\sigma(I)$)	0.0637
wR2 (F2) (all data)	0.1663
(Δ/σ)max	< 0.001
Largest diff peak / hole, e $Å^{-3}$	1.923 / –2.739
CCDC- Number	751878

[2,6-$Mes_2C_6H_3Sn(OH)_2(O_2PPh_2)]_2 \cdot 2\ CHCl_3$ (8)

Formula	$C_{74}H_{76}Cl_6O_8P_2Sn_2$
Formula weight, g mol^{-1}	1605.37
Crystal system	Monoclinic
Crystal size, mm	0.35 × 0.29 × 0.23
Space group	$P2_1/n$
Cell constants a, b, c (Å)	15.228(2), 14.933(6), 15.671(9)
Angle α, β, γ (º)	90, 98.17(7), 90
Cell volume ($Å^3$)	3528(4)
Z	2
Density, (g/cm^3)	1.511
Absorption coefficient (mm^{-1})	1.036
F(000)	1632
θ range, deg	2.21 to 26.00
Collected / independent reflections	19480 / 6914
Observed reflections with ($I>2\sigma(I)$)	4728
Completeness to θ max	99.6 %
Parameter	423
GooF	0.925
R1 (F) ($I > 2\sigma(I)$)	0.0455
wR2 (F2) (all data)	0.1476
(Δ/σ)max	< 0.001
Largest diff peak / hole, e $Å^{-3}$	0.849 / –1.357
CCDC- Number	749951

$Na_3(2,6\text{-}Mes_2C_6H_3Sn)_4O_6(OH)_3 \cdot 2$ toluene (9)

Formula	$C_{110}H_{119}Na_3O_9Sn_4$
Formula weight, g mol^{-1}	2128.78
Crystal system	Monoclinic
Crystal size, mm	0.39 × 0.23 × 0.21
Space group	*C*2/*c*
Cell constants a, b, c (Å)	26.14(2), 15.394(8), 26.50(2)
Angle α, β, γ (º)	90, 113.11(7), 90
Cell volume ($Å^3$)	9809(13)
Z	4
Density, (g/cm^3)	1.441
Absorption coefficient (mm^{-1})	1.077
F(000)	4332
θ range, deg	1.93 to 26.00
Collected / independent reflections	26979 / 9596
Observed reflections with ($I>2\sigma(I)$)	6762
Completeness to θ max	99.4 %
Parameter	573
GooF	0.928
R1 (F) ($I > 2\sigma(I)$)	0.0390
wR2 (F2) (all data)	0.0983
(Δ/σ)max	< 0.001
Largest diff peak / hole, e $Å^{-3}$	0.527 / –1.273
CCDC- Number	749952

(2,6-$Mes_2C_6H_3In)_2(\mu$-$Cl)_2Cl_2$ (10)

Formula	$C_{48}H_{50}Cl_4In_2$
Formula weight, g mol^{-1}	998.32
Crystal system	Orthorhombic
Crystal size, mm	0.18 × 0.17 × 0.15
Space group	Fdd2
Cell constants a, b, c (Å)	27.593(6), 14.179(3), 23.793(5)
Angle α, β, γ (º)	90, 90, 90
Cell volume ($Å^3$)	9309(3)
Z	8
Density, (g/cm^3)	1.425
Absorption coefficient (mm^{-1})	1.251
F(000)	4032
θ range, deg	0.99 to 25.25
Collected / independent reflections	16 640 / 2162
Observed reflections with ($I>2\sigma(I)$)	1767
Completeness to θ max	99.8 %
Parameter	250
GooF	1.033
R1 (F) ($I > 2\sigma(I)$)	0.0543
wR2 (F2) (all data)	0.1389
(Δ/σ)max	< 0.001
Largest diff peak / hole, e $Å^{-3}$	0.970 / –0.743
CCDC-Number	751065

2,6-$Mes_2C_6H_3InCl_2 \cdot H_2O$ (11)

Formula	$C_{24}H_{25}Cl_2InO$
Formula weight, g mol^{-1}	515.16
Crystal system	Orthorhombic
Crystal size, mm	0.25 × 0.25 × 0.11
Space group	$P2_12_12_1$
Cell constants a, b, c (Å)	8.292(4), 15.249(8), 19.409(9)
Angle α, β, γ (º)	90, 90, 90
Cell volume ($Å^3$)	2454(2)
Z	4
Density, (g/cm^3)	1.394
Absorption coefficient (mm^{-1})	1.191
F(000)	1040
θ range, deg	0.99 to 25.25
Collected / independent reflections	9466 / 4280
Observed reflections with ($I>2\sigma(I)$)	3519
Completeness to θ max	99.3 %
Parameter	253
GooF	0.956
R1 (F) ($I > 2\sigma(I)$)	0.0528
wR2 (F2) (all data)	0.1304
(Δ/σ)max	< 0.001
Largest diff peak / hole, e $Å^{-3}$	0.533 / –1.017
CCDC-Number	751066

[(2,6-$Mes_2C_6H_3In)_2(\mu$-$OH)_2Cl_2]\cdot 2CH_2Cl_2$ (12)

Formula	$C_{49}H_{50}Cl_4In_2O_2$
Formula weight, g mol^{-1}	1042.33
Crystal system	Monoclinic
Crystal size, mm	0.17 × 0.16 × 0.13
Space group	$P2_1/n$
Cell constants a, b, c (Å)	10.874(5), 16.852(7), 13.180(4)
Angle α, β, γ (º)	90, 91.89(3), 90
Cell volume ($Å^3$)	2413(2)
Z	2
Density, (g/cm^3)	1.434
Absorption coefficient (mm^{-1})	1.212
F(000)	1052
θ range, deg	1.96 to 25.25
Collected / independent reflections	11285 / 4321
Observed reflections with ($I>2\sigma(I)$)	3045
Completeness to θ max	99.2 %
Parameter	262
GooF	0.938
R1 (F) ($I > 2\sigma(I)$)	0.0343
wR2 (F2) (all data)	0.0910
(Δ/σ)max	< 0.001
Largest diff peak / hole, e $Å^{-3}$	1.015 / –1.017
CCDC-Number	751067

(2,6-$Mes_2C_6H_3In)_3(\mu$-OH)$_4Cl_2$ (13)

Formula	$C_{72}H_{75}Cl_2In_3O_4$
Formula weight, g mol^{-1}	1419.68
Crystal system	Triclinic
Crystal size, mm	0.50 × 0.50 × 0.14
Space group	P1
Cell constants a, b, c (Å)	13.300(8), 16.108(9), 18.934(7)
Angle α, β, γ (º)	89.87(4), 105.87(4), 90.73(5)
Cell volume (Å^3)	3901(3)
Z	2
Density, (g/cm^3)	1.208
Absorption coefficient (mm^{-1})	0.987
F(000)	1440
θ range, deg	1.69 to 25.25
Collected / independent reflections	28823 / 14021
Observed reflections with (I>2σ(I))	9660
Completeness to θ max	99.3 %
Parameter	730
GooF	1.040
R1 (F) (I > 2σ(I))	0.0581
wR2 (F2) (all data)	0.1943
(Δ/σ)max	< 0.001
Largest diff peak / hole, e Å^{-3}	1.916 / –1.025
CCDC-Number	751068

[(2,6-$Mes_2C_6H_3In)_4(\mu$-$OH)_8]\cdot H_2O\cdot 2CHCl_3$ (14)

Formula	$C_{98}H_{100}Cl_6In_4O_9$
Formula weight, g mol^{-1}	2093.76
Crystal system	Monoclinic
Crystal size, mm	0.48 × 0.20 × 0.06
Space group	C2/c
Cell constants a, b, c (Å)	24.77(1), 15.353(5), 27.74(1)
Angle α, β, γ (º)	90, 115.91(3), 90
Cell volume ($Å^3$)	9488(6)
Z	4
Density, (g/cm^3)	1.466
Absorption coefficient (mm^{-1})	1.183
F(000)	4232
θ range, deg	0.99 to 25.25
Collected / independent reflections	21866 / 8538
Observed reflections with ($I>2\sigma(I)$)	5172
Completeness to θ max	99.1 %
Parameter	532
GooF	0.890
R1 (F) ($I > 2\sigma(I)$)	0.0397
wR2 (F2) (all data)	0.0836
(Δ/σ)max	< 0.001
Largest diff peak / hole, e $Å^{-3}$	0.894 / –0.751
CCDC-Number	751069

[(2,6-$Mes_2C_6H_3In)_2(OH)_2(O_2PMe_2)_2$] (15)

Formula	$C_{52}H_{80}In_2O_6P_2$
Formula weight, g mol^{-1}	1092.74
Crystal system	Triclinic
Crystal size, mm	0.25 × 0.15 × 0.17
Space group	C2/c
Cell constants a, b, c (Å)	13.841(3), 22.730(5), 17.909(4)
Angle α, β, γ (º)	90, 111.72(3), 90
Cell volume ($Å^3$)	5234(2)
Z	4
Density, (g/cm^3)	1.387
Absorption coefficient (mm^{-1})	0.988
F(000)	2272
θ range, deg	1.76 to 25.25
Collected / independent reflections	4603 / 4603
Observed reflections with ($I>2\sigma(I)$)	2530
Completeness to θ max	97.0%
Parameter	279
GooF	0.990
R1 (F) ($I > 2\sigma(I)$)	0.0827
wR2 (F2) (all data)	0.2178
(Δ/σ)max	< 0.001
Largest diff peak / hole, e $Å^{-3}$	1.153 / –1.400

[(2,6-$Mes_2C_6H_3In)_2(OH)(O_2PPh_2)_3$] (16)

Formula	$C_{84}H_{80}In_2O_7P_3$
Formula weight, g mol^{-1}	1524.03
Crystal system	Monoclinic
Crystal size, mm	0.45 × 0.32 × 0.15
Space group	$P2_1/c$
Cell constants a, b, c (Å)	14.746(8), 23.594(19), 20.913(17)
Angle α, β, γ (º)	90, 95.38(6), 90
Cell volume ($Å^3$)	7244(9)
Z	4
Density, (g/cm^3)	1.397
Absorption coefficient (mm^{-1})	0.758
F(000)	3132
θ range, deg	1.81 to 29.24
Collected / independent reflections	49527 / 19461
Observed reflections with ($I>2\sigma(I)$)	7420
Completeness to θ max	98.5 %
Parameter	865
GooF	0.749
R1 (F) ($I > 2\sigma(I)$)	0.0542
wR2 (F2) (all data)	0.1127
(Δ/σ)max	< 0.001
Largest diff peak / hole, e $Å^{-3}$	0.464 / –1.079

[(2,6-$Mes_2C_6H_3In$)($Me_5C_3HPO_2$)$_2$(H_2O)$_2$] (17)

Formula	$C_{40}H_{62}InO_6P_2$
Formula weight, g mol^{-1}	815.66
Crystal system	Monoclinic
Crystal size, mm	0.50 × 0.31 × 0.21
Space group	$P2_1/a$
Cell constants a, b, c (Å)	24.88(2), 16.48(5), 26.03(2)
Angle α, β, γ (º)	90, 116.12(4), 90
Cell volume (Å^3)	9585(9)
Z	8
Density, (g/cm^3)	1.130
Absorption coefficient (mm^{-1})	0.596
F(000)	3432
θ range, deg	2.66 to 29.26
Collected / independent reflections	67449 / 25594
Observed reflections with (I>2σ(I))	5543
Completeness to θ max	97.9 %
Parameter	5543
GooF	0.542
R1 (F) (I > 2σ(I))	0.0533
wR2 (F2) (all data)	0.1076
(Δ/σ)max	< 0.001
Largest diff peak / hole, e Å^{-3}	0.364 / –0.379

[(2,6-$Mes_2C_6H_3In$)(*t*$Bu_2Sn)_2O(OH)_2Cl_2$]·$CHCl_3$ (18)

Formula	$C_{41}H_{62}Cl_5InO_3Sn_2$
Formula weight, g mol^{-1}	1132.36
Crystal system	Monoclinic
Crystal size, mm	0.15 × 0.15 × 0.08
Space group	$P2_1/c$
Cell constants a, b, c (Å)	19.705(1), 11.427(7), 22.201(1)
Angle α, β, γ (º)	90, 92.31(5), 90
Cell volume ($Å^3$)	4995(5)
Z	4
Density, (g/cm^3)	1.506
Absorption coefficient (mm^{-1})	1.750
F(000)	2264
θ range, deg	1.84 to 25.25
Collected / independent reflections	22361 / 9006
Observed reflections with ($I>2\sigma(I)$)	5838
Completeness to θ max	99.6 %
Parameter	469
GooF	0.922
R1 (F) ($I > 2\sigma(I)$)	0.0441
wR2 (F2) (all data)	0.1416
(Δ/σ)max	469
Largest diff peak / hole, e $Å^{-3}$	0.951 / –1.087

$(2,6\text{-}Mes_2C_6H_3In)_3(HCO_3)_2(OH)_4$ (20)

Formula	$C_{74}H_{81}In_3O_{10}$
Formula weight, g mol^{-1}	1474.85
Crystal system	Monoclinic
Crystal size, mm	0.18 × 0.17 × 0.12
Space group	$P2_1/n$
Cell constants a, b, c (Å)	13.741(1), 22.695(2), 24.07(3)
Angle α, β, γ (º)	90, 95.40(8), 90
Cell volume ($Å^3$)	7472(12)
Z	4
Density, (g/cm^3)	1.311
Absorption coefficient (mm^{-1})	0.970
F(000)	3008
θ range, deg	1.79 to 29.28
Collected / independent reflections	51309 / 19933
Observed reflections with ($I>2\sigma(I)$)	7234
Completeness to θ max	98.1%
Parameter	784
GooF	0.692
R1 (F) ($I > 2\sigma(I)$)	0.0487
wR2 (F2) (all data)	0.1106
(Δ/σ)max	< 0.001
Largest diff peak / hole, e $Å^{-3}$	0.569 / –0.728

(2,6-$Mes_2C_6H_3In)_4(CO_3)_2(OH)_4 \cdot 2\ H_2O$ (21)

Formula	$C_{98}H_{102}In_4O_{12}$
Formula weight, g mol^{-1}	1931.08
Crystal system	Monoclinic
Crystal size, mm	0.50 × 0.20 × 0.14
Space group	$P2_1/n$
Cell constants a, b, c (Å)	14.564(8), 20.232(9), 18.848(1)
Angle α, β, γ (º)	90, 109.676(5), 90
Cell volume ($Å^3$)	5229.8(5)
Z	2
Density, (g/cm^3)	1.226
Absorption coefficient (mm^{-1})	0.922
F(000)	1964
θ range, deg	1.79 to 29.28
Collected / independent reflections	40511 / 14070
Observed reflections with ($I>2\sigma(I)$)	9488
Completeness to θ max	98.6 %
Parameter	514
GooF	0.914
R1 (F) ($I > 2\sigma(I)$)	0.0442
wR2 (F2) (all data)	0.1231
(Δ/σ)max	< 0.001
Largest diff peak / hole, e $Å^{-3}$	0.603 / –1.364

[(2,6-$Mes_2C_6H_3In)_4(OCH_2CH_2O)_2(OH)_4$]·2THF (22)

Formula	$C_{108}H_{132}In_4O_{10}$
Formula weight, g mol^{-1}	2049.42
Crystal system	Orthorhombic
Crystal size, mm	0.22 × 0.32 × 0.20
Space group	$C222_1$
Cell constants a, b, c (Å)	14.936(5), 28.367(1), 22.525(10)
Angle α, β, γ (º)	90, 90, 90
Cell volume ($Å^3$)	9544(6)
Z	4
Density, (g/cm^3)	1.426
Absorption coefficient (mm^{-1})	1.013
F(000)	4224
θ range, deg	1.81 to 29.24
Collected / independent reflections	35342 / 12836
Observed reflections with ($I>2\sigma(I)$)	7719
Completeness to θ max	99.3 %
Parameter	553
GooF	0.825
R1 (F) ($I > 2\sigma(I)$)	0.0325
wR2 (F2) (all data)	0.0748
(Δ/σ)max	< 0.001
Largest diff peak / hole, e $Å^{-3}$	0.385 / –0.767

$(2,6\text{-}Mes_2C_6H_3In)_4(CO_3)_2(OCH_2CH_2OH)_2(OH)_2$ (23)

Formula	$C_{102}H_{110}In_4O_{12}$
Formula weight, g mol^{-1}	1987.18
Crystal system	Monoclinic
Crystal size, mm	0.22 × 0.18 × 0.06
Space group	$P2_1/n$
Cell constants a, b, c (Å)	13.372(8), 19.775(2), 17.780(1)
Angle α, β, γ (º)	90, 102.40(5), 90
Cell volume ($Å^3$)	4592(5)
Z	2
Density, (g/cm^3)	1.437
Absorption coefficient (mm^{-1})	1.052
F(000)	2028
θ range, deg	2.02 to 29.28
Collected / independent reflections	29014 / 12303
Observed reflections with ($I>2\sigma(I)$)	2756
Completeness to θ max	98.0%
Parameter	532
GooF	0.600
R1 (F) ($I > 2\sigma(I)$)	0.0572
wR2 (F2) (all data)	0.1330
(Δ/σ)max	< 0.001
Largest diff peak / hole, e $Å^{-3}$	0.541 / –0.622

(2,6-$Mes_2C_6H_3Tl)_2(\mu$-$Cl)_2Cl_2\cdot 1/2CH_2Cl_2$ (24)

Formula	$C_{49}H_{50}Cl_6Tl_2$
Formula weight, g mol^{-1}	1260.33
Crystal system	Monoclinic
Crystal size, mm	0.21 × 0.10 × 0.09
Space group	$P2_1/n$
Cell constants a, b, c (Å)	10.615(6), 16.90(1), 13.685(9)
Angle α, β, γ (º)	90, 94.10(5), 90
Cell volume ($Å^3$)	2448(3)
Z	2
Density, (g/cm^3)	1.710
Absorption coefficient (mm^{-1})	6.933
F(000)	1216
θ range, deg	1.92 to 25.25
Collected / independent reflections	13128 / 4413
Observed reflections with ($I>2\sigma(I)$)	3298
Completeness to θ max	99.5 %
Parameter	262
GooF	0.995
R1 (F) ($I > 2\sigma(I)$)	0.0375
wR2 (F2) (all data)	0.0973
(Δ/σ)max	< 0.001
Largest diff peak / hole, e $Å^{-3}$	1.569 / –1.579
CCDC-Number	751070

$[(2,6\text{-}Mes_2C_6H_3)_2Tl]TlCl_4 \cdot 2CHCl_3$ (25)

Formula	$C_{50}H_{52}Cl_{10}Tl_2$
Formula weight, g mol^{-1}	1416.16
Crystal system	Triclinic
Crystal size, mm	0.50 × 0.50 × 0.43
Space group	P1
Cell constants a, b, c (Å)	10.46(1), 15.55(3), 18.04(2)
Angle α, β, γ (º)	87.7(1), 75.30(9), 74.5(1)
Cell volume ($Å^3$)	2733(7)
Z	2
Density, (g/cm^3)	1.721
Absorption coefficient (mm^{-1})	6.411
F(000)	1368
θ range, deg	1.77 to 25.25
Collected / independent reflections	21358 / 9827
Observed reflections with ($I>2\sigma(I)$)	7923
Completeness to θ max	99.3 %
Parameter	554
GooF	1.029
R1 (F) ($I > 2\sigma(I)$)	0.0567
wR2 (F2) (all data)	0.1687
(Δ/σ)max	< 0.001
Largest diff peak / hole, e $Å^{-3}$	1.590 / –2.341
CCDC-Number	751071

(2,6-$Mes_2C_6H_3Tl)_2(\mu$-$OH)_2Cl_2\cdot 2H_2O$ (26)

Formula	$C_{48}H_{54}Cl_2O_4Tl_2$
Formula weight, g mol^{-1}	1174.55
Crystal system	Monoclinic
Crystal size, mm	0.50 × 0.28 × 0.27
Space group	$P2_1/n$
Cell constants a, b, c (Å)	10.84(2), 17.12(2), 13.36(2)
Angle α, β, γ (º)	90, 92.52(10), 90
Cell volume ($Å^3$)	2477(5)
Z	1
Density, (g/cm^3)	1.575
Absorption coefficient (mm^{-1})	6.642
F(000)	1140
θ range, deg	2.37 to 25.25
Collected / independent reflections	11063 / 4450
Observed reflections with ($I>2\sigma(I)$)	3342
Completeness to θ max	99.4 %
Parameter	261
GooF	1.072
R1 (F) ($I > 2\sigma(I)$)	0.0649
wR2 (F2) (all data)	0.2045
(Δ/σ)max	< 0.001
Largest diff peak / hole, e $Å^{-3}$	3.258 / –1.789
CCDC-Number	751072

(2,6-$Mes_2C_6H_3Tl)_4Tl_2(\mu_3$-O)$_4(\mu$-OH)$_6$ (27)

Formula	$C_{96}H_{100}O_{10}Tl_6$
Formula weight, g mol^{-1}	2639.98
Crystal system	Monoclinic
Crystal size, mm	0.50 × 0.17 × 0.16
Space group	$P2_1/n$
Cell constants a, b, c (Å)	14.30(1), 20.80(2), 18.082(2)
Angle α, β, γ (º)	90, 108.26(6), 90
Cell volume ($Å^3$)	5108(8)
Z	2
Density, (g/cm^3)	1.716
Absorption coefficient (mm^{-1})	9.478
F(000)	2484
θ range, deg	2.37 to 25.25
Collected / independent reflections	25482 / 9159
Observed reflections with ($I>2\sigma(I)$)	5464
Completeness to θ max	99.1 %
Parameter	568
GooF	1.006
R1 (F) ($I > 2\sigma(I)$)	0.0723
wR2 (F2) (all data)	0.1782
(Δ/σ)max	< 0.001
Largest diff peak / hole, e $Å^{-3}$	3.542 / –1.723
CCDC-Number	751073

Published results:

1. **Synthesis and Structure of Polynuclear Indoxanes and Thalloxanes Containing Bulky *m*-Terphenyl Substituents.**
   S. Usman Ahmad, Jens Beckmann
   Organometallics **2009**, 28, 6893.

2. **Hexameric Methylstannoxyl Carbonate Ion $[MeSn(O)CO_3]_6^{6-}$. A Missing Link with a Drum-Type Structure.**
   S. Usman Ahmad, Jens Beckmann, Andrew Duthie
   Organometallics **2009**, 28, 7053.

3. **New Insights into the Formation and Reactivity of Molecular Organostannonic Acids.**
   S. Usman Ahmad, Jens Beckmann, Andrew Duthie
   Chem. Asian J. **2010**, 5, 160.

7. Index

Compounds index

Nr.	Molecular formula
1	2,6-$Mes_2C_6H_3SnCl_3$
2	2,6-$Mes_2C_6H_3Sn(OH)Cl_2 \cdot H_2O$
3	*trans*-[2,6-$Mes_2C_6H_3Sn(O)OH]_3$
4	2,6-$Mes_2C_6H_3(OH)Sn(OSnt Bu_2)_2O$
5	[$t Bu_2Sn(OH)OSnR(OH)_2OC(OSnt Bu_2OH)_2(O)SnR(OH)(H_2O)]_2$ R = 2,6-$Mes_2C_6H_3$
6	$[MeSn(O)OH]_n$
7	$K_6[MeSn(O)CO_3]_6 \cdot 14\ H_2O$
8	$[2,6\text{-}Mes_2C_6H_3Sn(OH)_2(O_2PPh_2)]_2$
9	$Na_3(2,6\text{-}Mes_2C_6H_3Sn)_4O_6(OH)_3$
10	$(2,6\text{-}Mes_2C_6H_3In)_2(\mu\text{-}Cl)_2Cl_2$
11	$2,6\text{-}Mes_2C_6H_3InCl_2 \cdot H_2O$
12	$(2,6\text{-}Mes_2C_6H_3In)_2(\mu\text{-}OH)_2Cl_2$
13	$(2,6\text{-}Mes_2C_6H_3In)_3(\mu\text{-}OH)_4Cl_2$
14	$(2,6\text{-}Mes_2C_6H_3In)_4(\mu\text{-}OH)_8$
15	$[(2,6\text{-}Mes_2C_6H_3In)_2(OH)_2(O_2PMe_2)_2]$
16	$[(2,6\text{-}Mes_2C_6H_3In)_2(OH)(O_2PPh_2)_3]$
17	$[(2,6\text{-}Mes_2C_6H_3In)(Me_5C_3HPO_2)_2(H_2O)_2]$
18	$(2,6\text{-}Mes_2C_6H_3In)(t Bu_2Sn)_2O(OH)_2Cl_2$
19	$(2,6\text{-}Mes_2C_6H_3In)_2(t Bu_2Sn)O(OH)_2$
20	$(2,6\text{-}Mes_2C_6H_3In)_3(HCO_3)_2(OH)_4$
21	$(2,6\text{-}Mes_2C_6H_3In)_4(CO_3)_2(OH)_4 \cdot 2\ H_2O$
22	$(2,6\text{-}Mes_2C_6H_3In)_4(OCH_2CH_2O)_2(OH)_4$
23	$(2,6\text{-}Mes_2C_6H_3In)_4(CO_3)_2(OCH_2CH_2OH)_2(OH)_2$
24	$(2,6\text{-}Mes_2C_6H_3Tl)_2(\mu\text{-}Cl)_2Cl_2$
25	$[(2,6\text{-}Mes_2C_6H_3)_2Tl]TlCl_4$
26	$(2,6\text{-}Mes_2C_6H_3Tl)_2(\mu\text{-}OH)_2Cl_2$
27	$(2,6\text{-}Mes_2C_6H_3Tl)_4Tl_2(\mu_3\text{-}O)_4(\mu\text{-}OH)_6$

Figure Index

Scheme Index

Abbreviations

*t*Bu	*tert*- Butyl
*i*Pr	*iso*-Propyl
*trans*Myr	*trans*-Myrtanyl
*c*Hex	*cyclo*-Hexyl
Me	Methyl
Et	Ethyl
Ph	Phenyl
Mol. Wt	Molecular weight
Mes	Mesityl
m-Ter	*m*-Terphenyl substituent
Ph	Phenyl
R	Organic rest
rt	Room temperature
THF	Tetrahydrofurane
NMR	Nuclear magnetic resonance
IR	Infrared
ESI MS	Electrospray mass spectrometry
EA	Elemental analysis

8. References

1. (a) Hay, J.; Porter, D.; Raval, H. *Chem. Commun.* **1999**, 81. (b) Corriu, R. J. P.; Leclercq, D. *Angew. Chem. Int. Ed. Engl.* **1996**, 35, 1420. (c) Hay, J. N.; Raval, H. M. *Chem. Mater.* **2001**, 13, 3396.
2. Sarno, D. M.; Jiang, B; Grosfeld, D.; Afriyie, J. O.; Matienzo, L. J.; Wayne, Jr. E. *Langmuir* **2000**, 16, 6191.
3. (a) Biteau, J.; Chaput, F.; Lahlil, K.; Boilot, J. P. *Chem. Mater.* **1998**, 10, 1945. (b) Celio, H.; Lozaro, J.; Cabibi, H.; Ballast, L.; White, J. M. *J. Am. Chem. Soc.* **2003**,125, 3302 (c) Purkaystha, A.; Baruah, J. B. *Appl. Organometal. Chem.* **2001**, 15, 693. (d) Chung, M-K.; Orlova, G.; Goddard, J. D.; Schlaf, M.; Harris, R.; Beveridge, T. J.; White, G.; Hallett, F. R. *J. Am. Chem. Soc.* **2002**, 124,10508.
4. Corriu, R. J. P.; Cerveau, G., Framery, E. *Chem. Mater.* **2000**, 13, 3373.
5. Purkayastha, A.; Baruah, J. B. *Appl. Oranomet. Chem.* **2004**, 18, 166.
6. (a) Lickiss, P.D. *Adv. Inorg. Chem*. **1995**, 42, 147. (b) Lickiss, P.D. in: Rappoport, Z.; Apeloig, Y (Eds.), *Chemistry of Organic Silicon Compounds*, vol. 3, Wiley, Chichester, UK, **2001**, p. 695.
7. Unno, M.; Alias, S. B.; Arai, M.; Takada, K.; Tanaka, R.; Matsumoto, H. *Appl. Organomet. Chem*. **1999**, 13, 303.
8. (a) Nolte, J. -O.; Schneider, M.; Neumann, B.; Stammler, H.-G.; Jutzi, P.; *Organometallics*, **2003**, 22, 1010. (b) Murugavel, R.; Bhattacharjee, M.; Roesky, H. W. *Appl. Organomet. Chem*. **1999**, 13, 227.
9. Winkhofer, N.; Roesky, H. W.; Noltemeyer, M.; Robinson, W. T. *Angew. Chem*. **1992**,104, 670.
10. (a) Pietschnig, R.; Belaj, F.; Tirrée, J. J. *Organometallics*. **2004**, 23, 4897. (b) Spirk, S.: Belaj, F.: Baumgartner, J.: Pietschnig, R. *Z. Anorg. Allg. Chem*. **2009**, 635,1048.
11. Unno, M.; Takada, K.; Matsumoto, H. *Chem. Lett*. **1998**, 27, 489.
12. (a) Spirk, S.; Nieger, M.; Belaja, F.; Pietschnig, R. *Dalton Trans*., **2009**, 163, 163. (b) Lickiss, P. D.; Litster, S. A.; Redhouse, A, D.; Wisener, C. J. *J. Chem. Soc., Chem. Commun*., **1991**, 173.
13. Pietschnig, R.; Merz, K. *Organometallics* **2004**, 23, 1373.
14. Pietschnig, R.; Merz, K. *J. Chem. Soc., Chem. Commun*. **2001**,1210.

15. Unno, M.; Kishimoto, Y.; Matsumoto, H. *Organometallics*, **2004**, 23, 6221.
16. Ackerhans, C.; Roesky, H. W.; Labahn, T.;Magull. J. *Organometallics,* **2002**, 21, 3671.
17. Baugher, B. M.; Loy, D. A. *Mater. Res. Soc. Symp. Proc*. **1996,** 431, 323.
18. Nanjo, M.; Sasage, T.; Mochida, K. *J. Organomet. Chem*. **2003**, 667, 135.
19. (a) Puff, H.; Reuter, H. *J. Organomet*. *Chem*. **1989**, 364, 57. (b) Puff, H.; Reuter, H. *J.* Organomet. Chem. **1989**, 368, 173. (c) Puff, H.; Reuter,H. J. *Organomet*. *Chem*. **1989**, 373, 173. (d) Wraage, K.; Pape, T.; Herbst-Irmer, R.; Noltemeyer, M.; Schmidt, H. G.; Roesky, H. R. *Eur*. *J*. *Inorg*. Chem. **1999**, 369. (e) Janssen, J. Magull, Roesky, H. W. *Angew*. *Chem*. *Int*. Ed. **2002**, 41, 1365. (f) Prabusankar, G.; Jousseaume, B.; Toupance, T.; Allouchi, H. *Angew. Chem*. **2006**, 118, 1277; . Angew Chem ., Int. Ed. **2006**, 45,1255.
20. (a) Meyer, G. *Ber. Dtsch. Chem. Ges*. **1883**, 16, 1439. (b) Pfeiffer, P. *Z. Anorg. Allgem. Chem*. **1910**, *68*, 102. (c) Lambourne, H. *J. Chem. Soc*. **1922**, 121, 2533.
21. Luitjen, J. G. A. *Recl. Trav. Chim. Pays-Bas* **1966**, 85, 873.
22. Holmes, R. R.; Kaesz, H. D. *J. Am. Chem. Soc*. **1961**, 8*3*, 3903.
23. Puff, H.; Reuter, H. *J. Organomet. Chem*. **1989**, 364, 57.
24. Puff, H.; Reuter, H. *J. Organomet. Chem*. **1989**, 368, 173.
25. Puff, H.; Reuter, H. *J. Organomet. Chem*. **1989**, 373, 173.
26. Janssen, J.; Magull, J.; Roesky, H. W. *Angew. Chem. Int. Ed*. **2002**, 41, 1365.
27. Prabusankar, G.; Jousseaume, B.; Toupance, T.; Allouchi, H. *Angew. Chem. Int. Ed*. **2006**, *45*, 1255.
28. Wraage, K.; Pape, T.; Herbst-Irmer, R.; Noltemeyer, M.; Schmidt, H. -G.; Roesky, R. W. *Eur. J. Inorg. Chem*. **1999**, 869.
29. Bouŝka, M.; Dostál, L.; Jirásko, R.; Růžička, A.; Jambor, R. *Organometallics* **2009**, *28*, 4258.
30. Hall, D. G. (ed.) Boronic Acids, **2005**, Wiley-VCH, Weinheim and references cited therein.
31. (a) Braga, D.; Polito, M.; Bracaccini, M.; D'Addario, D.; Tagliavini, E.; Sturba, L.; Grepioni, F. *Organometallics* **2003**, 22, 2142. (b) Fournier, J.-H.; Maris, T.; Wuest, J. D.; Guo, W.; Galoppini, E. *J. Amer. Chem. Soc*. **2003**, 125, 1002. (c) Pedireddi, V. R.; Lekshmi, N. S. *Tetrahedron Lett*. **2004**, 45, 1903. (d) Fujita, N.; Shinkai, S.; James, T. D. *Chem. Asian J.* **2008**, 3, 1076. (e) Mastalerz, M.

Angew. Chem. Int. Ed. **2008**, 47, 445. (f) Severin, K. *Dalton Trans*. **2009**, 5254 and references cited therein.

32. James, T. D.; Sandanayake, K. R. A. S.; Shinkai, S. *Angew. Chem. Int. Ed*. **1996**, 35, 1910. (b) James, T. D.; Shinkai, S. *Topics Curr. Chem*. **2002**, 218, 159 and references cited therein.
33. Mason, M. R.; Smith, J. M.; Bott, S. G.; Barron, A. R. *J. Amer. Chem. Soc*. **1993**, 115, 4971.
34. Schnitter, C.; Roesky, H. W.; Albers, T.; Schmidt, H.-G.; Riipken, C.; Parisini, E.; Sheldrick, G. M. *Chem. Eur. J*. **1997**, 3, 1783.
35. Pasynkiewicz, *Polyhedron*, **1990**, 9, 429, and references cited therein.
36. Landry, C. C.; Harlan, C. J.; Bott, S. G. Barron, A. R. *Angew. Chem. Int. Ed*. **1995**, 34, 1201.
37. Wehmschulte, R. J.; Power, P. P. *J. Am. Chem. Soc*. **1997**, *119*, 8387.
38. Roesky, H. W.; Walawalkar, M. G.; Murugavel, R. *Acc. Chem. Res*. **2001**, *34*, 201 and references cited therein.
39. Storre, J.; Klemp, A.; Roesky, H. W.; Fleischer, R.; Stalke, D. *Organometallics* **1997**, 16, 3074

    Storre, S.; Klemp, A.; Roesky, H. W.; Schmidt, H.-G.; Noltemeyer, M.; Fleischer, R.; Stalke, D. *J. Amer. Chem. Soc*. **1996**, 118, 1380.
41. Roesky, H. W.; Walawalkar, M. G.; Murugavel, R. *Acc. Chem. Res*. **2001**, 34, 201 and references cited therein.
42. Al-Juaid, S. S.; Buttrus, N. H.; Eaborn, C.; Hitchcock, P.B.; Roberts, A. T. L.; Smith, J. D.; Sullivan, A. C. *J. Chem. Soc. Chem. Commun*. **1986**, 908.
43. Uhl, W.; Pohlmann, M. *Chem. Commun*. **1998**, 451.
44. Zhu, Z.; Wright, R. J.; Brown, Z. D.; Fox, A. R.; Phillips, A. D.; Richards, A. F.; Olmstead, M. M.; Power, P. P. *Organometallics* **2009**, *28*, 2512.
45. Beckmann, J.; Finke, P.; Hesse, M.; Wettig, B. *Angew. Chem. Int.Ed.* **2008**, 47,9982.
46. Beckmann, J.; Heek, T.; Takahashi, M. *Organometallics*. **2007**, 26, 3633.
47. Beckmann, J.; Bolsinger, J.; Finke, P.; Hesse, M. *Angew. Chem. Int. Ed*. **2010**, 49, 8030.
48. Ruhlandt-Senge, K.; Ellison, J. J.; Wehmschulte, R. J.; Pauer, F.; Power, P. P. *J. Am. Chem. Soc.* **1993**, 115, 11353.

49. Saito, M.; Hashimoto, H.; Tajima, T.; Ikeda, M. *J. Organomet. Chem*. **2007**, 692, 2729.
50. Lecomte, C.; Protas, J.; Devaud.M. *Acta Cryst*. **1976**, B32, 923.
51. Holmes, R. R.; Shafieezad, S.; Chandrasekhar, V.; Holmes, J. M.; Day, R. O. *J. Am. Chem. Soc*. **1988**, 110, 1174.
52. Beckmann, J.; Duthie, A.; Grassmann. M.; *J. Organomet. Chem*. **2009**, 694, 161.
53. (a) Beckmann, J.; Henn, M.; Jurkschat, k.; Schürmann, M.; Dakternieks, D.; Duthie, A. *Organometallics* **2002**, 21, 192. (b) Mehring, M.; Nolde, C.; Schürmann, M. *Inorg. Chim. Acta*. **2009**, 362, 745.
54. Prabusankar, G.; Jousseaume, B.; Toupance, T.; Allouchi, H. *Dalton Trans* **2007**, 3121.
55. Beckmann, J.; Jurkschat, K.; Kaltenbrunner, U.; Rabe, S.; Schürmann, M.; Dakternieks, D.; Duthie, A.; Müller, A. *Organometallics* **2000**, 19, 4887.
56. (a) Gibson , D. H. *Chem. Rev.* **1996***,* 96, 2063 *.(b)* Yin, *X*.; Moss, J*.* R*. Coord. Chem. Rev*. **1999** *,* 181 *,* 27*.*
57. Choi , J.-C.; Sakakura , T.; Sako , T. *J. Am. Chem. Soc.* **1999** , 121 , 3793.
58. Ballivet-Tkatchenko , D.;. Chambrey, S.; Keiski, R.; Ligabue, R.; Plasseraud, L.; Richard, P.; Turunen, H. *Catal. Today.* **2006** , 115 , 80.
59. Ballivet-Tkatchenko, D.; Chermette, H.; Plasseraud, L.; Walter , O. *Dalton Trans*. **2006** , 5167.
60. (a) Yin, S. F.; Maruyama , J.; Yamashita, T.; Shimada, S. *Angew. Chem***. 2008**, 120 *, Angew. Chem. Int. Ed. **2008***, 47, 6590. (b) Breunig, H. J.; Königsmann*,* L.; Lork, E.; Nema, M.; Philipp*,* N.; Silvestru*,* C.; Soran, A.; Varga, *R.* A.; Wagner, R*. Dalton Trans*. **2008**, 1831.
61. (a) Fujinami, T.; Sato, S.; Skai, S. *Chem. Lett*. **1981**, 749. (b) Davies, A.G.; Harrison, P.G. *J. Chem. Soc.* **1967**, 1313. (c) Choi, J.-C.; Sakakura, T.; Sako, T. *J. Amer. Chem. Soc*. **1999**, 121, 3793. (d) Ballivet-Tkatchenko, D.; Douteau, O.; Stutzmann, S. *Organometallics* **2000**, 19, 4563. (e) Kümmerlen, J.; Sebald, A.; Reuter, H. *J. Organomet. Chem*. **1992**, 427, 309. (f) Ballivet-Tkatchenko, D.; Jerphagnon, T.; Ligabue, R.; Plasseraud, L.; Poinsot, D. *Appl. Catal.* **2003**, 255, 93. (g) Beckmann, J.; Dakternieks, D.; Duthie, A.; Lewcenko, N. A.; Mitchell, C. *Angew. Chem. Int. Ed*. **2004**, *43*, 6683. (h) Zheng, G.-L.; Ma, J.-F.; Yang, J.; Li, Y.-Y.; Hao, X.-R. *Chem. Eur. J*. **2004**, 10,

3761. (i) Ballivet-Tkatchenko, D.; Chambrey, S.; Keiski, R.; Ligabue, R.; Plasseraud, L.; Richard, R.; Turunen, K. *Catal. Today*, **2006**, 115, 80. (j) Ballivet-Tkatchenko, D.; Chermette, H.; Plasseraud, L.; Walter,O. *Dalton Trans*. **2006**, 5167. (k) Padělková, Z.; Vaňkátová, H.; Císařová, I.; Nechaev, M.S.; Zevaco, T.A.; Walter, O.; Růžička,A. *Organometallics* **2009**, 28, 2629. (l) Dostál, L.; Jambor, R.; Růžiĉka, A.; Erben, M.; Jirásko, R.; Holeĉek, J. *Organometallics* **2009**, 28, 2633.

62. (a) Reuter, H. Ph.D. thesis, University of Bonn, Germany **1986**. (b) Ballivet-Tkatchenko, D.; Burgat, R.; Chambrey, S.; Plasseraud, L.; Richard, P. *J. Organomet. Chem*. **2006**, 691, 1498.

63. (a) Puff, H.; Hevendehl, H.; Hoefer, K.; Reuter, H.; Schuh, W. *J. Organomet. Chem*. **1985**, 287, 163. (b) Mokal, V. B.; Jain, V. K.; Tiekink, E. R. T. *J. Organomet. Chem*. **1992**, 431, 283. (c) Beckmann, J.; Jurkschat, K.; Mahieu, B.; Schürmann, M. *Main Group Met. Chem*. **1998**, 21, 113. (d) Sakamoto, K.; Hamada, Y.; Akashi, H.; Orita, A.; Otera, J. *Organometallics* **1999**, 18, 3555. (e) Sakamoto, K.; Ikeda, H.; Akashi, H.; Fukuyama, T.; Orita, A.; Otera, J. *Organometallics* **2000**, 19, 3242.

64. Beckmann, J.; Jurkschat, K.; Mahieu, B.; Schürmann, M. *Main Group Met. Chem*. **1998**, 21, 113

65. Beckmann, J.; Dakternieks, D.; Duthie, A.; Jurkschat, K.; Mehring, M.; Mitchell, C.; Schürmann, M. *Eur. J. Inorg. Chem*. **2003**, 4356.

66. Beckmann, J.: Bolsinger, J.: Duthie, A. *Z. Anorg. Allgem. Chem.* **2010**, 636, 5.

67. Kümmerlen , J.; Sebald , A.; Reuter , H. *J. Organomet. Chem.* **1992**, 427, 309.

68. Padělková, Z.; Vaňkátová, H.; Císařová, I.; Nechaev, M. S.; Zevaco, T. A.; Walter, O.; Růžička, A. *Organometallics* **2009** *,* 28 *,* 2629.

69. Dostál, L.; Jambor , R.; Růžiĉka, A.; Erben , M.; Jirásko , R.; Cernoškova , E.; Holeĉek, J. *Organometallics* **2009** *,* 28 *,* 2633.

70. (a) Davies, A. G.; Harrison, P. G. *J. Chem. Soc. C*, **1967**, 1313. (b) Fujinami, T.; Sato, S.; Skai, S. *Chem. Lett*. **1981**, 749. (c) Reuter, H. Ph.D. thesis, University of Bonn, Germany **1986**. (d) Kümmerlen, J.; Sebald, A.; Reuter, H. *J. Organomet. Chem*. **1992**, 427, 309. (e) Choi, J.-C.; Sakakura, T.; Sako, T. *J. Amer. Chem. Soc*. **1999**, 121, 3793. (f) Ballivet-Tkatchenko, D.; Douteau, O.; Stutzmann, S. *Organometallics* **2000**, 19, 4563. (g) Ballivet-Tkatchenko, D.; Jerphagnon, T.; Ligabue, R.; Plasseraud, L.; Poinsot, D. *Appl. Catal.* **2003**,

255, 93. (h) Zheng, G.-L.; Ma, J.-F.; Yang, J.; Li, Y.-Y.; Hao, X.-R. *Chem. Eur. J*. **2004**, 10, 3761. (i) Beckmann, J.; Dakternieks, D.; Duthie, A.; Lewcenko, N. A.; Mitchell, C. *Angew. Chem. Int. Ed*. **2004**, 43, 6683. (j) Ballivet-Tkatchenko, D.; Chambrey, S.; Keiski, R.; Ligabue, R.; Plasseraud, L.; Richard, R.; Turunen, K. *Catal. Today* **2006**, 115, 80. (k) Ballivet-Tkatchenko, D.; Chermette, H.; Plasseraud, L.; Walter, O. *Dalton Trans*. **2006**, 5167. (l) Ballivet-Tkatchenko, D.; Burgat, R.; Chambrey, S.; Plasseraud, L.; Richard, P. *J. Organomet. Chem*. **2006**, 691, 1498. (m) Padělková, Z.; Vaňkátová, H.; Císařová, I.; Nechaev, M. S.; Zevaco, T. A.; Walter, O.; Růžička, A. *Organometallics* **2009**, 28, 2629.

71. (a) Meyer, G. *Ber. Dtsch. Chem. Ges*. **1883**, 16, 1439. (b) Pfeiffer, P. *Z. Anorg. Allgem. Chem*. **1910**, 68, 102. (c) Lambourne, H. *J. Chem. Soc*. **1922**, 121, 533.

72. (a) Chandrasekhar, V.; Schmid, C. G.; Burton, S. D.; Holmes, J. M.; Day, R. O.; Holmes, R. R. *Inorg. Chem*. **1987**, 26, 1050. (b) Day, R. O.; Chandrasekhar, V.; Swamy, K. C. K.; Holmes, J. M.; Burton, S. D.; Holmes, R. R. *Inorg. Chem*. **1988**, 27, 2887. (c) Holmes, R. R. *Acc. Chem. Res.* **1989**, *22*, 190. (d) Mokal, V. B.; Jain, V. K.; Tiekink, E. R. T. *J. Organomet. Chem*. **1991**, 407, 173. (e) Tiekink, E. R. T. *Appl. Organomet. Chem*. **1991**, *5*, 1. (f) Tiekink, E. R. T. *Trends Organomet. Chem*. **1994**, 1, 71. (g) Ribot, F. O. Eychenne-Baron, C.; Sanchez, C. *Phosphorous Sulfur Silicon* **1999**, 150, 41. (h) Chandrasekhar, V.; Nagendran, S.; Bansal, S.; Cordes, A. W.; Vij, A. *Organometallics* **2002**, 21, 3297. (i) Chandrasekhar, V.; Nagendran, S.; Baskar, V. *Coord. Chem. Rev*. **2002**, *235*, 1. (j) Prabusankar, G.; Murugavel, R. *Organometallics* **2004**, 23, 5644. (k) Chandrasekhar, V.; Gopal, K.; Nagendran, S.; Steiner, A.; Zacchini, S. *Cryst. Growth Des*. **2006**, 6, 267. (l) Chandrasekhar, V.; Gopal, K.; Thilargar, P. *Acc. Chem. Res*. **2007**, 40, 420.

73. (a) Meyer, G. *Ber. Dtsch. Chem. Ges*. **1883**, 16, 1439. (b) Pfeiffer, P. *Z. Anorg. Allgem. Chem*. **1910**, 68, 102. (c) Lambourne, H. *J. Chem. Soc*. **1922**, 121, 2533.

74. Ribot, F.; Eychenne-Baron, C.; Fayon, F.; Massiot, D.; Bresson, B. *Main Group Met. Chem*. **2002**, 25, 115.

75. Banse, F.; Ribot, F. Toledano, P.; Maquet, J.; Sanchez, C. *Inorg. Chem*. **1995**, 34, 6371.

76. (a) Puff, H.; Reuter, H. *J. Organomet. Chem*. **1989**, 373, 173. (b) Dakternieks, D.; Zhu, H.; Tiekink, E. R. T.; Colton, R. *J. Organomet. Chem*. **1994**, 476, 33. (c) Eychenne-Baron, C.; Ribot, F.; Steunou, N.; Sanchez, C.; Fayon, F.; Biesemans, M.; Martins, J. C.; Willem, R. *Organometallics* **2000**, 19, 1940. (d) Beckmann, J.; Jurkschat, K.; Kaltenbrunner, U.; Rabe, S.; Schürmann, M.; Dakternieks, D.; Duthie, A.; Müller, D. *Organometallics* **2000**, 19, 4887.

77. (a) Holmes, R. R. *Acc. Chem. Res.* **1989**, 22, 190. (b) Chandrasekhar, V.; Nagendran, S.; Baskar, V. *Coord. Chem. Rev*. **2002**, 235, 1.

78. Holmes, R. R.; Kumara Swamy, K. C.; Schmid, C. G.; Day, R. O. *J. Am. Chem. Soc*. **1988**, 110, 7060.

79. Henn, M.; Jurkschat, K.; Mansfeld, D.; Mehring, M.: Schürmann, M. *J. Mol. Struc*. **2004**, 697, 213.

80. Blunden, S. J.; Hill, R. *Inorg. Chim. Acta* **1990**, 177, 219.

81. Reuter, H. *Angew. Chem. Int. Ed*. **1991**, 30, 1482.

82. Roesky, H. W.; Haiduc, I.; Hosmane, N. S. *Chem. Rev*. **2003**, 103, 2579.

83. (a) Mehring, M.; Mansfeld, D.; Costisella, B.; Schürmann ,M. *Eur. J. Inorg. Chem*. **2006**, 735. (b) Bremm, U.; Norrestam, R.; Nygren, M.; Westin, G. *Inorg. Chem*. **1995**, 34, 2367. (c) Evans, W. J.; Sollberger, M. S. *J. Am. Chem. Soc*. **1985**, 108, 6095.

84. Robinson, G. H.; Li, X.-W.; Pennington, W. T. *J. Organomet. Chem*. **1995**, 501, 399.

85. (a) Su, J.; Li, X.-W.; Robinson, G. H. *Chem. Commun*. **1998**, 2015. (b) Twamley, B.; Power, P. P. *Chem. Commun*. **1999**, 1805.

86. (a) Veith, M.; Hill, S.; Huch, V. *Eur. J. Inorg. Chem*. **1999**, 1343. (b) Hecht, E.; Gelbrich, T.; Thiele, K.-H.; Sieler, J. *Main Group. Chem*. **2000**, 3, 109. (c) Chitsaz, S.; Neumüller, B. *Z. Anorg. Allg. Chem*. **2001**, 627, 2451. (d) Chamazi, N. N.; Heravi, M. M.; Neumüller, B. *Z. Anorg. Allg.Chem*. **2006**, 632, 2043.

87. Roesky, H. W.; Haiduc, I.; Hosmane, N. S. *Organometallics* **2003**, 103, 2579 and references cited therein.

88. Coates, G. E..; Mukherjee, R. N. *J .Chem. Soc*. **1964**, 1295.

89. Mason, M. R. *J. Cluster Sci*. **1998**, 9, 1.

90. Hahn, F. E.; Schneider, B.; Reier, F.-W. *Z. Naturforsch. B.* **1990**, 45, 134.

91. Arif, A. M.; Barron, A. R. *Polyhedron* **1988**, 7, 2091.

92. The bulky 1,1,2,3,3-pentamethyltrimethylenephosphinic acid was recently introduced into group 14 and 15 element phosphinate chemistry. (a) Chandrasekhar, V.; Baskar, V.; Steiner, A.; Zacchini, S. *Organometallics* **2004**, 23, 1390. (b) Chandrasekhar, V.; Thirumoorthi, R. *Organometallics* **2009**, 28, 2637.

93. Mason, T. O.; Kammler, D. R.; Ingram, B. J.; Gonzalez, G. B.; Young, D. L.; Coutts. T. J. *Thin solid films* **2003**, 445, 186.

94. Shannon, R. D.; Gillson, J. L.; Bouchard, R. J. *J. Phys. Chem. Solids* **1977,** 38, 877.

95. Veith, M.; Kunze, K. *Angew. Chem. Int. Ed*. **1991**, 30, 1.

96. Veith, M.; Hill, S.; Huch, H. *Z. anorg. allg. Chem.* **2001***,* 627, 1495

97. (a) Ono, Y. *Appl. Catal. A: Gen*. **1997**, 155, 133. (b) Pacheco, M. A.; Marshall, C. L. *Energy Fuels*, **1997**, 11, 2. (c) Ono, Y. *Catal. Today*. **1997**, 35,15.

98. Chang, Y.; Jiang, T.; Han, B.; Liu, Z.; Wu, W.; Gao, L.; Li, J.; Gao, H.; Zhao, G.; Huang, *J. Applied Catalysis A: General*, **2004**, 263, 179.

99. (a) Tatsumi, T.; Watanabe, Y.; Koyano, K. A. *Chem. Commun*.**1996**, 2281.(b) Bhanage, B. M.; Fujita, S.I.; He, Y. F.; Ikushima, Y.; Torii, K.; Arai, M. *Green Chem*. **2003**, 5, 71.(c) Bhanage, B. M.; Fujita, S.I.; He, Y. F.; Ikushima, Y.; Shirai, M.; Torii, K.; Arai, M. *Catal. Lett*. **2002**, 83,137.

100 (a) Shaikh, A.A.; Sivaram, S. *Chem. Rev.*, **1996**, 96, 951. (b) Aresta, A.; Quaranta, E. *Chemtech*, **1997**, 32.

101. (a) Niemeyer, M.; Power, P. P. *Angew. Chem. Int. Ed*. **1998**, 37, 1277. (b) Wright, R. J.; Phillips, A. D.; Hino, S.; Power, P. P. *J. Amer. Chem. Soc*. **2005**, 127, 4794.

102. Laguna, A.; Fernandez, E. J.; Mendia, A.; Ruiz-Romero, M. E.; Jones, P. G. *J. Organomet. Chem.* **1989**, 365, 201.

103. Kuzu, I.; Neumüller, B. *Z. Anorg. Allg. Chem*. **2007**, 633, 941.

104. Niemeyer, M.; Power, P. P. *Organometallics* **1997**, 16, 3258.

105. Wehmschulte, R. J.; Steele, J. M.; Young, J. D.; Khan, M. A. *J. Am. Chem. Soc*. **2003**, 125, 1470.

106. Young, J. D.; Khan, M. A.; Wehmschulte, R. J. *Organometallics* **2004**, 23, 1965.

107. Rudawska-Frackiewicz, K.; Siekierski, S. *J. Coord. Chem*. **2004**, 57, 777.

108. Puff, H.; Schuh, W.; Sievers, R.; Wald, W.; Zimmer, R. *J. Org. Chem.* **1984**,

260, 271.
109. STOE X-Area and X-Red, 2004 Stoe & Cie GmbH, Darmstadt, Germany.
110. Farrugia, L. J. *J. Appl. Cryst.* **1999**, 32, 837.
111. DIAMOND V3.1d, Crystal Impact GbR, Brandenburg, K.; Putz, H. **2006**.